The Dissertation Committee for Laura Rosyle Geuss Certifies that this is the approved version of the following dissertation:

Manipulation of the embryoid body microenvironment to increase cardiomyogenesis

Committee:

Laura J. Suggs, Supervisor

Jennifer Maynard

Jeanne Stachowiak

Steven Vokes

Janeta Zoldan

Manipulation of the embryoid body microenvironment to increase cardiomyogenesis

by

Laura Roslye Geuss, B.A; M.S.

Dissertation

Presented to the Faculty of the Graduate School of

The University of Texas at Austin

in Partial Fulfillment

of the Requirements

for the Degree of

Doctor of Philosophy

The University of Texas at Austin

August 2014

Dedication

This dissertation is dedicated to those who supported my dream over the past decade and encouraged me through the setbacks. Without you, none of this would have been possible.

Acknowledgements

Firstly, I would like to thank Dr. Greg Altman and Dr. David Kaplan. I started my research journey with them at Tufts University, and it was them who got me excited about research to begin with. I also am thankful for the support of Dr. Jingsong Chen, my mentor while I was there, who truly provided the foundation of my career in research.

For those at UT, I want to thank my PI, Dr. Laura Suggs, for not giving up on me: your support was steadfast throughout my tenure here. I also want to thank my committee: Dr. Steve Vokes, Dr. Jeanne Stachowiak, Dr. Jennifer Maynard, and Dr. Janet Zoldan. Thank you for your guidance and advice over the years for this project.

I am also thankful for the support of my labmates during my time here – especially to those that indulged in my commiserating. I have been fortunate to have so many intelligent, gracious people around me to make this journey a little more bearable.

My friends have also played a huge supporting role. I want to thank my wonderful friend, Courtney, for being with me from the beginning. Having you around at the beginning of the program helped me keep going. Thank you Mary – it was nice having someone that shared similar experiences, someone to talk to.

And of course, there is absolutely no way I would have made it this far without my family. Thank you for always telling me you were proud, regardless of what the outcome was going to be. Thank you Tim, for putting up with me during the process, and for saying all the right things at the right time. I love you all, I am grateful for your

help getting me to this point, and I am so excited to close this chapter and start the next one.

Manipulation of the embryoid body microenvironment to increase cardiomyogenesis

Laura Roslye Geuss, PhD

The University of Texas at Austin, 2014

Supervisor: Laura J. Suggs

Myocardial Infarction (MI) is one of the most prevalent and deadliest diseases in the United States. Since the host myocardium becomes irreversibly damaged following MI, current research is focused on identification of novel, less invasive, and more effective treatment options for patients. Cellular cardiomyopathy, in which viable cells are transplanted into the necrotic tissue, has the potential to regenerate and integrate with the host myocardium. Stem cells, specifically pluripotent stem cells such as embryonic stem cells (ESCs) and induced pluripotent stem cells (iPSC), are ideal candidates for this procedure because they are pluripotent; however, ESCs must be predifferentiated to avoid teratoma formation *in vivo*. In this dissertation, our goal was improve upon current protocols to direct differentiation of ESCs into cardiomyocytes using an embryoid body (EB) model. We immobilized pro-cardiomyogenic proteins, specifically Sonic Hedgehog (SHH) and Bone Morphogenetic Protein 4 (BMP4) to paramagnetic beads and delivered them in the interior of the EB. While lineage commitment was indiscriminate, the presence of the beads alone appeared to guide differentiation into cardiomyocytes: there

were significantly more contracting areas in EBs containing beads than in the presence of SHH or BMP4. To take advantage of this result, we immobilized Arginine-Glycine-Aspartic Acid (RGD) peptides to the beads and magnetized them following incorporation into the EB. Magnetically mediated strain increased the expression of mechanochemical markers, and in combination with BMP4 increased the percentage of cardiomyocytes. Finally, PEGylated fibrin gels were used to investigate the effect of seeding method and fibrinogen concentration on cardiomyocyte behavior and maturation. Cells seeded on top of compliant hydrogels had the most contracting regions compared to stiffer PEGylated fibrin gels, whereas cardiomyocytes seeded within the hydrogels could not remodel the matrix or maintain contractility. As an alternative to 3D culture, we seeded cardiomyocytes within gel layers, which maintained viability as well as contractile activity. We observed that PEGylated fibrin gels can maintain ESC-derived cardiomyocytes; however, the ratio of cardiomyocytes and non-cardiomyocytes should be optimized to maintain contractile phenotypes. Therefore, this dissertation presents novel methods to differentiate ESCs into cardiomyocytes, and subsequently promote their maturation *in vitro*, for the treatment of MI.

Table of Contents

List of Tables

List of Figures

CHAPTER ONE

Introduction

1.1. INTRODUCTION

The overall goal of my research is to develop a tissue engineered construct, which uses a combination of cells and biocompatible materials, to treat cardiac disease such as myocardial infarction (MI). MI is one of the most prevalent forms of heart disease, and the focus of many studies has been on the discovery of less invasive methods to regenerate ischemic tissue damaged as a result of the MI event. Cardiomyocytes, which are the muscle cells that make up the myocardium, become necrotic and cannot regenerate following MI (Bergmann et al., 2009). Consequently, MI can be lethal without surgical intervention (Go et al., 2013).

In order to fully restore myocardial tissue function, there are two conditions that must be addressed: (1) identification of a cell population that can adequately repopulate the myocardium and (2) a medium to deliver the cells into the heart. Since millions of cells are needed to repair the damaged tissue, stem cells are ideal candidates to generate a large population of cardiovascular cells. Pluripotent stem cells (PSCs), which are stem cells that can differentiate into all three germ layers (mesoderm, endoderm, and ectoderm), have been under investigation for years due to their potential to differentiate into cardiovascular lineages. The bottleneck for their clinical use is finding the most effective regimen to guide differentiation specifically into cardiomyocytes and not other

cell types. Similarly, once the adequate cell source has been identified, the next challenge is to determine how to deliver the cells into the myocardium. This is especially important because injected cells are quickly lost from the myocardium following MI (Aicher et al., 2003).

In this project we focused on two specific needs for MI repair: (1) optimization of cardiomyocyte differentiation methods from PSCs and (2) development of a tissue engineered MI patch using cardiomyocytes and fibrin-based hydrogels. For the first part, our goal was to direct lineage commitment of mouse embryonic stem cells (mESCs) into mesoderm using biochemical stimulation or mechanical stimulation (Figure 1.1). Since current differentiation protocols using embryoid body (EB) models are not as efficient as 2D cell culture, we hypothesized that by delivering proteins into the interior of the EB, we could increase the percentage of cells that differentiate into mesoderm. Similarly, by delivering magnetic beads coated with cell adhesion peptides into the EB, we can induce strain on the cells via magnetic attraction. This method, known as mechanical stimulation, has also been used to drive differentiation towards cardiovascular lineages (Geuss & Suggs, 2013). Finally, we investigated the effect of fibrinogen concentration on the maintenance and maturity of mature cardiomyocytes and ESC-derived cardiomyocytes.

1.2. ORGANIZATION OF THE DISSERTATION

This dissertation is divided into six chapters. In Chapter 2, we describe the rationale for why cell therapy using PSCs has the most promise for tissue regeneration

following MI. The background of MI is introduced, as well as the most effective strategies currently being utilized. The most effective methods of ESC differentiation are presented, specifically biochemical means, as well as the mechanical stimulation regimens that have been used to derive cardiomyocytes from ESCs. This chapter also reviews the biomaterials that have been used to maintain cardiomyocytes for development of MI patches.

In Chapter 3, we describe the use of protein-immobilized beads to increase mesodermal commitment of mESCs. Specifically we investigate the effects of two proteins, Bone Morphogenetic Protein 4 (BMP4) and Sonic Hedgehog (SHH), which have both been used to either guide cardiomyogenesis or repair damaged myocardial tissue, respectively. As opposed to direct supplementation to cell culture medium, we have immobilized these proteins to paramagnetic beads and incorporated the beads into the EB interior. We assess cardiomyogenesis by the expression of lineage specific markers, as well as demonstration of functional characteristics of mature cardiomyocytes, such as contractile activity and sarcomeric α-actin expression. The results of this study suggested that while immobilizing proteins to beads may increase the percentage of cells exposed to the growth factors, the decreased potency of those growth factors when immobilized inhibits homogenous differentiation.

In Chapter 4, we use the paramagnetic beads to deliver mechanical stress to the cells, instead of for protein delivery applications. Beads were coated with Arginine-Glycine-Aspartic Acid (RGD) peptides, which promote cell attachment, and incorporated into the EB as described in Chapter 3. We observed that by magnetizing the cells with

neodymium magnets, we could activate mechanochemical signaling in the ESCs through the RGD-integrin interactions. By adjusting the timing of stimulation onset, we can direct differentiation towards specific cell lineages: here, application of stimulation on Day 3, in combination with BMP4, increases cardiomyogenesis over controls.

In Chapter 5, we use fibrin-based hydrogels for cardiomyocyte culture. Fibrinogen is conjugated with polyethylene glycol prior to crosslinking with thrombin to create a PEGylated fibrin gel. Changing the initial concentration of fibrinogen altered gel stiffness. Murine HL-1 cardiomyocytes were cultured in 3D and 2D on the hydrogels, and contractile activity rate as well as cardiomyocyte-specific marker expression was analyzed to assess the potential of the hydrogels as MI patches. We observed that while 3D culture inhibited contractile activity, 2D culture maintained contractility at rates within the range observed in other studies. We also performed initial experiments forming cell-gel layers, hereby referred to as 2DL culture, and observed that this could be an alternative *in vitro* seeding approach on PEGylated fibrin gels. Finally, in this chapter we describe early data of ESC-derived cardiomyocyte culture on 2D gels using the differentiation protocol in Chapter 4.

In Chapter 6, we present a summary of the findings in this dissertation, as well as conclusions and future work.

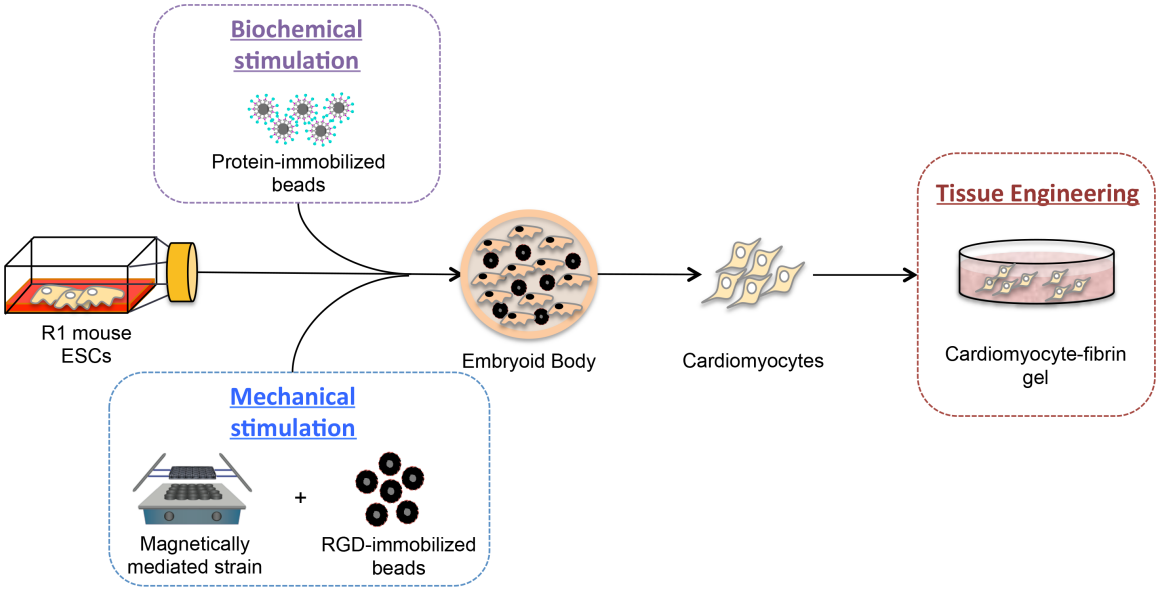

Figure 1.1: Overview of the Dissertation. Mouse ESCs are differentiated into cardiomyocytes using either biochemical stimulation (Chapter 3) or mechanical stimulation (Chapter 4). A tissue engineering approach is used to combine cardiomyocytes with PEGylated fibrin gels for potential use as an MI patch (Chapter 5).

1.3. REFERENCES

Aicher, A., Brenner, W., Zuhayra, M., Badorff, C., Massoudi, S., Assmus, B., et al. (2003). Assessment of the tissue distribution of transplanted human endothelial progenitor cells by radioactive labeling. *Circulation*, *107*(16), 2134–2139. doi:10.1161/01.CIR.0000062649.63838.C9

Bergmann, O., Bhardwaj, R. D., Bernard, S., Zdunek, S., Barnabe-Heider, F., Walsh, S., et al. (2009). Evidence for Cardiomyocyte Renewal in Humans. *Science (New York, N.Y.)*, *324*(5923), 98–102. doi:10.1126/science.1164680

Geuss, L. R., & Suggs, L. J. (2013). Making cardiomyocytes: how mechanical stimulation can influence differentiation of pluripotent stem cells. *Biotechnology Progress*, *29*(5), 1089–1096. doi:10.1002/btpr.1794

Go, A. S., Mozaffarian, D., Roger, V. L., Benjamin, E. J., Berry, J. D., Borden, W. B., et al. (2013). Heart disease and stroke statistics--2013 update: a report from the American Heart Association. *Circulation*, *127*(1), e6–e245. doi:10.1161/CIR.0b013e31828124ad

CHAPTER TWO

Background and Significance

2.1. MYOCARDIAL INFARCTION AND THERAPEUTIC STRATEGIES

Cardiovascular disease remains one of the most deadly diseases in America, accounting for approximately one of every 6 deaths in 2009 (Roger et al., 2012). Myocardial Infarction (MI) is one of the most prevalent manifestations of the disease: in 2008, 7.9 million Americans experienced MI, of which there were 134,000 deaths (Roger et al., 2012). Currently there are five different classifications of MI, which are listed in Table 2.1. The different classifications are predominantly recognized by increased levels of cardiac troponin (Tehrani & Seto, 2013; Thygesen, Alpert, Jaffe, Simoons, Chaitman, White, Joint ESC/ACCF/AHA/WHF Task Force for the Universal Definition of Myocardial Infarction, et al., 2012a), echocardiography, and other biomarkers for necrosis. The most common types are 1 and 2, which typically result from coronary artery blockage as a result of artherosclerosis (Figure 2.1). The loss of oxygenated blood flow leads to ischemia, and ultimately cardiomyocyte necrosis which if left untreated can be lethal (J. M. Alexander & Bruneau, 2010; M. Chen, Lin, Xie, Wu, & Wang, 2011; Duranteau, 1998; Xu et al., 2011). Currently, the most effective treatment strategies include fibrinolytic agents, percutaneous interventions, bypass grafting and heart transplantation; however, these treatments are not appropriate for all patients, and in the case of heart transplant is limited by supply (Pandur, 2005).

2.2. CELL THERAPY FOR MI

Terminally differentiated cells generally have limited regeneration potential, and this is especially true in tissues exposed to low perfusion or oxygen availability. As an alternative to more invasive treatment options, cell therapy, in which an exogenous cell population is injected into damaged tissue, can potentially repopulate the infarcted area. A challenge surrounding this treatment option is identification of a suitable cell source: millions of differentiated cardiomyocytes are needed to successfully replenish the damaged myocardium. Cardiac progenitor cells (CPCs) have been identified as a promising cell source as they have exhibited the greatest potential to differentiate into cardiomyocytes; however, scale-up of this population continues to be a limiting factor for their use clinically (Lyngbaek, Schneider, Hansen, & Sheikh, 2007).

Stem cells, which have the unique ability to self-renew and differentiate into multiple cells types, have also been explored as a cell source for their potential yield. Bone marrow stromal cells (MSCs) are multipotent stem cells that readily differentiate into osteoblasts, chondrocytes and adipocytes. There has also been evidence that these cells can differentiate into vascular fates, including cardiomyocytes, by supplementing the medium with 5-Azacytidine *in vitro* (Makino et al., 1999; X. Wang & Ha, 2013). *In vivo*, injection of MSCs into the myocardium of Lewis rats following ligation of the left anterior descending coronary artery (LAD) significantly decreased fibrosis and improved viability (Berry et al., 2006). Similar findings were also observed in rabbit models, in which significant improvements in vascular density were observed (M. Y. Tan et al., 2009); however, these results are most likely attributed to decreases in scar tissue other

than differentiation into cardiomyocytes, since few injected cells display cardiomyocyte-specific markers. Ultimately, for cell transplantation to be successful, cells must be able to integrate fully into the host tissue and electromechanically couple with native cardiomyocytes (Pandur, 2005; Ye, Zhou, Cai, & Tan, 2011).

2.3. EMBRYONIC STEM CELLS AS A SOURCE OF CARDIOMYOCYTES

As an alternative to adult stem cells, embryonic stem cells are pluripotent cells derived from the inner cell mass of the blastocyst. These cells are unique in that they can both self-renew as well as differentiate into all three germ layers, the endoderm, ectoderm and mesoderm (Martin, 1981). For this reason not only can ESCs differentiate specifically into cardiomyocytes, but they have greater potential to generate a higher concentration of cells.

On the other hand, these cells can become tumorigenic if implanted *in vivo* without pre-differentiation (Kolossov et al., 2006). To address this, studies have focused on optimizing methods to differentiate mouse and human ESCs and iPSCs into cardiomyocytes *in vitro*. Differentiation efficiency of ESCs into cardiomyocytes is evident by the expression of cardiomyocyte-specific genes and protein markers (Figure 2.2), as well as contractile phenotypes. Effective differentiation *in vitro* is demonstrated by the combined expression of all of these markers. Strategies have predominately involved stage-specific timing of protein supplementation (Yamashita et al., 2000). mirroring the factors that are involved in heart development such as Bone Morphogenetic Proteins (BMP), Activin, and Wnt inhibitors. These methods are very effective in

monolayer culture, as cardiomyocyte yields of up to 90-95% have been observed following this regimen (Lian et al., 2013). Cardiomyocyte differentiation from EB culture is significantly lower, averaging only 1-27% yields (Laflamme et al., 2007a; M. Y. Lee et al., 2011; Willems et al., 2011) as indicated by gene markers such as cardiomyocyte-specific gene Myosin Light Chain 6 (Myl6) (C. Williams, Johnson, Robinson, & Tranquillo, 2006) and contractile activity (Laflamme, Zbinden, Epstein, & Murry, 2007b; M. Y. Lee et al., 2011). These relatively low yields confirm the necessity to improve EB differentiation protocols for more high-throughput systems.

2.4. CARDIOVASCULAR DEVELOPMENT DURING EMBRYOGENESIS

The cardiovascular system is one of the first organ systems to develop in the embryo. Cardiac precursor cells can be found before the onset of gastrulation in the lateral posterior epiblast in pre-streak embryos (Van Vliet, Wu, Zaffran, & Pucéat, 2012). Formation of the mesendoderm, which is determined by Activin and Nodal signaling, is the result of ingression of the cells into the primitive streak (PS) (Berge et al., 2008; Evans, 2008; Harvey, 2002; Murry & Keller, 2010; Pandur, 2005; Ye et al., 2011). BMP2 signaling plays an important role in reprogramming the mesendoderm and promoting cardiogenesis (J. M. Alexander & Bruneau, 2010; Sucov, 1998; Van Vliet et al., 2012). Around embryonic day 7.5 (E7.5), the primary and secondary heart fields are formed and represented by expression of GATA4 and NK2 homeobox 5 (NKX 2.5) (Holtzinger, Rosenfeld, & Evans, 2010; Kolossov et al., 2006; D. Kumar, Kamp, & LeWinter, 2005). At E8.0, the linear heart tube forms, ultimately giving rise to the

formation of primitive ventricles and atria at E10.5. By E15, septation results in formation of the mature ventricles and atria, as well as formation of the heart valve (Xin, Olson, & Bassel-Duby, 2013) which are coordinated by multiple morphogens including the Hedgehog family (Astorga & Carlsson, 2007; Byrd et al., 2002; Lavine, Kovacs, & Ornitz, 2008; T. Mammoto & Ingber, 2010; Yamashita et al., 2000) and BMPs (Berge et al., 2008; Evans, 2008; Murry & Keller, 2010; Pandur, 2005; Tirosh-Finkel et al., 2010; Ye et al., 2011).

2.5. MECHANICAL FORCES IN DEVELOPMENT

Fluid forces play a significant role in heart morphogenesis during development. In the embryonic zebrafish heart, shear forces produced from blood flow have been measured between 2.5 dyn/cm^2 at 3.5 days post fertilization (d.p.f) and 75 dyn/cm^2 at 4.5 d.p.f (Hove et al., 2003; Lucitti et al., 2007). In the same study, glass beads were inserted into the heart to block blood flow, ultimately interfering with bulbus formation and proper heart looping. These forces are comparable to *in vitro* data suggesting that forces between 8 and 15 dyn/cm^2 cause cytoskeletal arrangement and increases in cardiovascular gene expression (Davies, Remuzzi, Gordon, Dewey, & Gimbrone, 1986). Similar results were also observed in Myosin Light Chain 2a (*Mlc2a*) null mice, which lack expression of myosin specific to the atrium and have defects in vascular remodeling (Lucitti et al., 2007). In these mice, when erythrocytes were unable to leave blood islands, blood cycling and vessel formation was severely impaired. These findings

provide strong support that mechanical forces play an important role in heart morphogenesis.

2.6. Effect of mechanical stimulation on embryonic stem cells

Upon ESC aggregation into Embryoid Bodies (EBs) following the withdrawal of Leukemia Inhibitory Factor (LIF) in mouse ESCs or basic Fibroblast Growth Factor (bFGF) in human ESCs, cells quickly lose their pluripotent phenotype, which is indicated by the presence of OCT4, NANOG and Stage-Specific Embryonic Antigen-1 (SSEA-1) in mouse ESCs, or SSEA-4, Tra-60 and Tra-81 in human ESCs (Figure 2.2) (Bai et al., 2010; Boheler et al., 2002; J. Cai et al., 2006; Nieden, Cormier, Rancourt, & Kallos, 2007; Xu, Police, Rao, & Carpenter, 2002). Cells start differentiating into three germ layers, marked by the expression of specific gene markers (Figure 2.2) resulting in a dynamic, heterogeneous population of cells. Investigation of pluripotent cell response to mechanical stress can employ various models, two of which will be discussed here: two-dimensional culture on tissue culture plastic, or three-dimensional culture in the form of EBs. These models have been used in studying the effects of cell stress, and also bring to question how the timing of stimulation onset can specify cell fate.

Similar to the developing embryo, ESCs sense environmental changes from mechanical stimulation through mechanosensitive ion channels, integrins and tyrosine kinase receptors (Labouesse, 2011). Current research has observed that the type of stimulation as well as the timing can have very different effects on ESC phenotype. Such

effects include both the maintenance of pluripotency as well as guidance of differentiation (summarized in Figure 2.3).

2.6.1. Guidance of cardiomyocyte differentiation

2.6.1.1. Fluid shear stress

The type of mechanical stress appears to play an important role on the determination of cell fate. This is especially evident by contrasting evidence that mechanical stress, such as shear and cyclic strain, drives pluripotent cell differentiation into various germ lineages. In cell culture, fluid shear stress is defined as the frictional force that is generated by the movement of fluid along a surface (Adamo & García-Cardeña, 2011). The effects of shear stress on stem cell differentiation towards vascular cell types, specifically endothelial cells, has been well-defined (Adamo & García-Cardeña, 2011; Ahsan & Nerem, 2010; Masumura, Yamamoto, Shimizu, Obi, & Ando, 2009; Metallo, Vodyanik, de Pablo, Slukvin, & Palecek, 2008; Nikmanesh, Shi, & Tarbell, 2012; Stolberg & McCloskey, 2009).

There is currently very limited information on how fluid shear can affect cardiomyogenesis *in vitro*, and the majority of these studies focus on mesodermal commitment in mouse ESC models. In one study, mouse ESCs cultured in monolayer in the absence of LIF were exposed to 10 dyn/cm^2 laminar shear stress for different periods of time ranging from 30 minutes to 8 hours (Illi et al., 2005). After 1 hour of exposure, expression of mesodermal and cardiomyocyte markers Vascular Endothelial Growth Factor 2 (VEGFR-2) and Myocyte Enhancer Factor 2c (*Mef2c*), respectively, were

increased, indicating the potential of shear stress to influence cardiomyogenesis; however, assessment of the functional characteristics of these cardiomyocytes was not performed. In a more recent study, mouse ESCs in monolayer exposed to longer durations of shear (4 days at 5 dyn/cm^2) expressed nearly 2-fold higher levels of mesodermal marker *T* (Wolfe, Leleux, Nerem, & Ahsan, 2012). Thus under the appropriate conditions, shear stress has the potential to drive mesodermal commitment in ESCs; however, clarification of how mesodermal commitment translates to cardiomyogenesis is necessary.

2.6.1.2. Cyclic strain

Similar to fluid shear forces, cyclic strain and stretch have been shown to rearrange the actin cytoskeleton.(Zhao et al., 1995) Cyclic stress is exerted upon cells using devices such as Flexercell strain units, which are flexible plates that promote cell elongation once deformed (Offenberg Sweeney et al., 2004; Riha et al., 2007). The current challenge for optimizing cyclic strain systems is to address the following parameters: (1) magnitude of strain, (2) timing of strain initiation, and (3) duration of strain.

The concept of using cyclic strain to induce differentiation is based on the biological function of cardiomyocytes. Cell stretching promotes elongation of the cell membrane and orientation of actin filaments, which facilitates the connections made between cells that are necessary to promote intracellular communication (Salameh et al., 2010). Cells near vasculature *in vivo* experience approximately 1 Hz of cyclic strain due

to pulsatile blood flow (Keung, Healy, Kumar, & Schaffer, 2009). The optimal amount and rate of strain for *in vitro* culture was contributed in part by a study performed by Schmelter *et al* (2006), in which Day 4 mouse EBs were attached to Flexercell plates and exposed to 5, 10 or 20% strain (Schmelter, Ateghang, Helmig, Wartenberg, & Sauer, 2006). In this study, application of 10% strain significantly increased the generation of reactive oxygen species (ROS) as well as beating areas within EBs.

2.6.1.2.1. Cyclic strain in monolayer culture

Cyclic strain has been shown to downregulate gene and protein expression associated with the maintenance of pluripotency in monolayer culture. In one of such studies, mouse ESCs monolayers were exposed to 10% cyclic stretch at 0.17Hz showed significant decreases in *Nanog* as well as increases in markers associated with endoderm after 2 days of exposure (Horiuchi, Akimoto, Hong, & Ushida, 2012). On the other hand, cyclic strain has also been observed to maintain pluripotency in human ESCs. In one study, 10% strain at 30 cycles per minute was applied to human ESCs in monolayer culture for 2 days. This regimen yielded a higher percentage of SSEA-4+ cells (85%), and was reversed to 36% SSEA-4+ when the strain was reduced to 8% at 10 cycles/min (Saha, Ji, de Pablo, & Palecek, 2006). The same group later reported that when 10% strain is applied to Day 1 human ESCs for 7-12 days, 67% of the cell population is OCT-4+, compared to 21% in cells cultured in the absence of strain (Saha, Ji, de Pablo, & Palecek, 2008). Alternatively, shorter periods of strain at Day 1 can promote differentiation. In a recent study, a loss in pluripotency marker expression was observed

in human iPSCs following a stretch regimen of 12 cycles per minute for 12 hours at 15% strain (Teramura et al., 2012). The latter was concurrent with inhibition of the Protein Kinase B (Akt/PKB) signaling cascade and activation of Rho-associated Protein Kinase (Rho/ROCK). These results suggest that extended cyclic strain can maintain pluripotency; however, short applications of higher magnitude strain can reverse this phenotype.

2.6.1.2.2. Cyclic strain in Embryoid Body culture

While the microenvironment for EBs is more complex than plated ESCs, cell differentiation is similarly influenced by strain. In these mechanical strain systems, mouse ESCs are allowed to aggregate into EBs and subsequently attached onto culture plates. In general, the timing of stimulation can have different effects on differentiation. In a microfluidic system, Day 9 mouse EBs were exposed to 24 hours of 10% strain at 1 Hz (Wan, Chung, & Kamm, 2011). Results demonstrated that α-MHC, a marker for cardiomyogenesis, was significantly decreased in Day 9 EBs exposed to strain, suggesting that stimulation regimens can potentially interfere with cardiomyocyte differentiation at later timepoints. Day 6 mouse EBs exposed to 5-10% cyclic uniaxial stretch at 1 Hz, on the other hand, have significantly increased expression of cardiomyocyte markers Connexin 43 (CX43) and NKX2.5 (Heo & Lee, 2011). Finally, Day 4 human (Tulloch et al., 2011) and mouse EBs (Gwak et al., 2008) exposed to 2-4 days of 5-10% strain have displayed increased cardiomyocyte gene expression (cardiac *α-MHC*, *Gata-4* and *Nkx2.5*) compared to static controls. Together, these results suggest

that in both mouse and human ESCs, earlier EB exposure to cyclic strain is beneficial for differentiation into cardiomyocyte phenotypes, while early and prolonged exposure to strain promotes pluripotency.

2.6.1.3. Magnetically mediated strain

While fluid shear and cyclic strain are the most common forms of mechanical strain, recent data suggests that magnetically mediated strain can also direct cell fate. Early studies investigating the cellular effects of this type of strain have employed Arginine-Glycine-Aspartic Acid (RGD)-conjugated magnetic beads. RGD is a cell binding sequence in fibronectin which has known interactions with β1 integrin (Meyer et al., 2000). When cells are bound to the RGD-magnetic beads, they can be displaced with magnets, producing a mechanical stress. This method was first employed to study signaling pathways involved in mechanotransduction (Laboureau, Dubertret, Lebreton-De Coster, & Coulomb, 2004; Plopper & Ingber, 1993; N. Wang, Butler, & Ingber, 1993).

Magnetically mediated strain was first developed by Wang *et al*, in which RGD-beads were attached to plated endothelial cells (N. Wang et al., 1993). Exposing the beads to a magnetic field imposed a 90° twist, equivalent to a shear stress of 0 to 68 dyn/cm^2 on the cell surface receptors. Manipulating integrins using this controlled stress increased expression of cytoskeletal proteins including talin and α-actinin, which are important proteins in contractile activity (Plopper & Ingber, 1993; N. Wang et al., 1993).

This study provided a foundation for future work to better understand the effects of controlled mechanical stress on cells using magnets.

The Magnetic Twisting Cytometry technique was built upon the technology used by Wang *et al*, allowing for more precise control of mechanical stress. Developed initially to study the effects of integrin twisting on endothelial cells (J. Chen, Fabry, Schiffrin, & Wang, 2001), this method has also been used to apply controlled stress to mouse ESCs. Following exposure to a twisting torque of 17.5 Pa at 0.3Hz, cells express significantly lower levels of OCT-4 over time compared to unstressed controls (Uda et al., 2011). While these studies have mostly focused on pluripotency, future work will need to specifically examine lineage commitment, and if this type of mechanical stress can positively influence cardiomyocyte differentiation.

2.7. CELL RESPONSE TO MECHANICAL STRESS

The mechanism for how stem cells translate external forces to the direction of cell fate is still under investigation. The effect of shear stress has been the most reviewed and studied to date (A. Mammoto, Mammoto, & Ingber, 2012; Stolberg & McCloskey, 2009). Extracellular matrix proteins can function as mediators between environmental forces and outside-in signaling. Heparin sulfate proteoglycans (HSPGs) have been observed to play such a role in ESCs (Gasimli, Linhardt, & Dordick, 2012; Stolberg & McCloskey, 2009). These adhesion-dependent proteins mediate the effects of multiple proteins, such as Fibroblast Growth Factor (FGF) (Toh & Voldman, 2011), Vascular Endothelial Growth Factor (VEGF) (Dias et al., 2012), and BMPs (Khan, Nelson, Pan,

Gaffney, & Gupta, 2008). The importance of HSPGs in regards to mouse ESCs' response to stress has recently been investigated (Toh & Voldman, 2011). Mouse ESCs exposed to shear stress at 1 dyn/cm^2 for 72 hours significantly decreased markers *Oct4* and *Nanog*, as well as decreasing proliferation, which is a hallmark of differentiation. These results were abrogated upon the addition of sodium chlorate, which inhibits proteoglycan sulfation, indicating the importance of ECM proteins for propagating external signals.

Expressed integrin types change during the course of development and can be specific to the differentiated cell type. During the earliest stages of development, integrin subunits α5 and αv bind to laminin and fibronectin (Hayashi et al., 2007). These subunits, along with β1 and β5, are important in ESC self-renewal and maintaining the pluripotent phenotype (Kalaskar, Downes, Murray, Edgar, & Williams, 2013; S. T. Lee et al., 2012; Rowland et al., 2010). As cells differentiate, the integrin profile changes, and consequently the cell's response to extracellular force changes. The differences in profiles have been well reviewed (Prowse, Chong, Gray, & Munro, 2011), especially in human ESCs. In recent work by Singh *et al*, hiPSCs were observed to have high levels of α6β1 integrin, with changes in adhesive properties over the course of differentiation (Singh et al., 2013). Response to mechanical stresses can therefore potentially be tailored to drive differentiation towards a desired cell type.

Redox signaling has also been observed in cells following mechanical stimulation. In this pathway, ROS, including superoxide anion radicals, hydroxyl radicals, and hydrogen peroxide, are generated by the membrane-bound enzyme complexes nicotinamide adenine dinucleotide phosphate-oxidase (NADPH oxidases)

(Son et al., 2011). The extent of radical production can have different effects on the cell. While higher concentrations of ROS can be toxic and lead to cell death, lower, localized levels can lead to cell differentiation or induce other signaling pathways. Both differentiated (Brewer & Shah, 2009; Lehoux, 2006; Offenberg Sweeney et al., 2004) and pluripotent (Bartsch et al., 2011; Buggisch et al., 2007; Sauer & Wartenberg, 2005) cells have been observed to generate ROS in response to shear or cyclic strain.

Mouse ESCs exposed to mechanical stress, especially cyclic strain, have been observed to produce ROS during cardiomyogenesis (Heo & Lee, 2011; Sauer & Wartenberg, 2005; Sauer, Rahimi, Hescheler, & Wartenberg, 2000; Schmelter et al., 2006); however, the exact mechanisms for how integrin-induced ROS production guides differentiation is still being elucidated. Using an EB model, Schmelter *et al* observed that 10% strain increased NADPH oxidase expression (Nox-4 and Nox-1) as well as cytosolic components p22phox, p47phox and p67phox (Schmelter et al., 2006). In the same study, ROS induced ERK1/2, JNK and p38 phosphorylation and subsequently *Mef2c* and *Gata4* gene expression in Day 4 EBs. In magnetic twisting studies, cyclic AMP (cAMP) and Extracellular-Signal-Regulated kinase (ERK) have also been increased by integrin-mediated cell stress (Chowdhury et al., 2009; Meyer et al., 2000); however, the effect of cAMP upregulation by magnetic mediated strain has not yet been assessed in ESCs. Heo *et al* also observed increases in DCF (5-(and-6)-chloromethyl-2',7'-dichlorodihydrofluorescein) fluorescence, a fluorescent marker for ROS, in the presence of strain, as well as CX43 and NKX 2.5 expression (Heo & Lee, 2011). Gene expression and ROS was decreased in the presence of ROS inhibitor, Vitamin C. Mechanical strain

also activated the Phosphatidylinositol 3-kinase (PI3k/Akt) signaling pathway and β-catenin translocation into the nucleus. These pathways have also been implicated in other stimulation regimens, such as electrical stimulation, to promote cardiomyocyte differentiation from pluripotent cells (Serena et al., 2009).

While various signaling pathway components have been observed to be involved in a mechanical pathway response, exactly how integrins mediate transduction of mechanical stimuli to activation of cardiomyogenesis is more complicated. Possible mechanisms for these responses are summarized in Figure 2.4. Combined results indicate that integrins are likely activating ROS production by NADPH oxidases, which subsequently activates the ERK and/or PI3k/Akt pathways to decrease *Nanog* and increase cardiomyocyte-specific markers (Hayashi et al., 2007; Heo & Lee, 2011). Recently, another group compared mouse ESC response to mechanical strain in the presence of LIF. They observed that *Nanog* expression decreased when ESCs were strained in the absence of LIF; however, with LIF supplementation, *Nanog* expression was maintained. The latter traditionally occurs via activation of the JAK/STAT and PI3k/Akt pathway (Burdon, Smith, & Savatier, 2002; Watanabe et al., 2006). While perhaps appearing to be in conflict, these results may support the theory that ERK can destabilize the PI3k/Akt pathway in ESCs during mechanical strain-induced differentiation (Lanner & Rossant, 2010; Patwari & Lee, 2008).

2.8. Effect of biomaterials on maturation of embryonic stem cell-derived cardiomyocytes

While deriving cardiomyocytes from ESCs addresses part of the bottleneck of cellular cardiomyoplasty, there is still debate over whether these cells are truly mature, differentiated cardiomyocytes that can restore damaged myocardium *in vivo*. While there are resemblances between ESC-CM and mature cardiomyocytes, such as contractile activity and expression of markers such as CX 43, sarcomeric α-actin and cardiac troponin, there are still distinct functional differences. Morphologically, adult cardiomyocytes have aligned sarcomeres, multiple nuclei (Robertson, Tran, & George, 2013), generally lack spontaneous contractile activity (Bistola et al., 2008), and only renew at a rate of 1% per year after age 25 (Bergmann et al., 2009). In contrast, ESC-CM are mononucleated, have fewer aligned sarcomeres, and have higher proliferation rates (Robertson et al., 2013).

In addition to mechanical stress, ESC-CM culture on biomaterials has also been observed to promote maturity towards adult cardiomyocyte phenotypes. Often, these materials mimic mechanical or biological properties that are present in the myocardium. Material stiffness is one of such properties, such that immature neonatal cardiomyocytes are more likely to adapt functional mature cardiomyocyte properties, such as sarcomeric α-actin alignment and spontaneous contractions, when cultured on materials with elastic moduli ranging from 1-11 kPa (Engler et al., 2008; Engler, Sen, Sweeney, & Discher, 2006). Similar observations have also been made for ESC differentiation: mesodermal commitment is enhanced when hESCs are cultured on synthetic materials (poly(lactic-co-

glycolic acid)/poly-l-lactic acid) with high elastic moduli ranging from 1.5-6 MPa (Zoldan et al., 2011).

Along with stiffness, the design of the scaffold can also influence ESC-CM maturity. Both porosity and anisotropic configurations can promote the formation of cell-cell connections and alignment, which is critical for electrical pacing *in vitro* and *in vivo* (Black, Meyers, Weinbaum, Shvelidze, & Tranquillo, 2009; Dar, Shachar, Leor, & Cohen, 2002; Gonnerman, Kelkhoff, McGregor, & Harley, 2012; A. W. Smith et al., 2012). In addition, matrix remodeling is also an important consideration when choosing a material: a balance between degradation rate and matrix deposition by the transplanted cells is also important (Luong & Gerecht, 2008).

A variety of materials, both synthetic and natural, have been examined for their potential in cardiac tissue engineering. For the former, poly(glycerol) sebacate polymers with micropatterned grooves were observed to promote neonatal cardiomyocyte actin alignment and contractile activity (Neal et al., 2013). Scaffolds containing naturally derived polymers, such as fibrinogen, are also popular for their biocompatibility. Further cross-linking fibrinogen with PEG, producing a PEGylated fibrin gels, can further enhance stability *in vitro* and *in vivo* (Drinnan, Zhang, Alexander, Pulido, & Suggs, 2010; G. Zhang, Wang, Wang, Zhang, & Suggs, 2006). Encapsulation of neonatal cardiomyocytes in 6 mg/ml PEGylated fibrin gels with a shear modulus of approximately 8 Pa promotes contractile activity compared to stiffer PEGylated fibrin gels (Shapira-Schweitzer & Seliktar, 2007; Shapira-Schweitzer, Habib, Gepstein, & Seliktar, 2009). Chitosan, which is a derivative of chitin with controllable degradation products, in

combination with fibrinogen, promotes improved neonatal cardiomyocyte contractility (Blan & Birla, 2008).

Finally, matrices can enhance cell retention in the myocardium to further promote regeneration and coupling of transplanted cells with the host tissue. By embedding myoblasts within injectable fibrin gels, cells can still be detected in the infarct 24 hours following transplantation, subsequently decreases the size of the infarct and restoring function (Christman et al., 2004; Ginis et al., 2004; Li & Gao, 2007). Therefore, the "gold-standard" of materials for cardiac tissue engineering must balance all of the aforementioned parameters to adequately restore myocardial function.

Table 2.1: Types of Myocardial Infarction and Current Treatment Strategies. (Tehrani & Seto, 2013; Thygesen, Alpert, Jaffe, Simoons, Chaitman, White, Joint ESC/ACCF/AHA/WHF Task Force for the Universal Definition of Myocardial Infarction, et al., 2012a)

Type of Myocardial Infarction (MI)	**Cause**	**Treatment**
Type 1: Spontaneous	Artherosclerotic coronary artery disease	Antithrombotic drugs, revascularization
Type 2: Due to ischemic imbalance	Supply-demand imbalance in myocardial perfusion	Blood vessel support or control; control of tachyarrhythmia; volume resuscitation
Type 3: Sudden cardiac death from MI	Death prior to biomarker assessment; have symptoms suggesting MI, electrocardiographic changes	
Type 4a: Due to percutaneous coronary intervention **Type 4b: Due to stent thrombosis** **Type 4c: Due to restenosis**	Must also have other symptoms associated with MI	Surgical intervention
Type 5: After coronary artery bypass grafting	Must also have other symptoms associated with MI	Surgical intervention

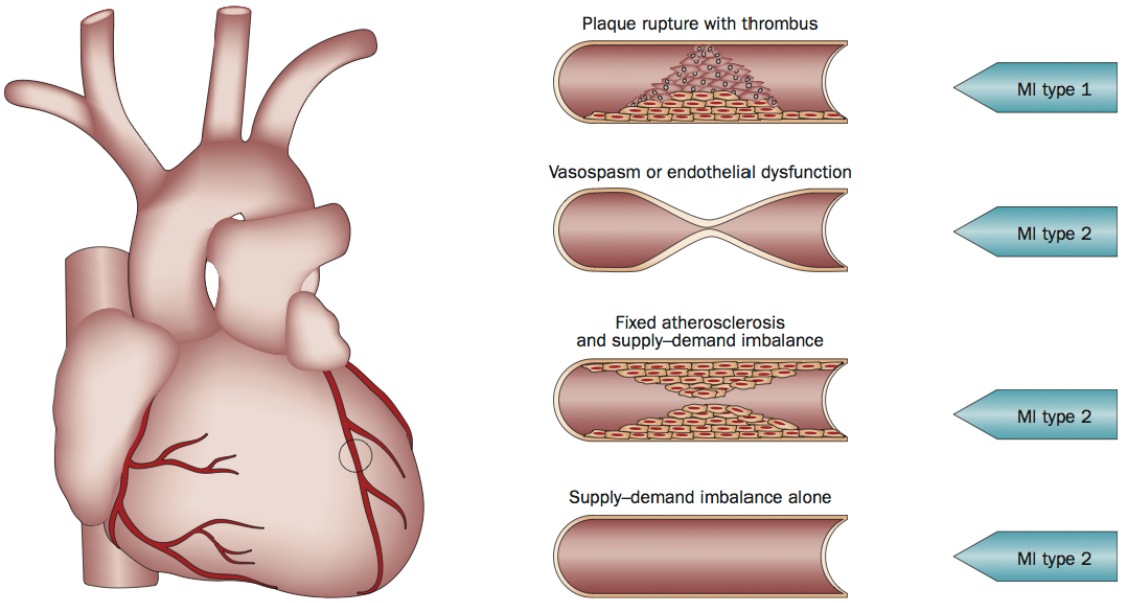

Figure 2.1. Differentiation between MI Types 1 and 2 according to the condition of the coronary artery. Reprinted with permissions from Thygesen et al, 2012 (Thygesen, Alpert, Jaffe, Simoons, Chaitman, White, Katus, et al., 2012b).

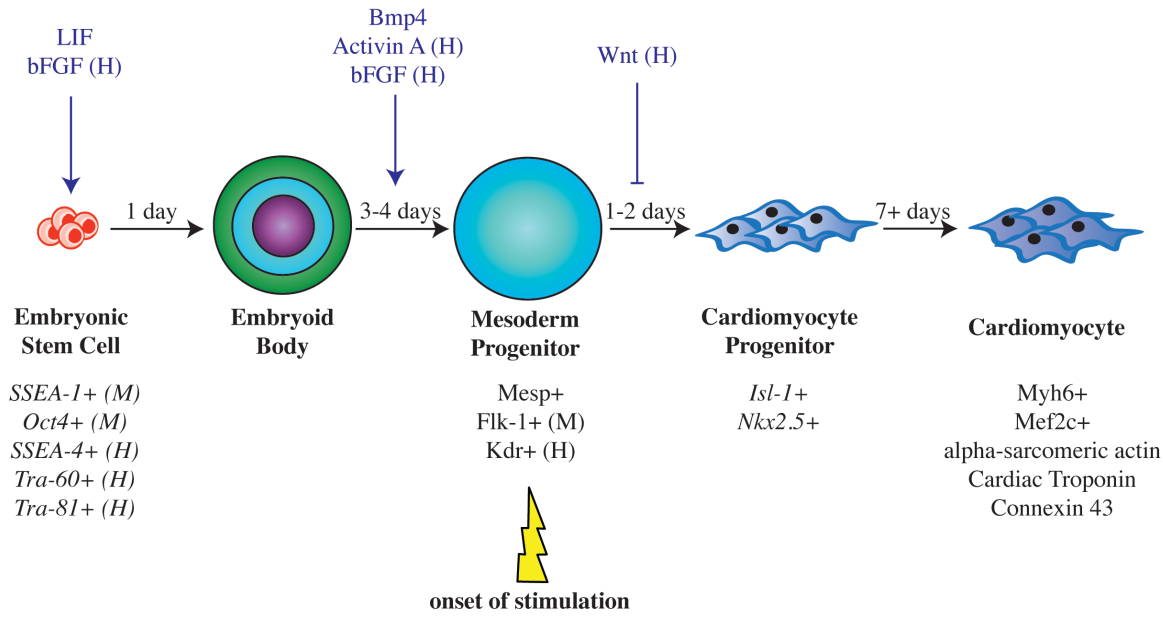

Figure 2.2: Stepwise commitment of Human and Mouse Embryonic Stem Cells using Biochemical and Mechanical Cues. In the absence of LIF, ESCs aggregate to form a triploblastic Embryoid Body (EB). To commit a higher percentage of cells toward mesoderm, a combination of BMP4 and Activin A is added to the medium. Inhibition of Wnt in mesodermal progenitor cells is also necessary to guide mesoderm progenitors specifically into cardiomyocytes (Nieden et al., 2007). Mechanical stimulation such as fluid shear or cyclic stress is typically initiated in Day 4-6 EBs, with a higher population of mesodermal progenitors. Gene (italics) and protein markers expressed in human (H) and mouse (M) pluripotent cells at the specific stages are indicated.

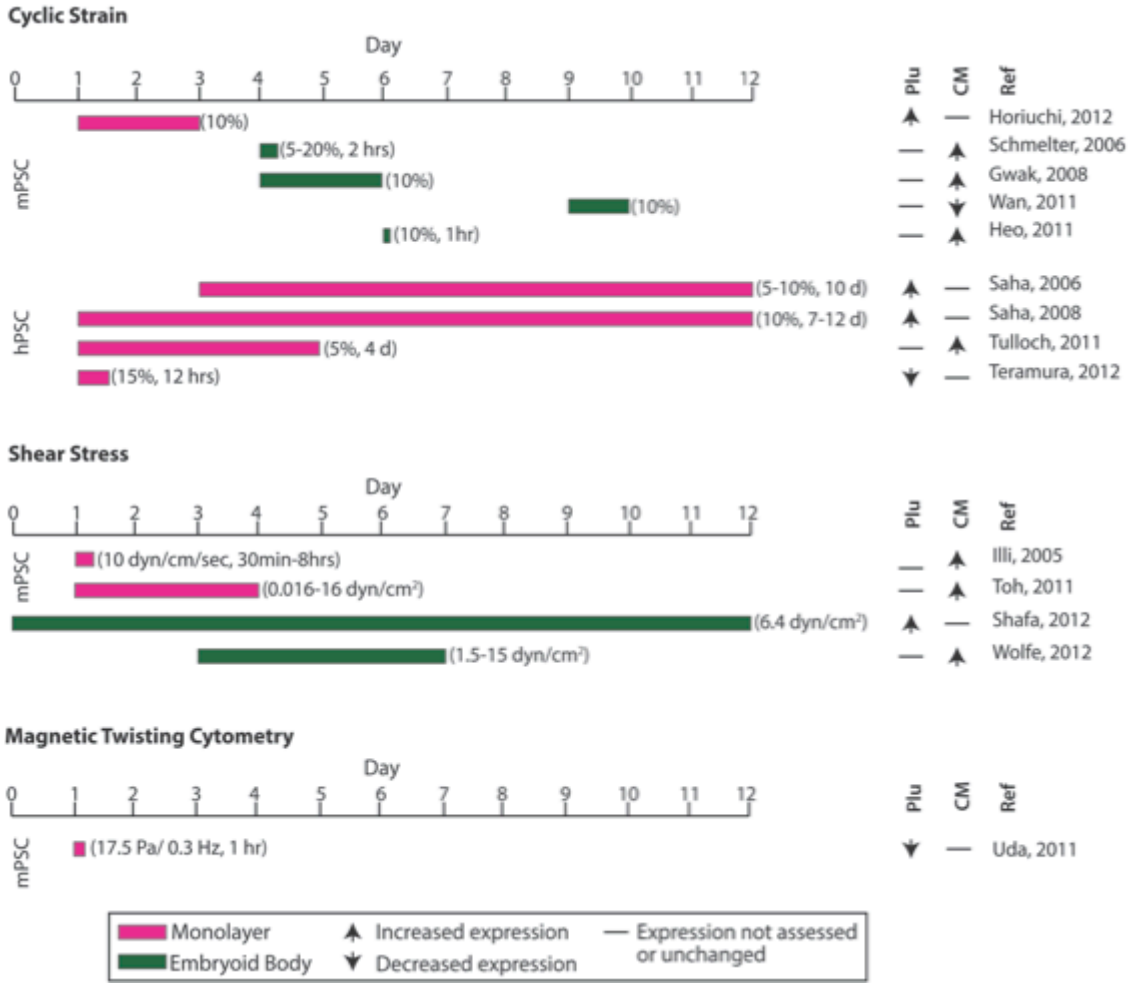

Figure 2.3: Summary of the effects of mechanical stimulation on Pluripotent Stem Cell differentiation towards cardiomyocytes. Boxes indicate the initiation and duration of stimulation, followed by the magnitude of stain for murine pluripotent stem cells (mPSC) and human pluripotent stem cells (hPSC). Arrows depict the observed increases or decreases in markers associated with pluripotency (Plu) or cardiomyocytes (CM). Ref: References.

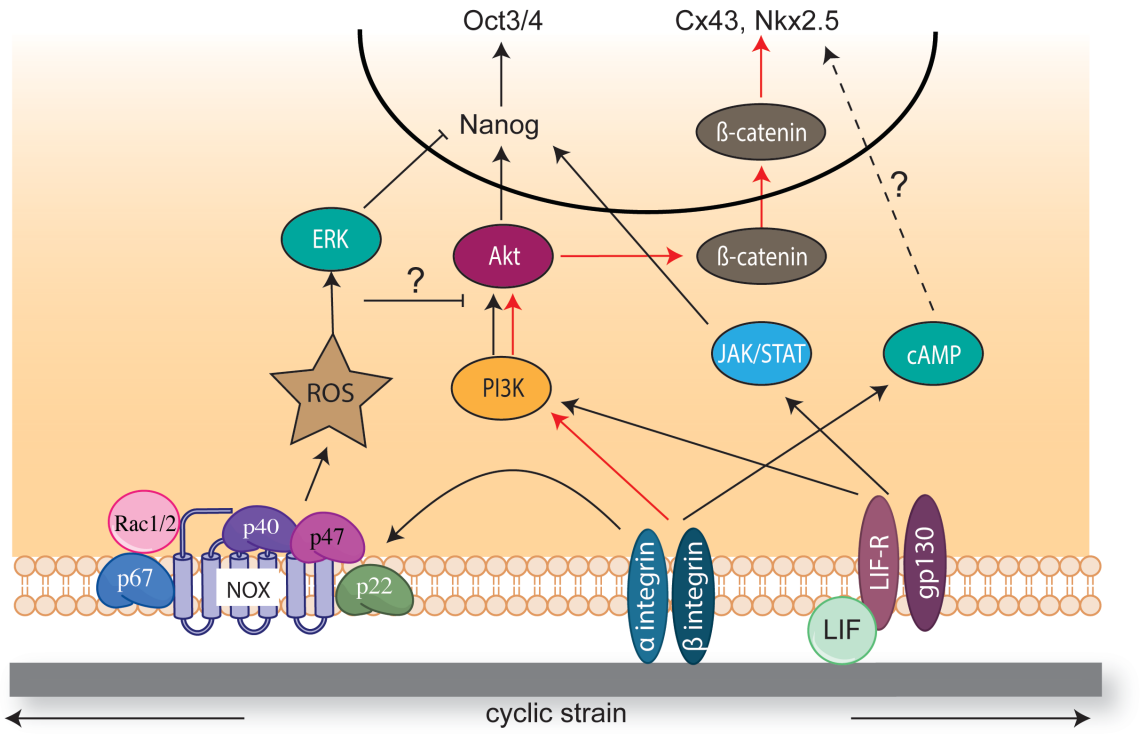

Figure 2.4: Signaling pathways involved in propagation of mechanical signals from cyclic stress. Application of stress deforms integrins on the cell surface, which have been shown to increase Reactive Oxygen Species (ROS) production by NADPH oxidase. ROS increases ERK phosphorylation, which inhibits pluripotency gene expression. Similarly, stress activates the PI3k/Akt pathway and translocation of β-catenin into the nucleus, which activates cardiomyocyte gene expression. While integrin activation can also increase cAMP expression, its function in ESCs has not been assessed. Given the known importance of PI3k/Akt in maintaining pluripotency, it is possible that ROS production can inhibit traditional Nanog activation to drive differentiation.

2.9. REFERENCES

Adamo, L., & García-Cardeña, G. (2011). Directed stem cell differentiation by fluid mechanical forces. *Antioxidants & Redox Signaling*, *15*(5), 1463–1473. doi:10.1089/ars.2011.3907

Ahsan, T., & Nerem, R. M. (2010). Fluid shear stress promotes an endothelial-like phenotype during the early differentiation of embryonic stem cells. *Tissue Engineering Part A*, *16*(11), 3547–3553. doi:10.1089/ten.TEA.2010.0014

Alexander, J. M., & Bruneau, B. G. (2010). Lessons for cardiac regeneration and repair through development. *Trends in Molecular Medicine*, *16*(9), 426–434. doi:10.1016/j.molmed.2010.06.003

Astorga, J., & Carlsson, P. (2007). Hedgehog induction of murine vasculogenesis is mediated by Foxf1 and Bmp4. *Development*, *134*(20), 3753–3761. doi:10.1242/dev.004432

Bai, H., Gao, Y., Arzigian, M., Wojchowski, D. M., Wu, W.-S., & Wang, Z. Z. (2010). BMP4 regulates vascular progenitor development in human embryonic stem cells through a Smad-dependent pathway. *Journal of Cellular Biochemistry*, *109*(2), 363–374. doi:10.1002/jcb.22410

Bartsch, C., Bekhite, M. M., Wolheim, A., Richter, M., Ruhe, C., Wissuwa, B., et al. (2011). NADPH oxidase and eNOS control cardiomyogenesis in mouse embryonic stem cells on ascorbic acid treatment. *Free Radical Biology & Medicine*, *51*(2), 432–443. doi:10.1016/j.freeradbiomed.2011.04.029

Berge, ten, D., Koole, W., Fuerer, C., Fish, M., Eroglu, E., & Nusse, R. (2008). Wnt signaling mediates self-organization and axis formation in embryoid bodies. *Cell Stem Cell*, *3*(5), 508–518. doi:10.1016/j.stem.2008.09.013

Bergmann, O., Bhardwaj, R. D., Bernard, S., Zdunek, S., Barnabe-Heider, F., Walsh, S., et al. (2009). Evidence for Cardiomyocyte Renewal in Humans. *Science (New York, N.Y.)*, *324*(5923), 98–102. doi:10.1126/science.1164680

Berry, M. F., Engler, A. J., Woo, Y. J., Pirolli, T. J., Bish, L. T., Jayasankar, V., et al. (2006). Mesenchymal stem cell injection after myocardial infarction improves myocardial compliance. *American Journal of Physiology Heart and Circulatory Physiology*, *290*(6), H2196–203. doi:10.1152/ajpheart.01017.2005

Bistola, V., Nikolopoulou, M., Derventzi, A., Kataki, A., Sfyras, N., Nikou, N., et al. (2008). Long-term primary cultures of human adult atrial cardiac myocytes: Cell

viability, structural properties and BNP secretion in vitro. *International Journal of Cardiology*, *131*(1), 113–122. doi:10.1016/j.ijcard.2007.10.058

Black, L. D., Meyers, J. D., Weinbaum, J. S., Shvelidze, Y. A., & Tranquillo, R. T. (2009). Cell-induced alignment augments twitch force in fibrin gel-based engineered myocardium via gap junction modification. *Tissue Engineering Part A*, *15*(10), 3099–3108. doi:10.1089/ten.TEA.2008.0502

Blan, N. R., & Birla, R. K. (2008). Design and fabrication of heart muscle using scaffold-based tissue engineering. *Journal of Biomedical Materials Research Part A*, *86A*(1), 195–208. doi:10.1002/jbm.a.31642

Boheler, K. R., Czyz, J., Tweedie, D., Yang, H.-T., Anisimov, S. V., & Wobus, A. M. (2002). Differentiation of pluripotent embryonic stem cells into cardiomyocytes. *Circulation Research*, *91*(3), 189–201.

Brewer, A. C., & Shah, A. M. (2009). Redox signalling and miRNA function in cardiomyocytes. *Journal of Molecular and Cellular Cardiology*, *47*(1), 2–4. doi:10.1016/j.yjmcc.2009.02.024

Buggisch, M., Ateghang, B., Ruhe, C., Strobel, C., Lange, S., Wartenberg, M., & Sauer, H. (2007). Stimulation of ES-cell-derived cardiomyogenesis and neonatal cardiac cell proliferation by reactive oxygen species and NADPH oxidase. *Journal of Cell Science*, *120*(Pt 5), 885–894. doi:10.1242/jcs.03386

Burdon, T., Smith, A., & Savatier, P. (2002). Signalling, cell cycle and pluripotency in embryonic stem cells. *Trends in Cell Biology*, *12*(9), 432–438.

Byrd, N., Becker, S., Maye, P., Narasimhaiah, R., St-Jacques, B., Zhang, X., et al. (2002). Hedgehog is required for murine yolk sac angiogenesis. *Development*, *129*(2), 361–372.

Cai, J., Chen, J., Liu, Y., Miura, T., Luo, Y., Loring, J. F., et al. (2006). Assessing self-renewal and differentiation in human embryonic stem cell lines. *Stem Cells*, *24*(3), 516–530. doi:10.1634/stemcells.2005-0143

Chen, J., Fabry, B., Schiffrin, E. L., & Wang, N. (2001). Twisting integrin receptors increases endothelin-1 gene expression in endothelial cells. *American Journal of Physiology-Cell Physiology*, *280*(6), C1475–84.

Chen, M., Lin, Y.-Q., Xie, S.-L., Wu, H.-F., & Wang, J.-F. (2011). Enrichment of cardiac differentiation of mouse embryonic stem cells by optimizing the hanging drop method. *Biotechnology Letters*, *33*(4), 853–858. doi:10.1007/s10529-010-0494-3

Chowdhury, F., Na, S., Li, D., Poh, Y.-C., Tanaka, T. S., Wang, F., & Wang, N. (2009). Material properties of the cell dictate stress-induced spreading and differentiation in embryonic stem cells. *Nature Materials*, *9*(1), 82–88. doi:10.1038/nmat2563

Christman, K. L., Vardanian, A. J., Fang, Q., Sievers, R. E., Fok, H. H., & Lee, R. J. (2004). Injectable fibrin scaffold improves cell transplant survival, reduces infarct expansion, and induces neovasculature formation in ischemic myocardium. *Journal of the American College of Cardiology*, *44*(3), 654–660. doi:10.1016/j.jacc.2004.04.040

Claycomb, W., Lanson, N., Stallworth, B., Egeland, D., Delcarpio, J., Bahinski, A., & Izzo, N. (1998). HL-1 cells: A cardiac muscle cell line that contracts and retains phenotypic characteristics of the adult cardiomyocyte. *Proceedings of the National Academy of Sciences of the United States of America*, *95*(6), 2979–2984.

Dar, A., Shachar, M., Leor, J., & Cohen, S. (2002). Cardiac tissue engineering - Optimization of cardiac cell seeding and distribution in 3D porous alginate scaffolds. *Biotechnology and Bioengineering*, *80*(3), 305–312. doi:10.1002/bit.10372

Davies, P. F., Remuzzi, A., Gordon, E. J., Dewey, C. F., & Gimbrone, M. A. (1986). Turbulent fluid shear stress induces vascular endothelial cell turnover in vitro. *Proceedings of the National Academy of Sciences of the United States of America*, *83*(7), 2114–2117.

Dias, J. V., Benslimane-Ahmim, Z., Egot, M., Lokajczyk, A., Grelac, F., Galy-Fauroux, I., et al. (2012). A motif within the N-terminal domain of TSP-1 specifically promotes the proangiogenic activity of endothelial colony-forming cells. *Biochemical Pharmacology*, *84*(8), 1014–1023. doi:10.1016/j.bcp.2012.07.006

Drinnan, C. T., Zhang, G., Alexander, M. A., Pulido, A. S., & Suggs, L. J. (2010). Multimodal release of transforming growth factor-β1 and the BB isoform of platelet derived growth factor from PEGylated fibrin gels. *Journal of Controlled Release : Official Journal of the Controlled Release Society*, *147*(2), 180–186. doi:10.1016/j.jconrel.2010.03.026

Duranteau, J. (1998). Intracellular Signaling by Reactive Oxygen Species during Hypoxia in Cardiomyocytes. *Journal of Biological Chemistry*, *273*(19), 11619–11624. doi:10.1074/jbc.273.19.11619

Engler, A. J., Carag-Krieger, C., Johnson, C. P., Raab, M., Tang, H.-Y., Speicher, D. W., et al. (2008). Embryonic cardiomyocytes beat best on a matrix with heart-like elasticity: scar-like rigidity inhibits beating. *Journal of Cell Science*, *121*(Pt 22),

3794–3802. doi:10.1242/jcs.029678

Engler, A. J., Sen, S., Sweeney, H. L., & Discher, D. E. (2006). Matrix elasticity directs stem cell lineage specification. *Cell*, *126*(4), 677–689. doi:10.1016/j.cell.2006.06.044

Evans, T. (2008). Embryonic Stem Cells as a Model for Cardiac Development and Disease. *Drug Discovery Today Disease Models*, *5*(3), 147–155. doi:10.1016/j.ddmod.2009.03.004

Gasimli, L., Linhardt, R. J., & Dordick, J. S. (2012). Proteoglycans in stem cells. *Biotechnology and Applied Biochemistry*, *59*(2), 65–76. doi:10.1002/bab.1002

Ginis, I., Luo, Y., Miura, T., Thies, S., Brandenberger, R., Gerecht-Nir, S., et al. (2004). Differences between human and mouse embryonic stem cells. *Developmental Biology*, *269*(2), 360–380. doi:10.1016/j.ydbio.2003.12.034

Gonnerman, E. A., Kelkhoff, D. O., McGregor, L. M., & Harley, B. A. C. (2012). The promotion of HL-1 cardiomyocyte beating using anisotropic collagen-GAG scaffolds. *Biomaterials*, *33*(34), 8812–8821. doi:10.1016/j.biomaterials.2012.08.051

Gwak, S.-J., Bhang, S. H., Kim, I.-K., Kim, S.-S., Cho, S.-W., Jeon, O., et al. (2008). The effect of cyclic strain on embryonic stem cell-derived cardiomyocytes. *Biomaterials*, *29*(7), 844–856. doi:10.1016/j.biomaterials.2007.10.050

Harvey, R. P. (2002). Patterning the vertebrate heart. *Nature Reviews Genetics*, *3*(7), 544–556. doi:10.1038/nrg843

Hayashi, Y., Furue, M. K., Okamoto, T., Ohnuma, K., Myoishi, Y., Fukuhara, Y., et al. (2007). Integrins regulate mouse embryonic stem cell self-renewal. *Stem Cells*, *25*(12), 3005–3015. doi:10.1634/stemcells.2007-0103

Heo, J. S., & Lee, J.-C. (2011). β-catenin mediates cyclic strain-stimulated cardiomyogenesis in mouse embryonic stem cells through ROS-dependent and integrin-mediated PI3K/Akt pathways. *Journal of Cellular Biochemistry*, *112*(7), 1880–1889. doi:10.1002/jcb.23108

Holtzinger, A., Rosenfeld, G. E., & Evans, T. (2010). Gata4 directs development of cardiac-inducing endoderm from ES cells. *Developmental Biology*, *337*(1), 63–73. doi:10.1016/j.ydbio.2009.10.003

Horiuchi, R., Akimoto, T., Hong, Z., & Ushida, T. (2012). Cyclic mechanical strain maintains Nanog expression through PI3K/Akt signaling in mouse embryonic stem cells. *Experimental Cell Research*. doi:10.1016/j.yexcr.2012.05.021

Hove, J. R., Köster, R. W., Forouhar, A. S., Acevedo-Bolton, G., Fraser, S. E., & Gharib, M. (2003). Intracardiac fluid forces are an essential epigenetic factor for embryonic cardiogenesis. *Nature*, *421*(6919), 172–177. doi:10.1038/nature01282

Illi, B., Scopece, A., Nanni, S., Farsetti, A., Morgante, L., Biglioli, P., et al. (2005). Epigenetic histone modification and cardiovascular lineage programming in mouse embryonic stem cells exposed to laminar shear stress. *Circulation Research*, *96*(5), 501–508. doi:10.1161/01.RES.0000159181.06379.63

Kalaskar, D. M., Downes, J. E., Murray, P., Edgar, D. H., & Williams, R. L. (2013). Characterization of the interface between adsorbed fibronectin and human embryonic stem cells. *Journal of the Royal Society, Interface / the Royal Society*, *10*(83), 20130139. doi:10.1098/rsif.2013.0139

Keung, A. J., Healy, K. E., Kumar, S., & Schaffer, D. V. (2009). Biophysics and dynamics of natural and engineered stem cell microenvironments. *Wiley Interdisciplinary Reviews. Systems Biology and Medicine*, *2*(1), 49–64. doi:10.1002/wsbm.46

Khan, S. A., Nelson, M. S., Pan, C., Gaffney, P. M., & Gupta, P. (2008). Endogenous heparan sulfate and heparin modulate bone morphogenetic protein-4 signaling and activity. *American Journal of Physiology-Cell Physiology*, *294*(6), C1387–97. doi:10.1152/ajpcell.00346.2007

Kolossov, E., Bostani, T., Roell, W., Breitbach, M., Pillekamp, F., Nygren, J. M., et al. (2006). Engraftment of engineered ES cell-derived cardiomyocytes but not BM cells restores contractile function to the infarcted myocardium. *The Journal of Experimental Medicine*, *203*(10), 2315–2327. doi:10.1084/jem.20061469

Kumar, D., Kamp, T. J., & LeWinter, M. M. (2005). Embryonic stem cells: differentiation into cardiomyocytes and potential for heart repair and regeneration. *Coronary Artery Disease*, *16*(2), 111–116.

Labouesse, M. (2011). *Forces and Tension in Development*. Academic Press. doi:10.1016/B978-0-12-385065-2.00008-6

Laboureau, J., Dubertret, L., Lebreton-De Coster, C., & Coulomb, B. (2004). ERK activation by mechanical strain is regulated by the small G proteins rac-1 and rhoA. *Experimental Dermatology*, *13*(2), 70–77. doi:10.1111/j.0906-6705.2004.00117.x

Laflamme, M. A., Chen, K. Y., Naumova, A. V., Muskheli, V., Fugate, J. A., Dupras, S. K., et al. (2007a). Cardiomyocytes derived from human embryonic stem cells in pro-

survival factors enhance function of infarcted rat hearts. *Nature Biotechnology*, *25*(9), 1015–1024. doi:10.1038/nbt1327

Laflamme, M. A., Zbinden, S., Epstein, S. E., & Murry, C. E. (2007b). Cell-based therapy for myocardial ischemia and infarction: pathophysiological mechanisms. *Annual Review of Pathology*, *2*, 307–339. doi:10.1146/annurev.pathol.2.010506.092038

Lanner, F., & Rossant, J. (2010). The role of FGF/Erk signaling in pluripotent cells. *Development*, *137*(20), 3351–3360. doi:10.1242/dev.050146

Lavine, K. J., Kovacs, A., & Ornitz, D. M. (2008). Hedgehog signaling is critical for maintenance of the adult coronary vasculature in mice. *The Journal of Clinical Investigation*, *118*(7), 2404–2414. doi:10.1172/JCI34561

Lee, M. Y., Bozkulak, E. C., Schliffke, S., Amos, P. J., Ren, Y., Ge, X., et al. (2011). High density cultures of embryoid bodies enhanced cardiac differentiation of murine embryonic stem cells. *Biochemical and Biophysical Research Communications*, *416*(1-2), 51–57. doi:10.1016/j.bbrc.2011.10.140

Lee, S. T., Yun, J. I., van der Vlies, A. J., Kontos, S., Jang, M., Gong, S. P., et al. (2012). Long-term maintenance of mouse embryonic stem cell pluripotency by manipulating integrin signaling within 3D scaffolds without active Stat3. *Biomaterials*, *33*(35), 8934–8942. doi:10.1016/j.biomaterials.2012.08.062

Lehoux, S. (2006). Redox signalling in vascular responses to shear and stretch. *Cardiovascular Research*, *71*(2), 269–279. doi:10.1016/j.cardiores.2006.05.008

Li, Y.-S., & Gao, B.-R. (2007). Transplantation of neonatal cardiomyocytes plus fibrin sealant restores myocardial function in a rat model of myocardial infarction. *Chinese Medical Journal*, *120*(22), 2022–2027.

Lian, X., Zhang, J., Azarin, S. M., Zhu, K., Hazeltine, L. B., Bao, X., et al. (2013). Directed cardiomyocyte differentiation from human pluripotent stem cells by modulating Wnt/β-catenin signaling under fully defined conditions. *Nature Protocols*, *8*(1), 162–175. doi:10.1038/nprot.2012.150

Lucitti, J. L., Jones, E. A. V., Huang, C., Chen, J., Fraser, S. E., & Dickinson, M. E. (2007). Vascular remodeling of the mouse yolk sac requires hemodynamic force. *Development*, *134*(18), 3317–3326. doi:10.1242/dev.02883

Luong, E., & Gerecht, S. (2008). Stem Cells and Scaffolds for Vascularizing Engineered Tissue Constructs. *Advances in Biochemical Engineering/Biotechnology*, *114*, 129–

172. doi:10.1007/10_2008_8

Lyngbaek, S., Schneider, M., Hansen, J. L., & Sheikh, S. P. (2007). Cardiac regeneration by resident stem and progenitor cells in the adult heart. *Basic Research in Cardiology*, *102*(2), 101–114. doi:10.1007/s00395-007-0638-3

Makino, S., Fukuda, K., Miyoshi, S., Konishi, F., Kodama, H., Pan, J., et al. (1999). Cardiomyocytes can be generated from marrow stromal cells in vitro. *The Journal of Clinical Investigation*, *103*(5), 697–705. doi:10.1172/JCI5298

Mammoto, A., Mammoto, T., & Ingber, D. E. (2012). Mechanosensitive mechanisms in transcriptional regulation. *Journal of Cell Science*, *125*(Pt 13), 3061–3073. doi:10.1242/jcs.093005

Mammoto, T., & Ingber, D. E. (2010). Mechanical control of tissue and organ development. *Development*, *137*(9), 1407–1420. doi:10.1242/dev.024166

Martin, G. R. (1981). Isolation of a pluripotent cell line from early mouse embryos cultured in medium conditioned by teratocarcinoma stem cells. *Proceedings of the National Academy of Sciences of the United States of America*, *78*(12), 7634–7638.

Masumura, T., Yamamoto, K., Shimizu, N., Obi, S., & Ando, J. (2009). Shear stress increases expression of the arterial endothelial marker ephrinB2 in murine ES cells via the VEGF-Notch signaling pathways. *Arteriosclerosis, Thrombosis, and Vascular Biology*, *29*(12), 2125–2131. doi:10.1161/ATVBAHA.109.193185

Metallo, C. M., Vodyanik, M. A., de Pablo, J. J., Slukvin, I. I., & Palecek, S. P. (2008). The response of human embryonic stem cell-derived endothelial cells to shear stress. *Biotechnology and Bioengineering*, *100*(4), 830–837. doi:10.1002/bit.21809

Meyer, C. J., Alenghat, F. J., Rim, P., Fong, J. H., Fabry, B., & Ingber, D. E. (2000). Mechanical control of cyclic AMP signalling and gene transcription through integrins. *Nature Cell Biology*, *2*(9), 666–668. doi:10.1038/35023621

Murry, C. E., & Keller, G. (2010). Differentiation of Embryonic Stem Cells to Clinically Relevant Populations: Lessons from Embryonic Development
. *Cell*, *132*, 661–680. doi:10.1016/j.cell.2008.02.008

Neal, R. A., Jean, A., Park, H., Wu, P. B., Hsiao, J., Engelmayr, G. C., et al. (2013). Three-dimensional elastomeric scaffolds designed with cardiac-mimetic structural and mechanical features. *Tissue Engineering Part A*, *19*(5-6), 793–807. doi:10.1089/ten.tea.2012.0330

Nieden, zur, N. I., Cormier, J. T., Rancourt, D. E., & Kallos, M. S. (2007). Embryonic stem cells remain highly pluripotent following long term expansion as aggregates in suspension bioreactors. *Journal of Biotechnology*, *129*(3), 421–432. doi:10.1016/j.jbiotec.2007.01.006

Nikmanesh, M., Shi, Z.-D., & Tarbell, J. M. (2012). Heparan sulfate proteoglycan mediates shear stress-induced endothelial gene expression in mouse embryonic stem cell-derived endothelial cells. *Biotechnology and Bioengineering*, *109*(2), 583–594. doi:10.1002/bit.23302

Offenberg Sweeney, von, N., Cummins, P. M., Birney, Y. A., Cullen, J. P., Redmond, E. M., & Cahill, P. A. (2004). Cyclic strain-mediated regulation of endothelial matrix metalloproteinase-2 expression and activity. *Cardiovascular Research*, *63*(4), 625–634. doi:10.1016/j.cardiores.2004.05.008

Pandur, P. (2005). What does it take to make a heart? *Biology of the Cell / Under the Auspices of the European Cell Biology Organization*, *97*(3), 197–210. doi:10.1042/BC20040109

Patwari, P., & Lee, R. T. (2008). Mechanical control of tissue morphogenesis. *Circulation Research*, *103*(3), 234–243. doi:10.1161/CIRCRESAHA.108.175331

Plopper, G., & Ingber, D. E. (1993). Rapid induction and isolation of focal adhesion complexes. *Biochemical and Biophysical Research Communications*, *193*(2), 571–578. doi:10.1006/bbrc.1993.1662

Prowse, A. B. J., Chong, F., Gray, P. P., & Munro, T. P. (2011). Stem cell integrins: implications for ex-vivo culture and cellular therapies. *Stem Cell Research*, *6*(1), 1–12. doi:10.1016/j.scr.2010.09.005

Riha, G. M., Wang, X., Wang, H., Chai, H., Mu, H., Lin, P. H., et al. (2007). Cyclic strain induces vascular smooth muscle cell differentiation from murine embryonic mesenchymal progenitor cells. *Surgery*, *141*(3), 394–402. doi:10.1016/j.surg.2006.07.043

Robertson, C., Tran, D. D., & George, S. C. (2013). Concise review: maturation phases of human pluripotent stem cell-derived cardiomyocytes. *Stem Cells*, *31*(5), 829–837. doi:10.1002/stem.1331

Roger, V. L., Go, A. S., Lloyd-Jones, D. M., Benjamin, E. J., Berry, J. D., Borden, W. B., et al. (2012). Heart Disease and Stroke Statistics—2012 Update A Report From the American Heart Association. *Circulation*, *125*(1), e2–e220.

Rowland, T. J., Miller, L. M., Blaschke, A. J., Doss, E. L., Bonham, A. J., Hikita, S. T., et al. (2010). Roles of integrins in human induced pluripotent stem cell growth on Matrigel and vitronectin. *Stem Cells and Development*, *19*(8), 1231–1240. doi:10.1089/scd.2009.0328

Saha, S., Ji, L., de Pablo, J. J., & Palecek, S. P. (2006). Inhibition of human embryonic stem cell differentiation by mechanical strain. *Journal of Cellular Physiology*, *206*(1), 126–137. doi:10.1002/jcp.20441

Saha, S., Ji, L., de Pablo, J. J., & Palecek, S. P. (2008). TGFbeta/Activin/Nodal pathway in inhibition of human embryonic stem cell differentiation by mechanical strain. *Biophysical Journal*, *94*(10), 4123–4133. doi:10.1529/biophysj.107.119891

Salameh, A., Wustmann, A., Karl, S., Blanke, K., Apel, D., Rojas-Gomez, D., et al. (2010). Cyclic mechanical stretch induces cardiomyocyte orientation and polarization of the gap junction protein connexin43. *Circulation Research*, *106*(10), 1592–1602. doi:10.1161/CIRCRESAHA.109.214429

Sauer, H., & Wartenberg, M. (2005). Reactive oxygen species as signaling molecules in cardiovascular differentiation of embryonic stem cells and tumor-induced angiogenesis. *Antioxidants & Redox Signaling*, *7*(11-12), 1423–1434. doi:10.1089/ars.2005.7.1423

Sauer, H., Rahimi, C., Hescheler, J., & Wartenberg, M. (2000). Role of reactive oxygen species and phosphatidylinositol 3-kinase in cardiomyocyte differentiation of embryonic stem cells. *FEBS Letters*, *476*(3), 218–223.

Schmelter, M., Ateghang, B., Helmig, S., Wartenberg, M., & Sauer, H. (2006). Embryonic stem cells utilize reactive oxygen species as transducers of mechanical strain-induced cardiovascular differentiation. *Faseb Journal*, *20*(8), 1182–. doi:10.1096/fj.05-4723fje

Serena, E., Figallo, E., Tandon, N., Cannizzaro, C., Gerecht, S., Elvassore, N., & Vunjak-Novakovic, G. (2009). Electrical stimulation of human embryonic stem cells: Cardiac differentiation and the generation of reactive oxygen species. *Experimental Cell Research*, *315*(20), 3611–3619. doi:10.1016/j.yexcr.2009.08.015

Shapira-Schweitzer, K., & Seliktar, D. (2007). Matrix stiffness affects spontaneous contraction of cardiomyocytes cultured within a PEGylated fibrinogen biomaterial. *Acta Biomaterialia*, *3*(1), 33–41. doi:10.1016/j.actbio.2006.09.003

Shapira-Schweitzer, K., Habib, M., Gepstein, L., & Seliktar, D. (2009). A photopolymerizable hydrogel for 3-D culture of human embryonic stem cell-derived

cardiomyocytes and rat neonatal cardiac cells. *Journal of Molecular and Cellular Cardiology*, *46*(2), 213–224. doi:10.1016/j.yjmcc.2008.10.018

Singh, A., Suri, S., Lee, T., Chilton, J. M., Cooke, M. T., Chen, W., et al. (2013). Adhesion strength-based, label-free isolation of human pluripotent stem cells. *Nature Methods*. doi:10.1038/nmeth.2437

Smith, A. W., Segar, C. E., Nguyen, P. K., MacEwan, M. R., Efimov, I. R., & Elbert, D. L. (2012). Long-term culture of HL-1 cardiomyocytes in modular poly(ethylene glycol) microsphere-based scaffolds crosslinked in the phase-separated state. *Acta Biomaterialia*, *8*(1), 31–40. doi:10.1016/j.actbio.2011.08.021

Son, Y., Cheong, Y.-K., Kim, N.-H., Chung, H.-T., Kang, D. G., & Pae, H.-O. (2011). Mitogen-Activated Protein Kinases and Reactive Oxygen Species: How Can ROS Activate MAPK Pathways? *Journal of Signal Transduction*, *2011*, 792639. doi:10.1155/2011/792639

Stolberg, S., & McCloskey, K. E. (2009). Can shear stress direct stem cell fate? *Biotechnology Progress*, *25*(1), 10–19. doi:10.1002/btpr.124

Sucov, H. M. (1998). Molecular insights into cardiac development. *Annual Review of Physiology*, *60*, 287–308. doi:10.1146/annurev.physiol.60.1.287

Tan, M. Y., Zhi, W., Wei, R. Q., Huang, Y. C., Zhou, K. P., Tan, B., et al. (2009). Repair of infarcted myocardium using mesenchymal stem cell seeded small intestinal submucosa in rabbits. *Biomaterials*, *30*(19), 3234–3240. doi:10.1016/j.biomaterials.2009.02.013

Tehrani, D. M., & Seto, A. H. (2013). Third universal definition of myocardial infarction: update, caveats, differential diagnoses. *Cleveland Clinic Journal of Medicine*, *80*(12), 777–786. doi:10.3949/ccjm.80a.12158

Teramura, T., Takehara, T., Onodera, Y., Nakagawa, K., Hamanishi, C., & Fukuda, K. (2012). Mechanical stimulation of cyclic tensile strain induces reduction of pluripotent related gene expressions via activation of Rho/ROCK and subsequent decreasing of AKT phosphorylation in human induced pluripotent stem cells. *Biochemical and Biophysical Research Communications*, *417*(2), 836–841. doi:10.1016/j.bbrc.2011.12.052

Thygesen, K., Alpert, J. S., Jaffe, A. S., Simoons, M. L., Chaitman, B. R., White, H. D., Joint ESC/ACCF/AHA/WHF Task Force for the Universal Definition of Myocardial Infarction, et al. (2012a). Third universal definition of myocardial infarction. (Vol. 126, pp. 2020–2035). Presented at the Circulation.

doi:10.1161/CIR.0b013e31826e1058

Thygesen, K., Alpert, J. S., Jaffe, A. S., Simoons, M. L., Chaitman, B. R., White, H. D., Katus, H. A., et al. (2012b). Third universal definition of myocardial infarction. *Nature Reviews Cardiology*, *9*(11), 620–633. doi:10.1038/nrcardio.2012.122

Tirosh-Finkel, L., Zeisel, A., Brodt-Ivenshitz, M., Shamai, A., Yao, Z., Seger, R., et al. (2010). BMP-mediated inhibition of FGF signaling promotes cardiomyocyte differentiation of anterior heart field progenitors. *Development*, *137*(18), 2989–3000. doi:10.1242/dev.051649

Toh, Y.-C., & Voldman, J. (2011). Fluid shear stress primes mouse embryonic stem cells for differentiation in a self-renewing environment via heparan sulfate proteoglycans transduction. *The FASEB Journal*, *25*(4), 1208–1217. doi:10.1096/fj.10-168971

Tulloch, N. L., Muskheli, V., Razumova, M. V., Korte, F. S., Regnier, M., Hauch, K. D., et al. (2011). Growth of engineered human myocardium with mechanical loading and vascular coculture. *Circulation Research*, *109*(1), 47–59. doi:10.1161/CIRCRESAHA.110.237206

Uda, Y., Poh, Y.-C., Chowdhury, F., Wu, D. C., Tanaka, T. S., Sato, M., & Wang, N. (2011). Force via integrins but not E-cadherin decreases Oct3/4 expression in embryonic stem cells. *Biochemical and Biophysical Research Communications*, *415*(2), 396–400. doi:10.1016/j.bbrc.2011.10.080

Van Vliet, P., Wu, S. M., Zaffran, S., & Pucéat, M. (2012). Early cardiac development: a view from stem cells to embryos. *Cardiovascular Research*, *96*(3), 352–362. doi:10.1093/cvr/cvs270

Wan, C.-R., Chung, S., & Kamm, R. D. (2011). Differentiation of embryonic stem cells into cardiomyocytes in a compliant microfluidic system. *Annals of Biomedical Engineering*, *39*(6), 1840–1847. doi:10.1007/s10439-011-0275-8

Wang, N., Butler, J. P., & Ingber, D. E. (1993). Mechanotransduction across the cell surface and through the cytoskeleton. *Science (New York, N.Y.)*, *260*(5111), 1124–1127.

Wang, X., & Ha, T. (2013). Defining Single Molecular Forces Required to Activate Integrin and Notch Signaling. *Science (New York, N.Y.)*, *340*(6135), 991–994. doi:10.1126/science.1231041

Watanabe, S., Umehara, H., Murayama, K., Okabe, M., Kimura, T., & Nakano, T. (2006). Activation of Akt signaling is sufficient to maintain pluripotency in mouse

and primate embryonic stem cells. *Oncogene*, *25*(19), 2697–2707. doi:10.1038/sj.onc.1209307

Willems, E., Spiering, S., Davidovics, H., Lanier, M., Xia, Z., Dawson, M., et al. (2011). Small-molecule inhibitors of the Wnt pathway potently promote cardiomyocytes from human embryonic stem cell-derived mesoderm. *Circulation Research*, *109*(4), 360–364. doi:10.1161/CIRCRESAHA.111.249540

Williams, C., Johnson, S. L., Robinson, P. S., & Tranquillo, R. T. (2006). Cell sourcing and culture conditions for fibrin-based valve constructs. *Tissue Engineering*, *12*(6), 1489–1502.

Wolfe, R. P., Leleux, J., Nerem, R. M., & Ahsan, T. (2012). Effects of shear stress on germ lineage specification of embryonic stem cells. *Integrative Biology : Quantitative Biosciences From Nano to Macro*, *4*(10), 1263–1273. doi:10.1039/c2ib20040f

Xin, M., Olson, E. N., & Bassel-Duby, R. (2013). Mending broken hearts: cardiac development as a basis for adult heart regeneration and repair. *Nature Reviews. Molecular Cell Biology*, *14*(8), 529–541. doi:doi:10.1038/nrm3619

Xu, C., Police, S., Hassanipour, M., Li, Y., Chen, Y., Priest, C., et al. (2011). Efficient generation and cryopreservation of cardiomyocytes derived from human embryonic stem cells. *Regenerative Medicine*, *6*(1), 53–66. doi:10.2217/rme.10.91

Xu, C., Police, S., Rao, N., & Carpenter, M. K. (2002). Characterization and enrichment of cardiomyocytes derived from human embryonic stem cells. *Circulation Research*, *91*(6), 501–508.

Yamashita, J., Itoh, H., Hirashima, M., Ogawa, M., Nishikawa, S., Yurugi, T., et al. (2000). Flk1-positive cells derived from embryonic stem cells serve as vascular progenitors. *Nature*, *408*(6808), 92–96. doi:10.1038/35040568

Ye, Z., Zhou, Y., Cai, H., & Tan, W. (2011). Myocardial regeneration: Roles of stem cells and hydrogels. *Advanced Drug Delivery Reviews*, *63*(8), 688–697. doi:10.1016/j.addr.2011.02.007

Zhang, G., Wang, X., Wang, Z., Zhang, J., & Suggs, L. (2006). A PEGylated fibrin patch for mesenchymal stem cell delivery. *Tissue Engineering*, *12*(1), 9–19. doi:10.1089/ten.2006.12.9

Zhao, S., Suciu, A., Ziegler, T., Moore, J. E., Bürki, E., Meister, J. J., & Brunner, H. R. (1995). Synergistic effects of fluid shear stress and cyclic circumferential stretch on

vascular endothelial cell morphology and cytoskeleton. *Arteriosclerosis, Thrombosis, and Vascular Biology*, *15*(10), 1781–1786.

Zoldan, J., Karagiannis, E. D., Lee, C. Y., Anderson, D. G., Langer, R., & Levenberg, S. (2011). The influence of scaffold elasticity on germ layer specification of human embryonic stem cells. *Biomaterials*, *32*(36), 9612–9621. doi:10.1016/j.biomaterials.2011.09.012

CHAPTER THREE

Guiding mouse embryonic stem cell mesodermal commitment with paramagnetic beads

Pluripotent stem cells are ideal candidates for cell therapy due to their potential to differentiate into any cell type. This potential is improved when embryonic stem cells (ESCs) are aggregated into embryoid bodies (EBs), further increasing the potential yield as the cells can differentiate into all three germ layers and are not limited by surface area. This is especially important for treatment of diseases such as heart disease, specifically following myocardial infarction, which requires millions of cells to repopulate the injured myocardium. A bottleneck for the use of EBs in cell therapy strategies is that consistency is limited by a number of factors including both the size of the EB, as well as heterogeneity of the cell population during differentiation. To uniformly guide differentiation, the most effective regimen to date involves the supplementation of growth factors or proteins that are known to be important for cardiomyogenesis during embryonic development. In addition, recent research into the gross morphology of the EB has demonstrated that a collagen-rich wall forming the endoderm develops around the EB three- to four-days after aggregation (Bratt-Leal, Carpenedo, & Mcdevitt, 2009). This renders the EB relatively impenetrable to larger molecules and thus cells in the interior are not exposed to these proteins, further increasing variation in the cell population. To address this issue, we hypothesized that by immobilizing proteins to microbeads and incorporating them into the interior of an EB, we can increase the population of cells exposed to pro-mesoderm growth factors and subsequently the yield

of cardiomyocytes. In this study we investigated the effects of two specific proteins, Sonic Hedgehog (SHH) and bone morphogenetic protein 4 (BMP4). We attached SHH and BMP4 to paramagnetic beads and incorporated the beads into EBs using Aggrewell plates and compared the percentage of EBs with contractile foci in the presence of the protein-immobilized beads. In this chapter, we found that there was little effect of SHH-immobilized beads on contractile activity due to the decreased potency of tagged SHH. The presence of tagged BMP4 also did not appear to affect cardiomyogenesis; however, the most significant effect on contractile activity was the result of the presence of the beads alone. This may be the result of an interaction with α1 integrin, as suggested by focal adhesion protein microarray.

3.1. INTRODUCTION

The ability of embryonic stem cells to aggregate into embryoid bodies provides an opportunity to derive a large population of cells from all germ lineages: ectoderm, endoderm, and mesoderm. This potential addresses a significant need for effective cell therapy, in which large concentrations of differentiated cells are used to repopulate damaged tissue as well as integrate with the host to promote full recovery. Traditionally, stem cell fate is guided by the addition of soluble factors to the medium. For cardiomyocyte differentiation, this has involved the supplementation of BMP4 to mouse ESCs, and a combination of BMP4, Activin, bFGF, and Wnt to human ESCs. While this differentiation strategy is quite effective for monolayer culture, the percentage of ESC-derived cardiomyocytes (ESC-CM) derived from EBs is lower: 90-95% yields in

monolayer culture (Lian et al., 2013) versus approximately 30% in EBs (Laflamme et al., 2007; Lee et al., 2011; Willems et al., 2011).

Electron microscopy of the EB over the course of culture has revealed that part of the difficulty with homogeneous ESC differentiation is overcoming diffusional limitations. Approximately three days after EB formation, a collagen-rich endodermal cell wall forms around the EB exterior (Bratt-Leal et al., 2009; Sachlos & Auguste, 2008). This suggests that the most exposure cells in the EB interior have to exogenous factors is through the first three days, after which proteins can no longer diffuse through the outermost cells (Sachlos & Auguste, 2008).

In an attempt to overcome these limitations, the possibility of delivering soluble factors to the interior of EBs has been explored. Microparticles composed of gelatin, Poly(lactic-co-glycolic acid) (PLGA) and agarose have been successfully incorporated into EBs, and have been shown to efficiently release soluble factors such as Retinoic Acid, ultimately promoting differentiation without impacting viability or gross morphology (Bratt-Leal, Carpenedo, Ungrin, Zandstra, & Mcdevitt, 2011; Bratt-Leal, Nguyen, Hammersmith, Singh, & Mcdevitt, 2013; Carpenedo et al., 2009). In addition, the presence of these particles alone have been observed to increase the expression of mesodermal markers (Carpenedo et al., 2009). Despite the potential of protein-loaded microspheres, this technique has only been demonstrated effective for small, hydrophobic molecules and not necessarily for larger proteins.

In addition to protein delivery strategies, alternative growth factors that enhance cardiomyogenesis are also being pursued. The hedgehog signaling pathway is also

activated in response to myocardial infarction (Thomas, Koudijs, van Eeden, Joyner, & Yelon, 2008), and Sonic Hedgehog (*Shh*) gene therapy has been shown to enhance healing post-MI in rodents (Ahmed, Haider, Shujia, Afzal, & Ashraf, 2010; Kusano et al., 2005). SHH signaling is essential for the regulation of patterning and growth of multiple embryonic organs (Ingham & McMahon, 2001; Thomas et al., 2008). *In vivo*, Hh signaling from the endoderm influences the fate of the embryonic mesoderm, guiding differentiation into vascular phenotypes, including cardiomyocytes (Bijlsma & Spek, 2010; Clement et al., 2009; Gianakopoulos & Skerjanc, 2005; Kusano et al., 2005). SHH induces its transcriptional response by binding to the receptor Patched (PTCH). In the absence of SHH, PTCH inhibits another receptor, Smoothened (SMO). SMO inhibition prevents GLI, a downstream transcription factor, from translocating into the nucleus and becoming activated. When SHH binds to PTCH, the signaling cascade is activated and SMO inhibition is relieved, leading to GLI activation and transcription of cardiovascular genes. In turn, *bmp4* transcripts are upregulated by SHH signaling (Gianakopoulos & Skerjanc, 2009).

Since microparticles have been observed to influence fate determination in EBs, we hypothesized that the incorporation of magnetic microbeads into the EB interior may guide differentiation into cardiomyocytes through biological or physical interactions. Similarly, these magnetic beads may also be used to deliver immobilized proteins, specifically those that promote cardiomyogenesis, to derive a larger population of mesodermal progenitors. In this chapter, we incorporated paramagnetic beads into EBs during aggregation and examined the effects on cardiomyocyte differentiation. The

efficiency of bead incorporation was confirmed by histology, and the nature of bead interactions with the cells was analyzed using a focal adhesion microarray. To assess the possibility of delivering immobilized proteins into EBs, 6xHis-tagged SHH and Maltose Binding Protein (MBP)-BMP4 were bound to anti-His or MBP magnetic beads and binding efficiency was confirmed by either ELISA or western blot. The effect of protein-immobilized beads on cardiomyocyte differentiation was analyzed by the percentage of EBs with spontaneous contracting foci. We observed that the magnetic beads do appear to increase cardiomyocyte differentiation, likely through integrin-mediated interactions; however, immobilized proteins have decreased potency, and consequently do not have a significant effect.

3.2. MATERIALS AND METHODS

3.2.1. Embryonic stem cell culture

R1 mouse ESCs (A. Nagy, Toronto, Canada) were expanded feeder-free on 0.1% gelatin-coated cell culture flasks (Stem Cell Technologies, Vancouver, Canada) in Growth Medium containing Knockout Dulbecco's Modified Eagle's Medium (Invitrogen, Grand Island, NY) supplemented with 15% ES-Cult Fetal Bovine Serum (Stem Cell Technologies), 1% Glutamax (Invitrogen), 1% Non-Essential Amino Acids (Invitrogen), 1% Nucleosides (Millipore, Billerica, MA), 1% Penicillin/Streptomycin (Invitrogen), 0.1mM β-Mercaptoethanol (Invitrogen) and 10^3 U/ml Leukemia Inhibitory

Factor (LIF; Millipore). Medium was changed in full each day, and cells were passaged every 2 days before reaching approximately 70% confluence.

3.2.2. Embryoid Body formation and Bead incorporation

The ESCs were enzymatically released from the gelatin-coated plates with trypsin/EDTA (ATCC, Manassas, VA) and resuspended in differentiation medium (growth medium without LIF supplementation). Aggrewell 400™ plates (Stem Cell Technologies) were used to facilitate ESC aggregation as directed by the manufacturer. To form the EBs, 1.2 x 10^6 cells were added to each well of the Aggrewell plate, shaken briefly on an orbital shaker, and centrifuged for 3 min at 100 x g, resulting in a final EB size of 1000 cells/EB. The Aggrewell plates were incubated at 37°C/5% CO_2 for 30 minutes to allow the cells to settle into the wells. Paramagnetic beads, either without protein or immobilized with SHH or BMP4, were resuspended in differentiation medium and pipetted directly into the Aggrewell plate. The groups and concentrations of reagents used for the SHH and the BMP4 experiments are listed in Table 3.1. After 72 hours, the EBs were removed from the wells with wide bore tips and transferred to ultra-low attachment plates (Corning, Lowell, MA). The EBs were maintained in differentiation medium in suspension culture for 7 days. Viability was assessed by Trypan Blue exclusion.

3.2.3. Protein immobilization to Paramagnetic Beads

Recombinant mouse SHH with a 6x His tag (R&D Systems, Minneapolis, MN) was immobilized to anti-His tag magnetic Dynabeads (DBs) according to the manufacturer's protocol with modifications. A 1x Binding Buffer was diluted in PBS (Mediatech, Manassas, VA) from a 2x Binding Buffer containing 100 mM sodium phosphate pH 8.0, 600 mM sodium chloride and 0.02% tween-20 (Sigma-Aldrich, St. Louis, MO) and sterile filtered prior to use. To immobilize the SHH to the DBs, 1 µg of SHH was combined with 40 µg of DBs in 300 µl of sterile 1x Binding Buffer. The SHH-Dynabead solution (Shh-DB) was incubated on an end-to-end shaker for 3 hours at 4°C. The SHH-DBs were pulled out of solution using a Dynal magnet (Invitrogen, Carlsbad, CA).

For BMP4 studies, recombinant human BMP4 with a MBP tag (rhBMP4-MBP, Abcam, Cambridge, MA) was combined with Anti-MBP paramagnetic beads (New England Biolabs, Ipswitch, MA) at a final concentration of 10 µg protein/ mg beads. The beads were first rinsed in Rinse Buffer (0.1M sodium phosphate, pH 8) prior to resuspension in PBS containing 2.5 µg rhBMP4-MBP on an end-to-end shaker for 1 hour at 4°C. The protein-bound beads (hereafter referred to as BMP4-beads) were rinsed again three times in Rinse Buffer. The beads were resuspended in medium (200 µl per Aggrewell) prior to transfer to the Aggrewell plate.

3.2.4. Prussian Blue staining

To assess bead loading efficiency into EBs, beads at concentrations ranging from 10 μg to 400 μg were added to each well of an Aggewell plate. The EBs were removed on Day 3 and transferred to ultra low attachment dishes for an additional 4 days. On day 7, the EBs were fixed with 4% buffered formalin, rinsed in PBS, and resuspended in OCT solution (Thermo Scientific) for cryosectioning. Frozen sections (10 μm) were rehydrated for 10 minutes in PBS. Prussian Blue staining was performed to locate the beads within the EBs. The sections were incubated in a 1:1 solution of 20% aqueous hydrochloric acid: 10% aqueous potassium ferrocyanide for 20 minutes at room temperature. Following three rinses in distilled water, the slides were counterstained in Nuclear Fast Red (Sigma-Aldrich) for 5 minutes at room temperature. The slides were rinsed twice in distilled water, cleared and mounted with Cytoseal (Thermo Scientific). EBs were imaged using a Leica DMI2000B microscope with a Leica DFC290 camera.

3.2.5. Enzyme Linked Immunosorbent Assay

The concentration of SHH bound to beads was assessed at Day 0, 1, 3, 5 and 7 (n=3 per time point) using a SHH Enzyme Linked Immunosorbent Assay (ELISA; R&D systems, Minneapolis, MN). SHH was immobilized to beads as described above. Immediately following the 3-hour incubation, SHH-beads were collected with a Dynal magnet and the Binding Solution was removed. The SHH-beads were incubated in 300mM Imidazole, 50mM sodium phosphate pH 8.0, 300mM sodium chloride and 0.01% Tween-20 (His-elution Buffer) overnight at 4°C on an end-to-end shaker to isolate the

bound Shh. Day 1-7 samples were incubated in PBS at 37ºC for the duration of the study, and Shh was eluted at each time point using the same procedure. The SHH ELISA (R&D systems) was carried out as directed by the manufacturer.

3.2.6. Western Blot

A BMP4 western blot was used to confirm rhBMP4-MBP binding efficiency to anti-MBP beads. After binding the BMP4 to beads as described in Section 3.2.1, the BMP4-beads were incubated in PBS at 37ºC/5%CO_2 over 7 days. On Days 1, 3, 5 and 7, the BMP4-beads were rinsed in PBS and incubated in 1x Laemmli Buffer containing β-Mercaptoethanol (Bio-Rad) for 5 minutes at 70ºC. The BMP4-Laemmli solution was separated from the beads using a Dynal magnet. The protein fraction was run on a 10% tris-HCl Page gel (Bio-Rad) for 1 hour at 100V. The Page gel was transferred onto a PVDF membrane (Bio-Rad) at 100V for 1 hour. After blocking for 1 hour in 5% Milk in TBST (Tris Buffered Saline with 0.05% Tween-20), the blots were incubated in rabbit anti-mouse BMP4 primary antibody (Abcam, 1:500 in 5% Milk/TBST) overnight at 4ºC. The blot was incubated in goat anti-rabbit IgG HRP (Abcam, 1:2000 in 5% Milk/TBST) for 1 hour at room temperature. After three rinses in TBST, the blots were developed with SuperSignal West Pico Substrate (Thermo Scientific) as directed by the manufacturer, and images were obtained with a FluorChem HD2 digital imager (Protein Simple, Santa Clara, CA). Band intensity was calculated and analyzed using AlphaView software (Protein Simple). Soluble BMP4 at the same concentration in PBS was included as a control.

3.2.7. Focal Adhesion Protein PCR Array

To determine potential binding interactions with beads and the ESCs, we performed a Focal Adhesions PCR Array (SA Biosciences, Valencia, CA). EBs were formed using Aggrewell plates as described in Section 3.2.2. Day 1 EBs containing 20 μg beads were compared to controls without beads. RNA was isolated using an RNeasy mini kit (Qiagen). Following RNA isolation, 500 ng RNA was reverse transcribed using the RT^2 First Strand Reverse Transcription kit (SA Biosciences) and a Veriti Thermal Cycler (Invitrogen) at the following conditions: 15 minutes at 42ºC, and 5 minutes at 95ºC. Following dilution in RNase free water, the cDNA was mixed with one volume of 2x RT^2 SYBR Green Master Mix (SA Biosciences) and added to each well of the Microarray. The PCR products were amplified with a ViiA 7™ Real Time Polymerase Chain Reaction (PCR; Life Technologies) system under the following conditions: 95ºC for 10 minutes for one cycle, 15 seconds at 95ºC followed by 1 minute at 60ºC for 40 cycles. The results were analyzed using the RT^2 Profiler™ PCR array data analysis program (SA Biosciences).

3.2.8. Gli1-response assay

For RNA extraction, EBs were rinsed in PBS and disrupted using a QIAshredder kit as recommended by the manufacturer (Qiagen). RNA was further extracted using an RNeasy Mini kit (Qiagen). Total RNA was calculated using a BioTek plate reader (BioTek, Winooski, VT). A 100ng sample of RNA was reverse transcribed to cDNA using a High-Capacity Reverse Transcription kit (Life Technologies) and Veriti Thermal

Cycler (Invitrogen) as recommended by the manufacturer. To assess the activity of His-tagged SHH, we compared *Gli1* transcriptional activation to the Shh agonist Stemolecule™ Purmorphamine (Stemgent, Cambridge, MA) as described previously with some modifications (Frank-Kamenetsky et al., 2002). ESCs were cultured on gelatin-coated tissue culture plastic in growth medium containing LIF. After 24 hours, the cells were changed to 0.5% serum growth medium containing 1-100nM purmorphamine or His-tagged Shh. After 24 hours of exposure, the RNA was collected and isolated as described in Section 3.2.7. RT-PCR was performed using the inventoried *Gli1* TaqMan assay Mm00494654_m1 (Life Technologies).

3.2.9. Contractile activity

The spontaneous development of contracting foci within EBs was analyzed as described previously with a few modifications (Sargent, Berguig, & Mcdevitt, 2009). On Day 7, single EBs were transferred from the ultra-low attachment plates to individual wells of 0.1% gelatin-coated 48-well plates. At least 10-15 EBs were transferred for each group with an n=3. On Days 8, 10, 12, and 14, the number of EBs with spontaneously contracting areas was recorded.

3.2.10. Statistics

Statistical analysis was performed using StatPlus LE (AnalystSoft). All groups analyzed represent three independent experiments. Data from each of the groups was compared using one-way ANOVA coupled with Tukey's HSD test for differences

between means. Values are reported as mean ± standard deviation unless indicated otherwise. *p*-values less than 0.05 were considered statistically significant.

3.3. RESULTS

3.3.1. Bead incorporation into EBs

Since our objective was to expose cells within the EB to as many beads as possible, we delivered a range of bead concentrations to EBs in the Aggrewell plates and stained them with Prussian Blue (Figure 3.1) to examine distribution. Very few beads were detectable in EBs loaded with 10-50 μg beads per well (Figure 3.1D,E). Slight increases in staining were observed in EBs containing 100 to 500 μg beads (Figure 3.1A-C).

3.3.2. Effect of beads on focal adhesion protein expression

Previous reports have suggested that the presence of microparticles alone increase mesodermal commitment in EBs (Carpenedo et al., 2009). To better understand the interactions between magnetic beads and the cells, we performed a Focal Adhesion Protein (FAP) microarray to investigate which extracellular proteins are being activated and upregulated in response to bead exposure. After incubating the EBs with Anti-His beads for 24 hours, we compared transcript expression of FAPs to control EBs. The presence of the beads increased Integrin α1 (*Itga1*) expression 3.2-fold compared to EBs without beads (Figure 3.2A,B). Expression of Integrin β1 (*Itgb1*), the subunit that comprises the α1β1 heterodimer, decreased 1.28-fold compared to controls. Slight

increases were also observed in Protein Kinase b (*Prkcb*, 1.55-fold), ras-related C3 botulinum toxin substrate 2 (*Rac2*, 1.46-fold) and Son of Sevenless 2 (*Sos2*, 1.38-fold).

3.3.3. Effect of Shh-beads on EB viability

After confirming that beads could be incorporated into the EBs, we next assessed the effect of protein-immobilized beads on cardiomyogenesis. SHH has been observed to guide differentiation of cells into cardiovascular phenotypes via activation of the transcription factor GLI1 (Figure 3.3). We first assessed the efficiency and stability of SHH binding to anti-His tagged beads. To ensure maximum SHH loading to the beads, 155 ng of SHH was combined with 20 μg of Dynabeads for 3 hours as suggested by the manufacturer. We calculated that the final concentration of bound SHH was approximately $9.3x10^5$ molecules of SHH/μg beads (or 15.5±3.3 pmol SHH/μg beads; Figure 3.4A). To determine the stability of bound SHH, we measured the amount of SHH bound to the beads over the course of 7 days in culture at 37ºC/5%CO_2 by ELISA. Following elution of the protein from the beads, we found that traces of SHH remained on the beads through Day 7 (Figure 3.4B).

After establishing the binding efficiency of SHH to beads, we incorporated the SHH-beads into the EBs using Aggrewell plates (Figure 3.4C). After 24 hours, we measured the percentage of living and dead cells by Trypan blue dye exclusion. Regardless of the presence of beads, no significant differences in viability were observed (Figure 3.4D).

3.3.4. Effect of Shh-beads on contractile activity

To investigate the effect of SHH-beads on cardiomyogenesis, the EBs were plated on Day 7 and the percentage of EBs with contracting areas was recorded (Figure 3.5). Contractile activity in all groups was observed 3 days after plating (Day 7+3). After 12 days (Day 7+5), there was approximately a 2-fold increase in contractile activity in all treatment groups compared to controls. Contractile activity returned to levels comparable to the control without SHH or beads by Day 14 (Day 7+7).

3.3.5. Preparation of BMP4-beads and loading optimization

In addition to His-tagged SHH, we also examined the effect of bead immobilized BMP4 on cardiomyogenesis in EBs, since BMP4 is the most common protein used to direct mesodermal commitment in ESCs. RhBMP4 with MBP tags were combined with Anti-MBP paramagnetic beads (Figure 3.6A) and the binding stability was assessed by western blot (Figure 3.6B). Over the course of seven days *in vitro*, the amount of BMP4 eluted from the beads was relatively unchanged: approximately 80% of the initial BMP4 concentration was detected throughout the incubation period (Figure 3.6C). In comparison, the concentration of soluble, tagged BMP4 decreased more quickly, such that only 30% of the initial BMP4 concentration was detectable by Day 7.

3.3.6. Effect of BMP4-Beads on contractile activity

To examine the differentiated cardiomyocyte phenotype, we plated the EBs containing BMP-beads on Day 7 (Figure 3.7). By Day 14, increases in contractile

activity were observed in EBs exposed to low concentrations of both soluble BMP4 (6%±6% versus 2%±4% in high concentration groups) and immobilized BMP4 (13%±6% versus 4%±4% in high concentration groups). The only group that displayed significant increases in contractile activity by Day 14 were the EBs containing 400 μg unbound beads (19%±10%). No significant differences were observed between EBs with low concentrations of unbound beads compared to controls.

3.3.7. Comparison of SHH-bead and purmorphamine potency

Due to the inconsistent effects on contractile activity, we assessed the effectiveness of His-tagged SHH to increase transcript levels of the transcription factor *Gli1*. The ESCs were exposed to 1 – 100 nM of His-tagged SHH or purmorphamine in serum-free medium for 24 hours prior to RNA isolation. We observed that purmorphamine was significantly more potent, increasing *Gli1* gene expression almost 8-fold at 100 nM (Figure 3.8) compared to controls. Only a 2-fold change in *Gli1* expression was observed in the presence of 50 nM His-tagged SHH. As a comparison, approximately 52 nM His-tagged SHH is delivered to EBs via beads on Day 0.

3.4. DISCUSSION

Successful development of an MI patch requires (1) a stable, biocompatible material to retain cells at the infarct site and (2) a population of cardiomyocytes or cardiomyocyte progenitors that can replace the necrotic tissue. While differentiation of ESCs in monolayer culture yields approximately 95% cardiomyocytes, optimizing EB

culture methods could potentially further increase this percentage. The low cardiomyocyte yields from EBs have been partially attributed to the development of a thick visceral endoderm layer composed primarily of collagen starting around day 3 after ESC aggregation. Diffusional assays using Methylene Blue, a dye with a molecular weight of 320 Da, was shown to readily diffuse through EBs on day 3; however, diffusion decreased 80% by day 7 (Sachlos & Auguste, 2008). To address this issue, the idea of entrapping or attaching proteins to microparticles has been explored (Bratt-Leal et al., 2011; Carpenedo et al., 2009).

Previous reports have demonstrated that the presence of microparticles alone within an EB can direct lineage commitment; however, the nature of the interaction between particles and the cells is unclear (Carpenedo et al., 2009). We also observed that the presence of paramagnetic beads inside the EBs was sufficient to increase the contractile phenotype. Regardless of whether SHH (Figure 3.5) or BMP4 (Figure 3.7) were immobilized to beads, cardiomyogenesis was most influenced by the presence of un-immobilized beads. The microarray results clarify this, since after 24 hours the gene most predominantly upregulated compared to control EBs without beads was *Itga1* (integrin α1) (Figure 3.2). Integrin heterodimer α1β1 is the major receptor for collagen *in vivo* (Louis et al., 2007). The α subunit of the heterodimer plays an important role in protein-ligand binding coordination with the β subunit (Srichai & Zent, 2009). Activation of the α and β subunits leads to both clustering of the actin cytoskeleton, and activation of integrin-mediated signaling pathways ("outside-in signaling"). Similarly, the collagen-β1 integrin binding interaction is necessary for both proper EB formation

and subsequently ESC differentiation into cardiomyocytes (Zeng et al., 2013). The increase in *Itga1* gene expression suggests that the beads are interacting directly with the cells via integrin α1. While *Itgb1* expression was not significantly changed by the presence of the beads, it is possible that gene expression could increase at a later time point. Since integrin heterodimers mediate outside-in signaling in response to mechanical signals (Aikawa et al., 2002), this may explain why unbound beads alone can have an effect on cardiomyogenesis; however, integrin α1 and β1 blocking experiments would be necessary to confirm this possibility.

While SHH has been observed to promote angiogenesis and also improve recovery following myocardial infarction (Gianakopoulos & Skerjanc, 2005; Kusano et al., 2005; Renault et al., 2010; Vokes et al., 2004), its effect on directing differentiation in EBs has not yet been assessed. For this reason, we examined the effect of immobilized SHH on (1) overcoming EB diffusional limitations and (2) influencing differentiation into cardiomyocytes. Our preliminary data demonstrated that His-tagged SHH could be stably bound to beads and remained bound for up to 7 days *in vitro* (Figure 3.4); however, there was no effect on contractile activity (Figure 3.5). The *Gli1* transcript expression data clarified the possible reason for this: since *Gli1* expression is significantly higher following exposure to the SHH agonist purmorphamine as compared to His-SHH (Figure 3.8), this suggests that the potency of tagged SHH is insufficient to induce a biological response in ESCs. Since contractile activity was similarly unaffected in our BMP4 group, we could conclude that tagged-BMP4 is insufficient for the same reason. This was confirmed by western blot results, in which tagged BMP4 did not

increase SMAD1/5/8 expression, a downstream target of BMP4 (Figure 3.3), at any of the concentrations tested (data not shown). Therefore, while we cannot conclude that controlled delivery of proteins such as SHH or BMP4 into the EB interior have no effect on cardiomyogenesis, delivery of tagged proteins appear not to be effective.

3.5. CONCLUSIONS

In this chapter, we confirmed previous findings that microparticles, such as paramagnetic beads, can influence differentiation into cardiomyocyte phenotypes, and this is most likely the result of $\alpha 1\beta 1$ integrin binding interactions. Due to the decreased potency of tagged SHH and BMP4, we were unable to confirm the potential of localized delivery of these proteins on fate determination. In regards to SHH, another option to investigate the potential of SHH on mesodermal commitment is the soluble delivery of agonists such as purmorphamine. Purmorphamine (520 Da) is a smaller protein compared to Shh (49,607 Da) and may better penetrate the thick, collagen layer comprising the EB endoderm. In the future, we may further increase cardiomyogenesis by combining the mechanical interactions between cells and beads with biological cues, either delivered in microparticles or in soluble form.

Table 3.1. Concentrations of Shh and BMP4 used in protein-immobilized bead experiments.

Protein	Group	Abbreviation	Protein concentration/well	Bead concentration/well
Shh	Control	C	--	--
	DB	B	--	20 μg
	Shh	S	155 ng	--
	Shh-DB	SD	155 ng	20 μg
BMP4	Control	C	--	--
	Low [Beads]	LD	--	10 μg
	High [Beads]	HD	--	400 μg
	Low [BMP]	LB	62.5 ng	--
	High [BMP4]	HB	2.5 μg	--
	Low [BMP4-Beads]	LBD	62.5 ng	10 μg
	High [BMP4-Beads]	HBD	2.5 μg	400 μg

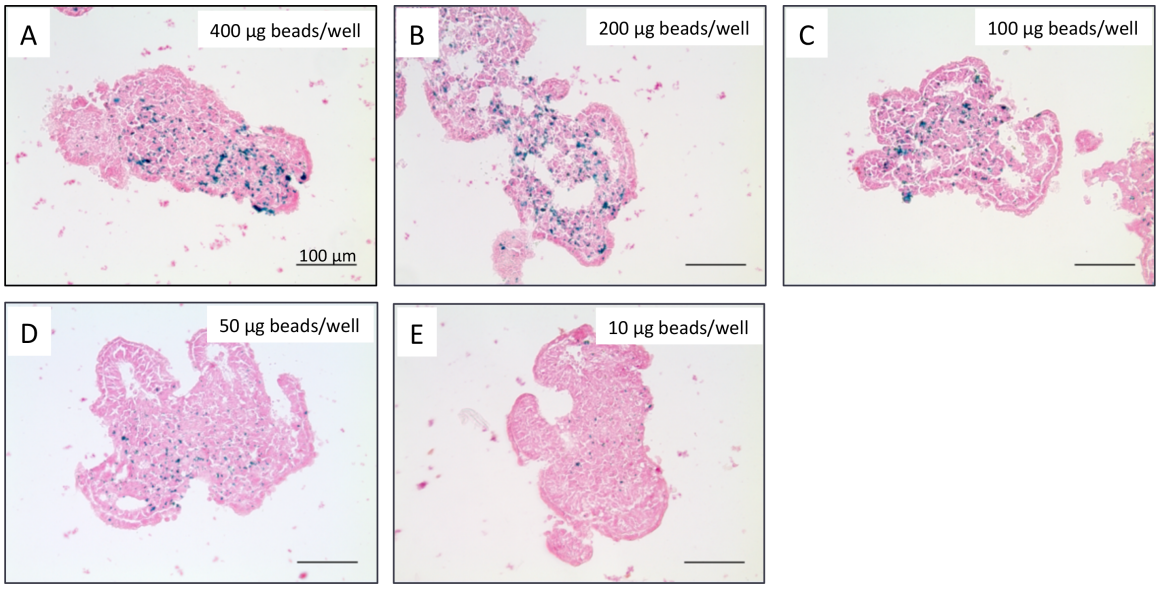

Figure 3.1: Prussian Blue staining of Day 7 EBs containing serial dilutions of paramagnetic beads. A range of bead concentrations was added to the Aggrewells, from 400µg/well to 10µg/well. Blue: beads, red: Nuclear Fast Red. Scale = 100 µm.

A

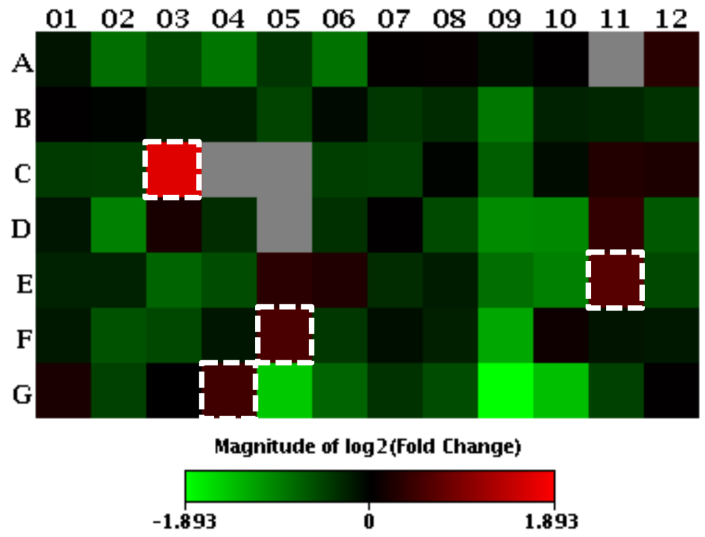

B

Layout	01	02	03	04	05	06	07	08	09	10	11	12
A	Actn1 **-1.10** OKAY	Actn2 **-1.76** B	Actn4 **-1.45** OKAY	Akt1 **-1.83** OKAY	Akt2 **-1.30** OKAY	Akt3 **-1.80** A	Arhgap5 **1.02** OKAY	Bcar1 **1.03** OKAY	Capn2 **-1.08** OKAY	Cav1 **1.01** B	Cav2 **1.17** C	Cav3 **1.23** B
B	Cdc42 **1.01** OKAY	Crk **-1.02** OKAY	Crkl **-1.18** OKAY	Ctnnb1 **-1.16** OKAY	Diap1 **-1.42** OKAY	Dock1 **-1.06** OKAY	Dst **-1.32** OKAY	Flna **-1.24** OKAY	Flnb **-1.86** OKAY	Fyn **-1.20** OKAY	Grb2 **-1.22** OKAY	Gsk3b **-1.29** OKAY
C	Hras1 **-1.35** OKAY	Ilk **-1.37** OKAY	Itga1 **3.17** B	Itga11 **1.17** C	Itga2 **1.17** C	Itga2b **-1.37** B	Itga3 **-1.39** OKAY	Itga4 **-1.02** B	Itga5 **-1.63** OKAY	Itga6 **-1.06** B	Itga7 **1.19** B	Itga8 **1.16** B
D	Itga9 **-1.12** B	Itgal **-1.92** B	Itgam **1.13** B	Itgav **-1.25** OKAY	Itgax **1.17** C	Itgb1 **-1.28** OKAY	Itgb2 **1.01** B	Itgb3 **-1.47** B	Itgb4 **-2.05** OKAY	Itgb5 **-2.03** OKAY	Itgb6 **1.29** B	Pak1 **-1.57** OKAY
E	Pak2 **-1.19** OKAY	Pak3 **-1.19** B	Pak4 **-1.67** OKAY	Parva **-1.47** A	Parvb **1.24** OKAY	Parvg **1.18** B	Pdpk1 **-1.26** OKAY	Pip5k1c **-1.16** A	Plec **-1.77** OKAY	Prkca **-1.93** B	Prkcb **1.55** B	Prkcc **-1.44** B
F	Pten **-1.13** OKAY	Ptk2 **-1.53** OKAY	Pxn **-1.45** OKAY	Rac1 **-1.12** OKAY	Rac2 **1.46** B	Raf1 **-1.31** OKAY	Rap1a **-1.07** OKAY	Rap1b **-1.17** OKAY	Rapgef1 **-2.37** OKAY	Rasgrf1 **1.07** B	Rhoa **-1.11** OKAY	Rock1 **-1.13** OKAY
G	Rock2 **1.14** OKAY	Shc1 **-1.40** OKAY	Sos1 **1.01** OKAY	Sos2 **1.38** B	Src **-2.84** A	Tln1 **-1.67** OKAY	Tns1 **-1.30** B	Vasp **-1.48** OKAY	Vav1 **-3.71** B	Vav2 **-2.67** A	Vcl **-1.38** OKAY	Zyx **1.01** OKAY

Figure 3.2: Focal Adhesion Protein expression of EBs containing unbound beads. The expression of focal adhesion proteins were compared between unloaded controls and bead-containing EBs 24 hours after EB formation. (A) Heat map of focal adhesion proteins. Highlighted boxes depict increased expression of proteins in bead-containing EBs. (B) Changes in transcript levels between bead-containing EBs and controls.

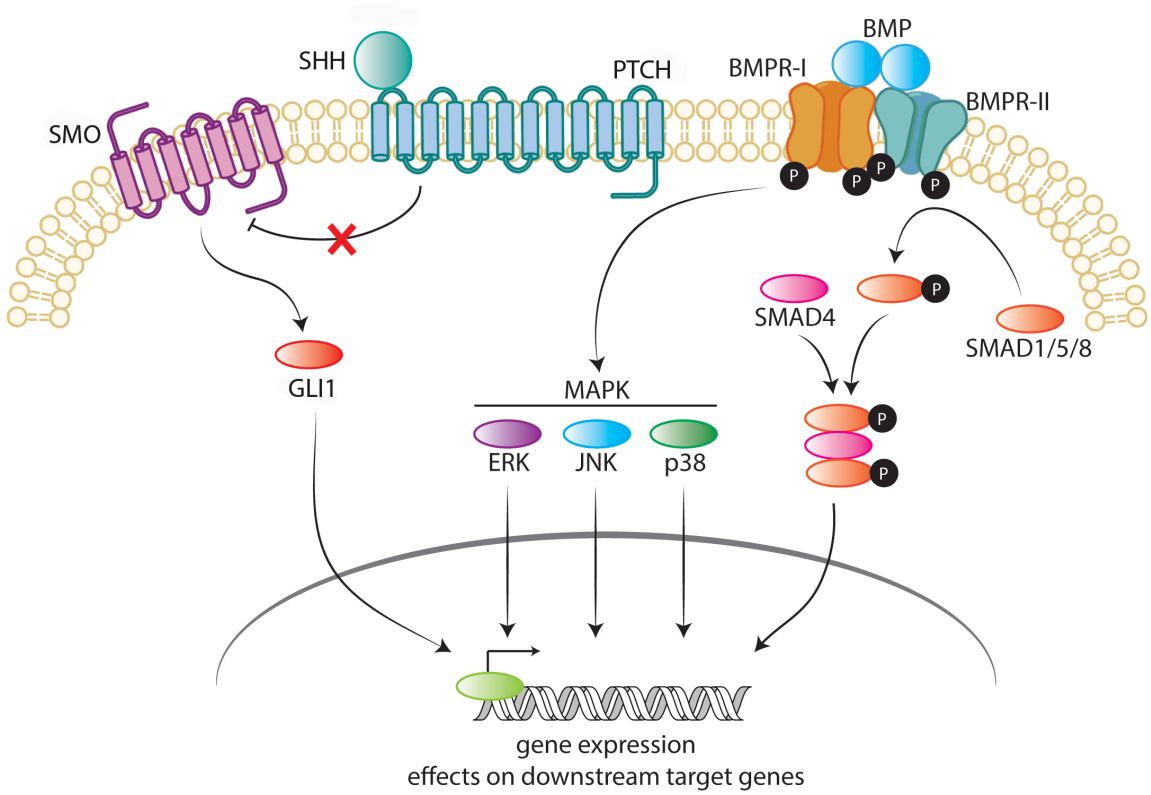

Figure 3.3. SHH and BMP signaling pathway overview. Shh binding to PTCH relieves Ptc inhibition of the receptor SMO. Activation of SMO results in the translocation of transcription factor GLI1 into the nucleus. BMP4 binds to serine-threonine kinase receptors, which results in signal transduction via the SMAD and MAP kinase pathways. Adapted from Anderson and Darshan, 2008 (Anderson & Darshan, 2008).

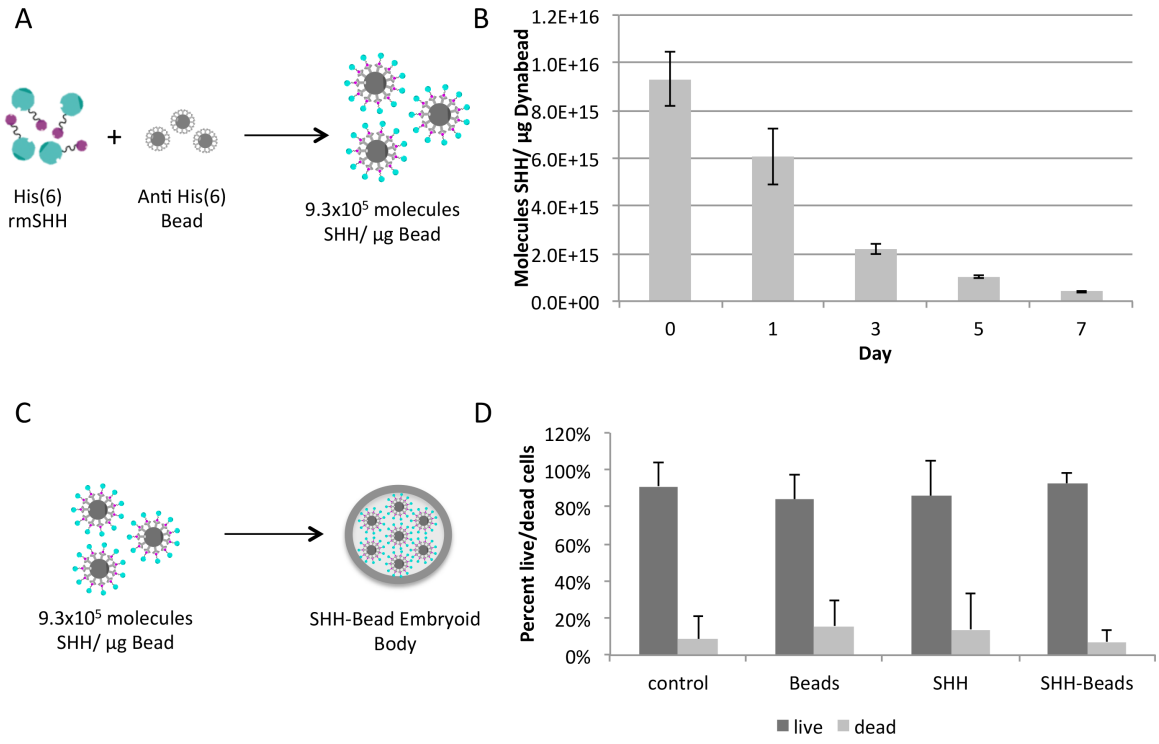

Figure 3.4: Efficiency of SHH-immobilization to beads and effect on cell viability. (A) His-tagged recombinant mouse SHH and Anti-His tag beads were co-incubated as recommended by the manufacturer to yield $9.3x10^5$ molecules of SHH/µg bead. (B) Viability of EBs with immobilized beads was unaffected compared to controls. Scale bars: standard deviation.

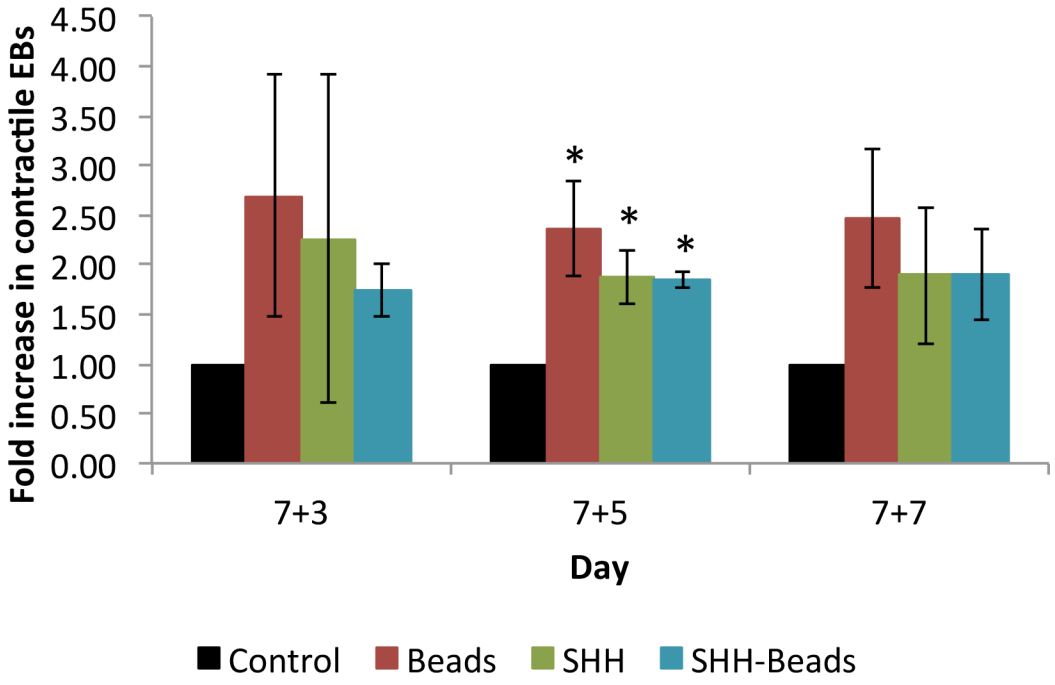

Figure 3.5: Minimal changes in contractile activity were observed in Bead- and SHH-treated groups. Only Day 12-EBs (5 days after plating Day 7-EBs on gelatin-coated plastic) showed significantly increased numbers of contractile cells compared to unloaded controls. Bars: standard error of the mean. *p<0.05.

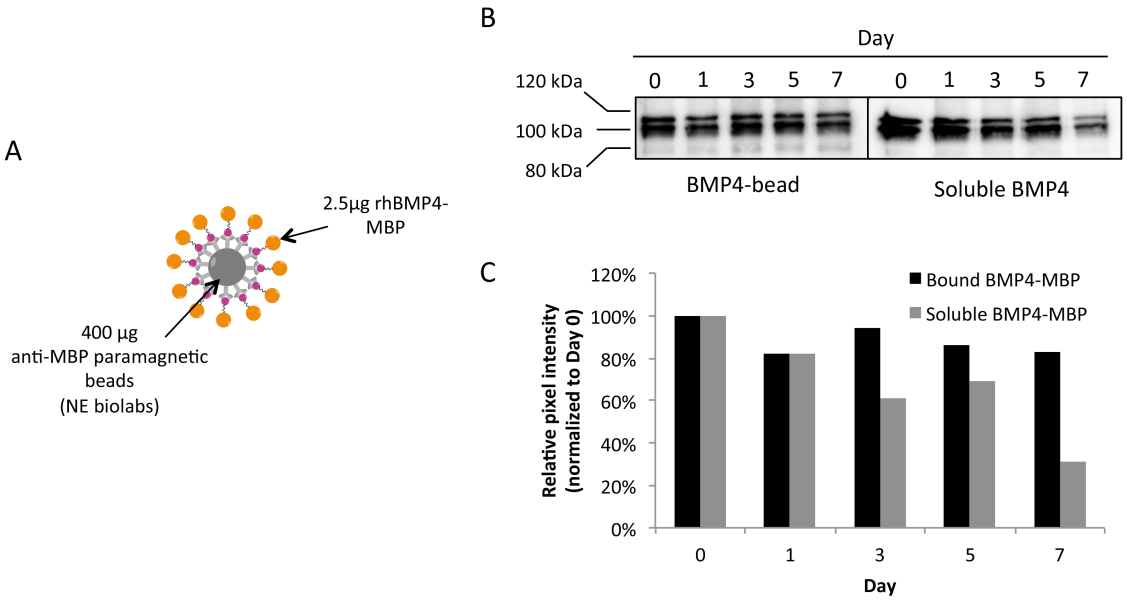

Figure 3.6: Efficiency of immobilizing BMP4-MBP to Anti-MBP paramagnetic beads. (A) 2.5 µg of BMP4 with a MBP tag was immobilized to 400 µg anti-MBP paramagnetic beads as directed by the manufacturer. (B) Concentration of eluted or soluble BMP4 detected on beads. (C) Relative pixel intensity of Western Blot bands in (B). Band intensity was normalized to Day 0 protein levels.

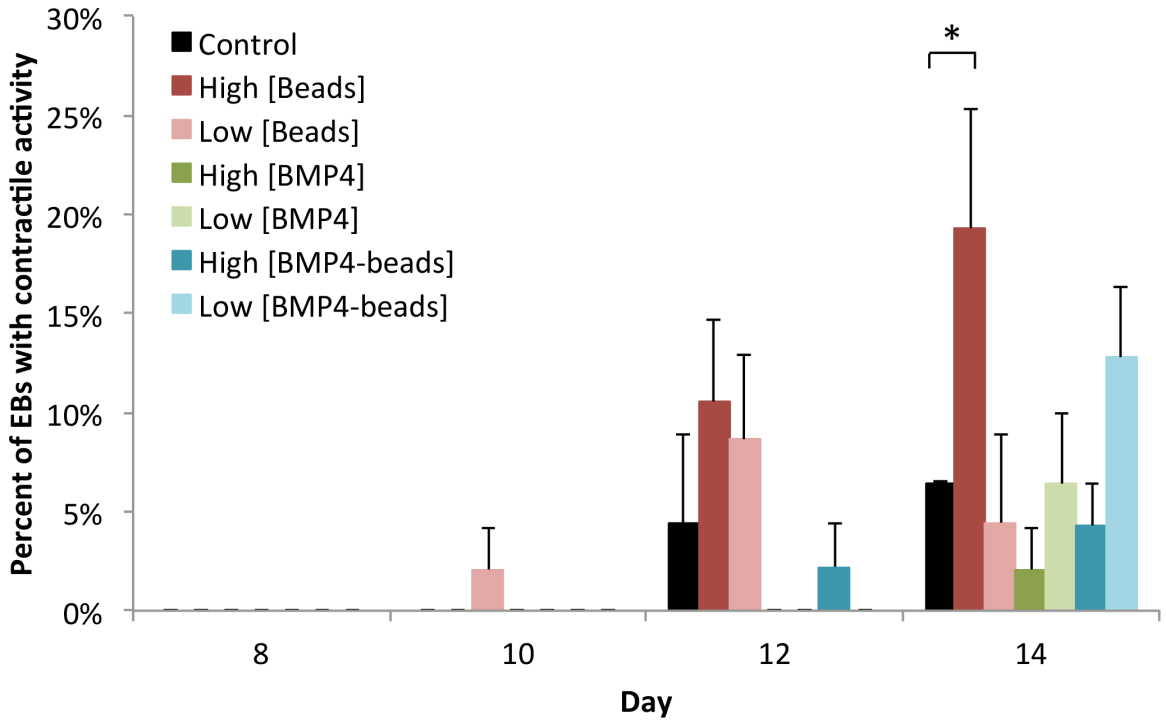

Figure 3.7: Contractile activity in EBs loaded with BMP4-beads. Contractile activity in EBs was monitored from Days 8 through 14. *p<0.05. Bars: standard error of the mean.

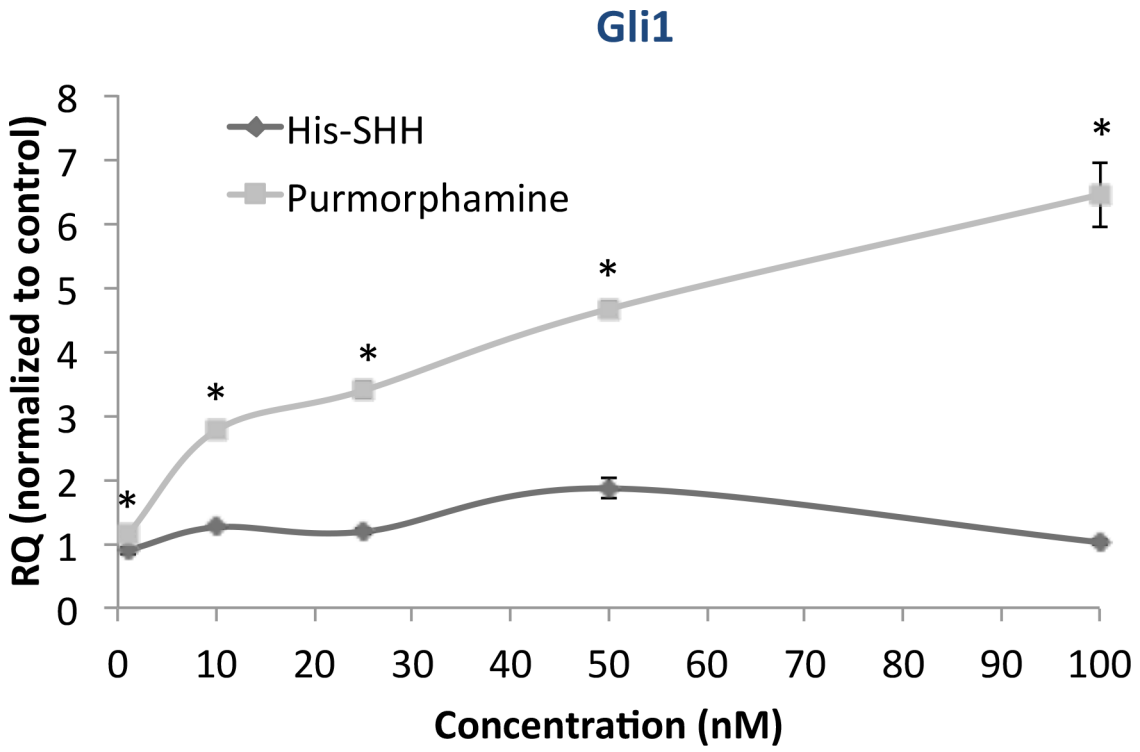

Figure 3.8: His-tagged SHH is less potent than the SHH agonist Purmorphamine. ESCs were incubated in low serum for 24 hours and supplemented with varying concentrations of His-tagged SHH or Purmorphamine. *Gli1* transcript expression was significantly higher in Purmorphamine-treated samples than His-tagged SHH-treated samples. Bars: standard deviation. *$p<0.05$.

3.6. REFERENCES

Ahmed, R. P. H., Haider, K. H., Shujia, J., Afzal, M. R., & Ashraf, M. (2010). Sonic Hedgehog gene delivery to the rodent heart promotes angiogenesis via iNOS/netrin-1/PKC pathway. *Plos One*, *5*(1), e8576. doi:10.1371/journal.pone.0008576

Aikawa, R., Nagai, T., Kudoh, S., Zou, Y., Tanaka, M., Tamura, M., et al. (2002). Integrins play a critical role in mechanical stress-induced p38 MAPK activation. *Hypertension*, *39*(2), 233–238.

Anderson, G. J., & Darshan, D. (2008). Small-molecule dissection of BMP signaling. *Nature Chemical Biology*, *4*(1), 15–16. doi:10.1038/nchembio0108-15

Bijlsma, M. F., & Spek, C. A. (2010). The Hedgehog morphogen in myocardial ischemia-reperfusion injury. *Experimental Biology and Medicine (Maywood, N.J.)*, *235*(4), 447–454. doi:10.1258/ebm.2009.009303

Bratt-Leal, A. M., Carpenedo, R. L., & Mcdevitt, T. C. (2009). Engineering the embryoid body microenvironment to direct embryonic stem cell differentiation. *Biotechnology Progress*, *25*(1), 43–51. doi:10.1002/btpr.139

Bratt-Leal, A. M., Carpenedo, R. L., Ungrin, M. D., Zandstra, P. W., & Mcdevitt, T. C. (2011). Incorporation of biomaterials in multicellular aggregates modulates pluripotent stem cell differentiation. *Biomaterials*, *32*(1), 48–56. doi:10.1016/j.biomaterials.2010.08.113

Bratt-Leal, A. M., Nguyen, A. H., Hammersmith, K. A., Singh, A., & Mcdevitt, T. C. (2013). A microparticle approach to morphogen delivery within pluripotent stem cell aggregates. *Biomaterials*, *34*(30), 7227–7235. doi:10.1016/j.biomaterials.2013.05.079

Carpenedo, R. L., Bratt-Leal, A. M., Marklein, R. A., Seaman, S. A., Bowen, N. J., Mcdonald, J. F., & Mcdevitt, T. C. (2009). Homogeneous and organized differentiation within embryoid bodies induced by microsphere-mediated delivery of small molecules. *Biomaterials*, *30*(13), 2507–2515. doi:10.1016/j.biomaterials.2009.01.007

Clement, C. A., Kristensen, S. G., Møllgård, K., Pazour, G. J., Yoder, B. K., Larsen, L. A., & Christensen, S. T. (2009). The primary cilium coordinates early cardiogenesis and hedgehog signaling in cardiomyocyte differentiation. *Journal of Cell Science*, *122*(17), 3070–3082. doi:10.1242/jcs.049676

Frank-Kamenetsky, M., Zhang, X. M., Bottega, S., Guicherit, O., Wichterle, H., Dudek,

H., et al. (2002). Small-molecule modulators of Hedgehog signaling: identification and characterization of Smoothened agonists and antagonists. *Journal of Biology*, *1*(2), 10.

Gianakopoulos, P. J., & Skerjanc, I. S. (2005). Hedgehog signaling induces cardiomyogenesis in P19 cells. *The Journal of Biological Chemistry*, *280*(22), 21022–21028. doi:10.1074/jbc.M502977200

Gianakopoulos, P. J., & Skerjanc, I. S. (2009). Cross talk between hedgehog and bone morphogenetic proteins occurs during cardiomyogenesis in P19 cells. *In Vitro Cellular & Developmental Biology. Animal*, *45*(9), 566–572. doi:10.1007/s11626-009-9228-z

Ingham, P. W., & McMahon, A. P. (2001). Hedgehog signaling in animal development: paradigms and principles. *Genes & Development*, *15*(23), 3059–3087. doi:10.1101/gad.938601

Kusano, K. F., Pola, R., Murayama, T., Curry, C., Kawamoto, A., Iwakura, A., et al. (2005). Sonic hedgehog myocardial gene therapy: tissue repair through transient reconstitution of embryonic signaling. *Nature Medicine*, *11*(11), 1197–1204. doi:10.1038/nm1313

Laflamme, M. A., Chen, K. Y., Naumova, A. V., Muskheli, V., Fugate, J. A., Dupras, S. K., et al. (2007). Cardiomyocytes derived from human embryonic stem cells in pro-survival factors enhance function of infarcted rat hearts. *Nature Biotechnology*, *25*(9), 1015–1024. doi:10.1038/nbt1327

Lee, M. Y., Bozkulak, E. C., Schliffke, S., Amos, P. J., Ren, Y., Ge, X., et al. (2011). High density cultures of embryoid bodies enhanced cardiac differentiation of murine embryonic stem cells. *Biochemical and Biophysical Research Communications*, *416*(1-2), 51–57. doi:10.1016/j.bbrc.2011.10.140

Lian, X., Zhang, J., Azarin, S. M., Zhu, K., Hazeltine, L. B., Bao, X., et al. (2013). Directed cardiomyocyte differentiation from human pluripotent stem cells by modulating Wnt/β-catenin signaling under fully defined conditions. *Nature Protocols*, *8*(1), 162–175. doi:10.1038/nprot.2012.150

Louis, H., Kakou, A., Regnault, V., Labat, C., Bressenot, A., Gao-Li, J., et al. (2007). Role of alpha(1)beta(1)-integrin in arterial stiffness and angiotensin-induced arterial wall hypertrophy in mice. *American Journal of Physiology Heart and Circulatory Physiology*, *293*(4), H2597–H2604. doi:10.1152/ajpheart.00299.2007

Renault, M.-A., Roncalli, J., Tongers, J., Thorne, T., Klyachko, E., Misener, S., et al.

(2010). Sonic hedgehog induces angiogenesis via Rho kinase-dependent signaling in endothelial cells. *Journal of Molecular and Cellular Cardiology*, *49*(3), 490–498. doi:10.1016/j.yjmcc.2010.05.003

Sachlos, E., & Auguste, D. T. (2008). Embryoid body morphology influences diffusive transport of inductive biochemicals: A strategy for stem cell differentiation. *Biomaterials*, *29*(34), 4471–4480. doi:10.1016/j.biomaterials.2008.08.012

Sargent, C. Y., Berguig, G. Y., & Mcdevitt, T. C. (2009). Cardiomyogenic differentiation of embryoid bodies is promoted by rotary orbital suspension culture. *Tissue Engineering Part A*, *15*(2), 331–342. doi:10.1089/ten.tea.2008.0145

Srichai, M. B., & Zent, R. (2009). Integrin Structure and Function. In R. Zent & A. Pozzi, (pp. 19–41). New York, NY: Springer New York. doi:10.1007/978-1-4419-0814-8_2

Thomas, N. A., Koudijs, M., van Eeden, F. J. M., Joyner, A. L., & Yelon, D. (2008). Hedgehog signaling plays a cell-autonomous role in maximizing cardiac developmental potential. *Development*, *135*(22), 3789–3799. doi:10.1242/dev.024083

Vokes, S. A., Yatskievych, T. A., Heimark, R. L., McMahon, J., McMahon, A. P., Antin, P. B., & Krieg, P. A. (2004). Hedgehog signaling is essential for endothelial tube formation during vasculogenesis. *Development*, *131*(17), 4371–4380. doi:10.1242/dev.01304

Willems, E., Spiering, S., Davidovics, H., Lanier, M., Xia, Z., Dawson, M., et al. (2011). Small-molecule inhibitors of the Wnt pathway potently promote cardiomyocytes from human embryonic stem cell-derived mesoderm. *Circulation Research*, *109*(4), 360–364. doi:10.1161/CIRCRESAHA.111.249540

Zeng, D., Ou, D.-B., Wei, T., Ding, L., Liu, X.-T., Hu, X.-L., et al. (2013). Collagen/β(1) integrin interaction is required for embryoid body formation during cardiogenesis from murine induced pluripotent stem cells. *BMC Cell Biology*, *14*, 5. doi:10.1186/1471-2121-14-5

CHAPTER FOUR

Magnetically mediated strain guides mouse embryonic stem cell differentiation into cardiomyocytes

Mechanical forces play an important role in proper embryologic development, and similarly such forces can directly impact pluripotency and differentiation of mouse embryonic stem cells (mESC) *in vitro*. In this study, we developed a mechanical stimulation regimen using permanent neodymium magnets to magnetically attract cells within an embryoid body (EB). Arginine-Glycine-Aspartic Acid (RGD)-conjugated paramagnetic beads were incorporated into the interior of the EBs during aggregation, allowing us to exert force on individual cells using short-term magnetization. EBs were stimulated for one hour at different magnetic field strengths, subsequently exerting a range of force intensity on the cells at different stages of early EB development. Our results demonstrated that following exposure to a 0.2 Tesla magnetic field, ESCs respond to magnetically mediated strain by activating Protein Kinase A (PKA) and increasing phosphorylated extracellular signal-regulated kinase 1/2 (pERK1/2) expression. The timing of stimulation can also be tailored to guide ESC differentiation: the combination of bone morphogenetic protein 4 (BMP4) supplementation with one hour of magnetic attraction on Day 3 enhances cardiomyogenesis by increasing contractile activity and the percentage sarcomeric α-actin-expressing cells compared to control samples with BMP4 alone. Together these results suggest that magnetically mediated strain can be used to increase the percentage of mouse ESC-derived cardiomyocytes over current differentiation protocols.

4.1. INTRODUCTION

Myocardial Infarction (MI) is one of the most prevalent diseases in America, accounting for approximately 50% (7.6 million) of the 15.4 million Americans suffering from coronary heart disease (Go et al., 2013). As an alternative to invasive surgical treatment options, cell therapy holds promise in promoting recovery following heart failure. For this strategy to be effective in a clinical setting, an adequate cardiomyocyte cell source must be identified. Differentiation of cardiomyocytes from progenitor cells such as pluripotent stem cells (PSCs) has the most potential to derive a large enough population to be a clinically relevant source. The most effective differentiation regimens include the addition of bone morphogenetic protein 4 (BMP4) to mouse embryonic stem cells (mESCs), as well as the supplementation of basic Fibroblast Growth Factor (bFGF), Activin, and Wnt to human embryonic stem cell (hESC) cultures (Yamashita et al., 2000). While the highest purity of the differentiated cardiomyocyte population is generated from ESC monolayer culture (up to 90-95% cardiomyocytes from hESCs) (Lian et al., 2013), establishing a protocol to efficiently differentiate ESCs within an embryoid body (EB) could potentially increase the final cell yield, which is a bottleneck for the clinical use of ESC-derived cardiomyocytes. To date, the highest cardiomyocyte yield from murine EB culture is approximately 20% (M. Y. Lee et al., 2011).

Mechanical stimulation has been well demonstrated to direct differentiation of many progenitor cell types, including ESCs. A variety of stimulation regimens have been used to differentiate PSCs into cardiomyocytes, the most common being fluid shear and cyclic strain (Geuss & Suggs, 2013). In general, the onset and duration of stimulation can

have the most profound effects on cardiomyogenesis. Short durations of cyclic strain in Day 4-6 mouse EBs increase the expression of CX 43 and mesodermal marker NKX 2.5 (Gwak et al., 2008; Heo & Lee, 2011; Schmelter, Ateghang, Helmig, Wartenberg, & Sauer, 2006), while exposure to strain at later time points (after Day 9) can inhibit mESC differentiation (Wan, Chung, & Kamm, 2011). In hESC monolayers, earlier exposure (Day 1 through 4) has been demonstrated to increase α-actinin expression and alignment (Tulloch et al., 2011). In Day 1 mouse ESC monolayers, as little as 30 minutes exposure to 10 dyn/cm^2 shear stress increases cardiovascular marker expression compared to controls (Toh & Voldman, 2011). Similar magnitudes have also been effective on Day 3 EBs attached to tissue culture plastic (Wolfe, Leleux, Nerem, & Ahsan, 2012).

Magnetic Twisting Cytometry (MTC) is another stimulation technique that has been widely used to study mechanotransduction in cells (Laboureau, Dubertret, Lebreton-De Coster, & Coulomb, 2004; Plopper & Ingber, 1993; N. Wang, Butler, & Ingber, 1993). This technique employs Arginine-Glycine-Aspartic Acid (RGD)-coated paramagnetic beads, which when attached to the cell surface via integrins induce strain on the cell during magnetization. MTC has recently been used to demonstrate that integrin-mediated forces can decrease pluripotency in mESCs (Chowdhury et al., 2009; Uda et al., 2011). In these experiments, single mESCs were plated and attached to RGD-Beads. The cells were exposed to an oscillatory stress (17.5 Pa and 0.3 Hz) for one hour, and changes in pluripotency marker expression were examined over time. The authors discovered that only an hour of stimulation was required to significantly decrease OCT 3/4 24 hours after exposure. These results demonstrated that pluripotency in ESCs can be

linked to integrin-RGD interactions and manipulation; however, the effects on terminal differentiation are still not well understood.

A challenge with mechanical stimulation of EBs is obtaining homogenous exposure of all cells within the EB to a similar magnitude of stress. In addition, few studies have compared the combinatorial effect of biochemical supplementation and mechanical stimulation. In this study, we hypothesized that magnetization of RGD-immobilized beads within an EB can activate stress-dependent signaling pathways in ESCs, and subsequently increase the population of cardiomyocytes. We have adapted the MTC-stimulation regimen by loading mouse EBs with RGD-beads and have examined the effect of magnetization at the earliest stages of EB development. Here, we report that magnetization directs lineage commitment in EBs, and the terminal phenotype is influenced by the onset of stimulation.

4.2. MATERIALS/METHODS

4.2.1. Embryonic Stem Cell Culture

R1 mouse ESCs (A. Nagy, Toronto, Canada) were expanded feeder-free on 0.1% gelatin-coated cell culture flasks (Stem Cell Technologies, Vancouver, Canada) in Growth Medium containing Knockout Dulbecco's Modified Eagle's Medium (Invitrogen, Grand Island, NY) supplemented with 15% ES-Cult Fetal Bovine Serum (Stem Cell Technologies), 1% Glutamax (Invitrogen), 1% Non-Essential Amino Acids (Invitrogen), 1% Nucleosides (Millipore, Billerica, MA), 1% Penicillin/Streptomycin (Invitrogen), 0.1mM β-Mercaptoethanol (Invitrogen) and 10^3 U/ml Leukemia Inhibitory

Factor (LIF; Millipore). Medium was changed in full each day, and cells were passaged every 2 days before reaching approximately 70% confluence.

4.2.2. Bead Preparation

RGD-Beads were prepared as previously described, with a few modifications (Laboureau et al., 2004; Plopper & Ingber, 1993). Briefly, 50 μg Peptite 2000 (Advanced Biomatrix, San Diego, CA) was bound to 1 mg of 1 μm BcMag™ tosyl-activated paramagnetic beads (Bioclone, San Diego, CA) for 72 hours at 4ºC in 0.1M Carbonate Buffer, pH 9 as suggested by the manufacturer. Acetylated-Low Density Lipoprotein (AcLDL, Biomedical Technologies, Stoughton, MA), which does not bind integrins or support stress transfer across the cell membrane (Maniotis, Chen, & Ingber, 1997), was used as a negative control and immobilized to the beads at the same concentration (50 μg protein/mg beads). The protein-bound beads were rinsed three times in PBS containing calcium and magnesium with a Dynal magnet (Invitrogen) and blocked for 1 hour in PBS containing 5% Bovine Serum Albumin (Sigma-Aldrich, St. Louis, MO). Following an additional three rinses in PBS, the beads were resuspended in medium and added to the Aggrewell 400™ plates at 1 mg beads per well.

4.2.3. Embryoid Body Formation and Bead Incorporation

ESCs were enzymatically released from the gelatin-coated plates with trypsin/EDTA (ATCC, Manassas, VA) and resuspended in Differentiation Medium (Growth Medium without LIF). Approximately 1.2 million cells were added to each well

of a 24-well Aggrewell 400™ plate (Stem Cell Technologies) as directed by the manufacturer. The final EB sizes were approximately 1,000 cells/EB. Once the EBs were allowed to settle for 30 minutes at 37ºC/5%CO_2, the beads were distributed to the appropriate wells. The EBs were kept in the Aggrewell 400™ plates for 3 days, and medium was partially changed daily. Day 3 EBs were transferred to suspension culture in ultra-low attachment plates and medium was changed in full every 2 days. In the BMP4-treated group, 10 ng/ml BMP4 was added from Days 1 through 7 as described previously (Taha & Valojerdi, 2008). On Day 7, the EBs were allowed to attach to gelatin-coated plates and maintained for up to 18 days at 37ºC/5%CO_2.

4.2.4. EB viability

EB viability was evaluated on Day 2 and Day 7 with a live/dead viability kit (Life Technologies) as described previously with a few modifications (Hwang et al., 2009). At each timepoint, the EBs were collected and rinsed in PBS containing calcium and magnesium and incubated in 2 μM calcein-AM and 4 μM ethidium homodimer diluted in PBS for 30 minutes at 37ºC on an end-to-end shaker. The EBs were imaged using a Zeiss scanning confocal microscope. Live and dead cells were labeled with calcein-AM (green) and ethidium homodimer (red), respectively.

4.2.5. β1 integrin inhibition

For β1 integrin blocking experiments, ESCs were trypsinized and incubated in 500 μg/ml Gly-Arg-Gly-Asp-Ser (GRGDS; Anaspec Inc, Fremont, CA) in serum-free

growth medium containing 10^3 U/ml LIF to prevent aggregation. The ESCs were incubated in ultra-low attachment plates at 37°C/5%CO_2 for 4 hours with gentle shaking. Immediately following incubation, the ESCs were aggregated using Aggrewell 400™ plates as described previously.

4.2.6. Spontaneous contractile activity

The presence of contractile areas in EBs was assessed as described previously (Sargent, Berguig, & Mcdevitt, 2009; Taha & Valojerdi, 2008). After 7 days of suspension culture, EBs were transferred to a 0.1% gelatin-coated 48-well plate using a 1 ml wide bore tip. Approximately 1-2 EBs were added to each well for a final count of 10-15 EBs per group. The EBs were monitored for 10 days after plating, with 70% medium changes every 2 days. At each timepoint, the percentage of EBs with contractile areas was calculated relative to the total number of EBs per group.

4.2.7. Flow Cytometry

EBs were collected on Day 18 to measure sarcomeric α-actin as described previously with a few modifications (Sargent et al., 2009). Following dissociation in Accumax (Stem Cell Technologies), the ESCs were incubated in anti-mouse sarcomeric α-actin (5c5, Sigma-Aldrich; 0.2 µl/100 µl reaction) for 45 minutes at room temperature in the dark with rotation. Mouse IgM isotype controls (Stem Cell Biotechnology) were included. Following another three rinses, the cells were incubated with goat anti-mouse IgM FITC (Stem Cell Biotechnology) for 30 minutes in the dark. The ESCs were

resuspended in 500 μl cold PBS at a final concentration of $1x10^6$ cells/ml. The number of sarcomeric α-actin positive cells was analyzed using an Accuri C6 Flow Cytometer (BD Biosciences) to capture a minimum of 10,000 events. Positive gates were set at 1% of the isotype control population. Analysis was performed using FlowJo software (Tree Star Inc, Ashland, OR).

4.2.8. SDS-Page and Western Blotting

Immediately following magnetization, EBs were collected from Aggrewell 400™ plates, rinsed in PBS, and disrupted in cold RIPA buffer (Santa Cruz Biotechnology, Santa Cruz, CA). The suspension was centrifuged for 10 minutes at 10,000xg at 4ºC. The supernatant was transferred to a 10 kDa MWCO filter unit (Millipore, Billerica, MA) and centrifuged at 10,000xg for 4 minutes at room temperature to concentrate the protein fraction. The protein was then inverted into a new tube and collected at 1,000xg for 2 minutes at room temperature. Total protein was analyzed by BCA assay (Thermo Scientific), and 10 μg protein was loaded into each lane of a 10% Mini-Protean TGX precast gel (Bio-rad, Hercules, CA). Following western transfer, the PVDF membranes were blocked for 1 hour in 5% Milk in TBST (Tris Buffered Saline with 0.05% Tween-20) and incubated overnight at 4ºC in rabbit anti-cAMP protein kinase catalytic subunit antibody (Abcam, 1:3000), rabbit anti-pERK1/2 antibody (Cell Signaling Technology, 1:400) or rabbit anti-ERK1/2 (Cell Signaling Technology, 1:1000) diluted in blocking buffer. After rinsing, the blots were incubated for 1 hour at room temperature in goat-anti rabbit HRP antibody (Santa Cruz Biotechnology, 1:1000). The signal was developed

using SuperSignal West Pico Substrate (Thermo Scientific) as directed by the manufacturer, and images were obtained with a FluorChem HD2 digital imager (Protein Simple, Santa Clara, CA). Band intensity was calculated and analyzed using AlphaView software (Protein Simple). The data represent the results of protein isolated from at least three independent experiments.

4.2.9. Histology and Immunostaining

EBs were fixed with 4% buffered formalin, rinsed in PBS, and resuspended in OCT solution (Thermo Scientific) for cryosectioning. Frozen sections (10 μm) were rehydrated for 10 minutes in PBS. Prussian Blue staining was performed to locate the beads within the EBs. The sections were incubated in a 1:1 solution of 20% aqueous hydrochloric acid: 10% aqueous potassium ferrocyanide for 20 minutes at room temperature. Following three rinses in distilled water, the slides were counterstained in Nuclear Fast Red (Sigma-Aldrich) for 5 minutes at room temperature. The slides were rinsed twice in distilled water, cleared and mounted with Cytoseal (Thermo Scientific).

For immunostaining, epitope retrieval was performed using 0.25% trypsin solution (Thermo Scientific) for 20 minutes at 37ºC in a humidified chamber. To detect intracellular protein, samples were permeabilized in 0.5% Triton-X in PBS for 10 minutes at room temperature. After rinsing, sections were blocked for 1 hour at room temperature in 10% normal goat serum (NGS) or normal donkey serum (NDS). The samples were incubated overnight at 4ºC in rat anti-integrin β1 (Abcam, Cambridge, MA, 1:100 in 1% NDS), mouse anti-sarcomeric α-actin (5c5, Sigma Aldrich, 1:500 in 1%

NGS) or rabbit anti-connexin 43 (CX 43, Cell Signaling Technologies, 1:250 in 1% NGS). The sections were rinsed in TBST and incubated in goat anti-mouse IgM FITC (Abcam, 1:100 in 1% NGS), goat anti-rabbit Alexa Fluor 488 (Invitrogen, 1:500 in 1% NGS) or donkey anti-rat Alexa Fluor 594 (Invitrogen, 1:500 in 1% NDS) for 1 hour at room temperature. The samples were counterstained with 5 μg/ml 4',6-diamidino-2-phenylindole (DAPI, Life Technologies) for 15 minutes and mounted with Prolong Gold antifade reagent (Life Technologies). Beta 1 integrin images were taken using a Leica DMI2000B microscope with a Leica DFC290 camera. CX 43 and sarcomeric α-actin images were taken using a Zeiss scanning confocal microscope.

4.2.10. Statistics

Statistical analysis was performed using StatPlus LE software (AnalystSoft). All groups analyzed represent three independent experiments. Data from each of the groups was compared using one-way ANOVA coupled with Tukey's Post Hoc test. Values are reported as mean ± standard deviation unless indicated otherwise. *p*-values less than 0.05 were considered statistically significant.

4.3. RESULTS

4.3.1. Paramagnetic beads do not affect EB morphology

To prepare the EBs, we used Aggrewell 400™ plates to aggregate the ESCs and also facilitate bead incorporation within the aggregate. By FACS analysis, we calculated that the approximate number of beads loaded into each EB was 500 beads/EB (data not

shown). We confirmed the bead incorporation procedure by light microscopy and Prussian Blue staining on sectioned EBs, in which the latter stains ferric ions a blue color. In comparison to the control EBs with no beads (Figure 4.1 A, A'), the EBs with the magnetic beads were darker in light micrographs (Figure 4.1B), and the beads appeared distributed throughout the entire EB (Figure 4.1B'). To examine the effects of beads or magnetization on EB gross morphology, we quantified EB size 24 hours after magnetic attraction. No significant differences were observed regardless of bead incorporation or magnetization (Figure 4.1C).

4.3.2. Magnetic field strength proportionally increases force on cells by RGD-Beads

In this study, we used RGD-immobilized paramagnetic beads to exert mechanical stimuli to cells within the interior of EBs. As mentioned previously, Uda *et al* (2011) demonstrated that one hour of MTC using RGD-beads decreased pluripotency markers in mESCs (Uda et al., 2011). In this study, we investigated how magnetization at different field strengths can affect mechanotransduction in murine EBs. We had previously observed that cycling neodymium magnets underneath EBs resulted in a continuous attraction of the EBs to the magnets. In our stimulation regimen, an array of neodymium magnets with different thicknesses and field strengths were placed on an orbital shaker at 37ºC/5%CO_2 (Figure 4.2A). These magnets were cycled at 42 rpm one quarter inch underneath an immobilized Aggrewell plate, which allowed us to exert a continuous magnetic field while minimizing fluid shear forces on the cells.

For our magnetic attraction experiments, we compared three types of neodymium magnets with different magnetic field strengths: ¾" x ⅛" N42 neodymium magnets, ¾" x ¼" N42 neodymium magnets, and ¾" x ½" N42 neodymium magnets (K&J Magnetics). Using a gaussmeter, we calculated that the magnetic field strengths were 0.128 Tesla, 0.2 Tesla and 0.4 Tesla respectively with the EBs placed one-quarter inch above the magnets. To model the force acting on the EBs, the cycle of magnet rotation was divided into 126 frames using a customized Matlab program (Mathworks, Natick, MA) where each frame differs by 0.05 radians. At every frame, the magnetic field at each position was modeled. The force ($\vec{F}$) acting on each point within the wells was calculated using

$$\vec{F} = \frac{v_m \Delta x}{\mu_0} \left(\vec{B} \cdot \nabla\right) \vec{B} \quad (1)$$

where B is the magnetic field, v_m is the total volume of the magnetic material, Δx is the effective magnetic susceptibility of the RGD-Bead attached to the cell and μ_0 is the magnetic constant in a classical vacuum as described previously (Zborowski, Sun, Moore, Stephen Williams, & Chalmers, 1999). The magnitude of force applied to the cells during magnetization was summarized for each of the points and averaged for each Aggrewell over 1 minute (42 cycles). From these calculations, we approximated that the force exerted on the cells was 10 piconewton (pN) at 0.128 Tesla (Figure 4.2B), 20 pN at 0.2 Tesla (Figure 4.2C), and 80pN at 0.4 Tesla (Figure 4.2D).

4.3.3. High field strengths negatively affect short term but not long term viability

We next sought to determine whether there was any negative effect of magnetic attraction on cell viability. We performed live/dead staining on the EBs 24 hours following stimulation to examine any effects on immediate cytotoxicity, as well as on Day 7 to compare effects on long-term viability. After 24 hours, there was no difference in the number of dead cells within the EBs containing RGD-Beads maintained under static conditions (Figure 4.3A), 0.128 Tesla (Figure 4.3B) or 0.2 Tesla magnetic fields (Figure 4.3C); however, more dead cells were stained in EBs exposed to a 0.4 Tesla magnetic field (Figure 4.3D). In contrast, there was no evident effect of magnetic field strength on long-term viability in EBs with RGD-Beads (Figure 4.3A'-D'). No effect on viability was observed in EBs containing AcLDL-Beads, which do not bind to integrins, or EBs without beads at any of the field strengths tested (Figure 4.4).

4.3.4. Mechanotransduction in EBs in response to magnetization

Integrins have been well established to play an integral role in the transmission of mechanical signals in cells (Matthews, Overby, Mannix, & Ingber, 2006), and their manipulation via mechanical forces has been observed to increase small molecule expression and subsequent activation of a variety of signaling cascades (Alenghat, Tytell, Thodeti, Derrien, & Ingber, 2009; Laboureau et al., 2004). In response to mechanical stress, cAMP levels increase, subsequently activating cAMP protein kinase (Protein Kinase A, PKA) (Bukoreshtliev, Haase, & Pelling, 2013; Meyer et al., 2000). In this study, we investigated the effects of magnetically mediated strain on PKA levels in EBs.

As a negative control, we also incorporated AcLDL-beads within EBs, which is a standard control for MTC because they do not specifically bind integrin (N. Wang et al., 1993).

In the absence of magnetic attraction, PKA expression was observed in all samples regardless of the presence of RGD- or AcLDL-Beads (Figure 4.5A,E). Following one hour of exposure to a 0.128 Tesla field, there was no difference in the amount of PKA observed between samples (Figure 4.5B,F). As the field strength increased to 0.2 Tesla, significant differences in PKA expression could be observed between groups. While there was no difference in PKA between controls and AcLDL-Bead groups, levels increased approximately 6-fold in EBs containing RGD-Beads (Figure 4.5C,G). As the field strength increased to 0.4 Tesla, PKA levels decreased to the level of the unloaded and AcLDL-Bead controls (Figure 4.5D,H).

To further verify that the increases in PKA were the result of integrin activation by RGD-Beads, we examined the effects of magnetization on β1 integrin expression and blocking by GRGDS. Positive β1 integrin immunostaining was observed in EBs containing both AcLDL- and RGD-Beads (Figure 4.5I,J). Following GRGDS inhibition, PKA levels were decreased in magnetized samples containing RGD-Beads (Figure 4.5K). The involvement of β1 integrin was also verified by PKA levels in AcLDL-Bead containing EBs: there was no change in PKA expression between static and magnetized groups.

Since the onset of mechanical stimulation can have different effects on ESC differentiation (Geuss & Suggs, 2013), we also investigated how the timing of magnetic

mediated stress affects mechanotransduction in EBs. Regardless of whether stimulation was initiated on Day 1 (Figure 4.6A), Day 2 (Figure 4.6B) or Day 3 (Figure 4.6C), the expression of pERK1/2, whose expression is correlated to integrin activation (Laboureau et al., 2004; Offenberg Sweeney et al., 2004), was significantly increased following magnetic attraction. PKA expression was also significantly increased in Day 1 and 3 samples (Figure 4.6A,C). These results demonstrate that EBs can sense and respond to mechanical stress throughout the earliest stages of differentiation.

4.3.5. Timing of stimulation affects cardiomyogenesis in EBs

Based on our observation that EBs are able to respond to mechanical signals at different timepoints (Figure 4.6), we sought to examine the effect of attraction timing on differentiation. ESC differentiation into cardiomyocytes has been observed following exposure to multiple types of mechanical stimuli, including shear (Wan et al., 2011) and cyclic (Gwak et al., 2008; Salameh et al., 2010; Shimizu et al., 2008) forces; however, the effect of magnetic attraction on cardiomyogenesis from pluripotent cells has not yet been investigated. To investigate the effect of magnetically mediated strain on ESC differentiation, we exposed the EBs to a 0.2 Tesla magnetic field, as this strain magnitude most effectively increased PKA expression while maintaining cell viability (Figures 4.3, 4.4, 4.5). EBs were stimulated for 1 hour on Day 1, Day 2 or Day 3. Since BMP4 supplementation is currently the most effective regimen for differentiating mouse ESCs into cardiomyocytes (Taha & Valojerdi, 2008), we also compared the combinatorial effects of BMP4 and mechanical stimulation (Figure 4.7A).

Stimulation of early EBs, specifically on Day 1 (Figure 4.7B) or Day 2 (Figure 4.7C), did not appear to have any significant effect on cardiomyocyte differentiation, as the percentage of contractile foci were comparable to controls with or without BMP4 supplementation. When BMP4 was added to the medium during suspension culture, Day 3-stimulated EBs (Figure 4.7D) containing the RGD-Beads had significantly higher percentages of contractile foci compared to controls by Day 17 (33%±14% versus 4%±7%). The presence of beads alone also appeared to have an effect on contractile activity compared to controls; however, only AcLDL-Bead-containing EBs had significantly higher levels than controls (18%±8%). These trends were not observed when BMP4 was omitted from the medium (Figure 4.7D).

Considering the difference in contractile activity, we further examined the expression of sarcomeric α-actin within the Day 3-stimulated EBs on Day 18 by FACS analysis and immunostaining. For the former, in the presence of BMP4 there was a shift in fluorescence intensity in all EBs (Figure 4.8B) compared to those which were not exposed to BMP4 (Figure 4.8A). In the absence of BMP4, there were no significant differences between the control and EBs containing either AcLDL-Beads or RGD-Beads (Figure 4.8C). With BMP4 added to the medium, there were significantly more sarcomeric α-actin positive cells in stimulated EBs containing RGD-Beads (33.2%±3.8%) compared to unloaded controls (22.0%±1.1%)(Figure 4.8D). Connexin 43 (Figure 4.8E) and sarcomeric α-actin (Figure 4.8F) immunostaining was observed sections of Day 18 EBs released from gelatin-coated plastic. Expression was observed in

the vicinity of beads (labeled as "b"), which could not be observed directly by confocal microscopy but appeared as a shadow in the micrographs.

4.4. DISCUSSION

In this study, we developed a unique method to expose a larger population of ESCs within an EB to mechanical strain. We demonstrated that RGD-Beads, such as those used for MTC, can be incorporated into the interior of the EB and bind to cells within that EB. By adjusting the thickness of the magnets, and consequently the magnetic field strength, we can take advantage of the RGD-integrin interactions to induce strain on the individual cells without compromising viability. A complication that occurs with current mechanical stimulation regimens is that ESCs experience non-uniform forces, which produce the same heterogeneous cell population that would occur naturally without stimulation. Immobilization of RGD-Beads within the EB interior has the potential to reduce this variability. In addition, this process does not impact differentiation protocols that would depend on suspension culture during downstream processing.

A benefit of this mechanical stimulation regimen is that it is a cost-effective method to present a permanent magnetic field to cells in culture. The magnetic field strength can be easily adjusted by altering the strength of the neodymium magnets, and the force acting on the cells in response to magnetization can be deduced using the equation developed by Zborowski *et al* (1999) for a magnetized cell in a quadripole field (Equation 1) (Zborowski et al., 1999). Overall, our results confirm previous findings that

ESCs are responsive to integrin-mediated forces, and these forces lead to outside-in signaling cascades that can direct cell fate (Chowdhury et al., 2009; Uda et al., 2011). These forces can be assessed by the expression of small molecules and proteins, such as PKA and pERK1/2, which are well established to be directly regulated by mechanical stimulation (Figures 4.5, 4.6) (Alenghat et al., 2009; Laboureau et al., 2004; Meyer et al., 2000). Consequently, the same methods that are used to study mechanical signal transmission in differentiated cells can be applied to pluripotent stem cells.

In general, there is limited information about the amount of force required by cells to activate signaling or respond to external stress. This has been most recently addressed by Wang *et al* (2013), whom have developed a Tension Gauge Tether (TGT) technique to quantify the amount of force required to activate integrin and Notch signaling cascades in immortalized CHO cells (X. Wang & Ha, 2013). The authors reported that Notch signaling was activated by less than 12 pN force, and that cells apply approximately 40 pN force to single integrin-ligand adhesions. Forces above 40 pN result in stress fiber formation *in vitro*. Based on our model, 0.2 Tesla magnetic fields exert approximately 20 pN force on the ESCs. Doubling the magnetic field to 0.4 Tesla exerts almost 80 pN force, which negatively affects signal transduction and viability. While we would predict that 20 pN would be too low to transmit mechanical signals, our results suggest that this magnitude is sufficient to activate integrins. There are a few possible explanations for this discrepancy: (1) there may be differences in force sensitivity between differentiated and pluripotent stem cells or (2) there may be other forces experienced by the cells within the EB, such as shear forces between cells, that are not adequately represented by either

model. In the future, a better understanding of the range of forces and force strengths being experienced during ESC aggregation may clarify these questions.

Cell-matrix interactions, and their manipulation, have been widely observed to play important roles in directing pluripotent cell fate (Battista et al., 2005; Brafman, Phung, Kumar, & Willert, 2013; Chowdhury et al., 2009; Dawson et al., 2011; Pimton et al., 2011; Yanada et al., 2006). Considering mechanical stimulation can direct cardiomyogenesis from pluripotent cells (Geuss & Suggs, 2013), we asked whether magnetic attraction can similarly direct differentiation. Timing the onset of mechanical stimulation can have drastic effects on fate determination in regards to cardiovascular phenotypes. While short term applications of cyclic strain between days 4 and 7 during EB development increase the percentage of differentiated cardiomyocytes (Gwak et al., 2008; Heo & Lee, 2011; Schmelter et al., 2006), early and prolonged exposure maintains pluripotency (Saha, Ji, de Pablo, & Palecek, 2006; 2008). Our results similarly suggest that cardiomyogenesis in EBs is most effective when mechanical stimulation is initiated later during EB development, around Day 3. This was made evident by maintained contractile activity at Day 17 and significantly increased sarcomeric α-actin expression (Figures 4.7, 4.8). Interestingly, this is only observed when BMP4, which is the most effective morphogen for mESC differentiation into cardiomyocytes, is supplemented to culture medium. Considering that Brachyury expression, a marker for mesendoderm (Kattman, Huber, & Keller, 2006), peaks around Day 3 and 4 of EB development (Boheler et al., 2002; Bratt-Leal, Nguyen, Hammersmith, Singh, & Mcdevitt, 2013; Czyz & Wobus, 2001), this would suggest that pre-differentiation of EBs towards mesodermal

fates prior to the onset of mechanical stimulation is optimal for cardiomyogenesis *in vitro*. Therefore, while mechanical stimulation by magnetization is alone not sufficient to drive differentiation, it can be combined with other protocols to enhance cardiomyocyte differentiation.

To date, there are few studies that have been able to investigate the effects of early mechanical stimulation on the terminal phenotype of ESCs. Often this issue is due to logistics: there is a minimum amount of time required to allow EBs to attach to culture surfaces and also acclimate to new environments prior to exposure to stress. While this study primarily focused on cardiomyocyte differentiation, earlier exposure to magnetization (Days 1-2) may be driving differentiation into other phenotypes. This is suggested by preliminary data, in which EBs magnetized on Day 1 express significantly less SSEA-1, a marker for mouse ESC pluripotency, by Day 7 compared to EBs stimulated on Day 2 or 3 (data not shown). Further investigation into the effects of integrin-RGD interactions, and how they change during the first few days of EB differentiation, will be useful for tailoring magnetic attraction to derive specific differentiated cells.

4.5. CONCLUSIONS

Our data showed that magnetically mediated strain applied by RGD-immobilized paramagnetic beads activates mechanochemical signaling in murine EBs. We also observed that ESC response to strain is dependent on the magnetic field strength, as high field strengths can apply too much force on the cells, resulting in cell death.

Magnetically mediated strain can also be used to direct differentiation of mESCs into cardiomyocytes; however guiding the mesodermal commitment of mESCs prior to the onset of stimulation is required. Conceivably, this system may be tailored to derive other cell types that are similarly influenced by mechanical forces by altering the medium supplements and timing accordingly.

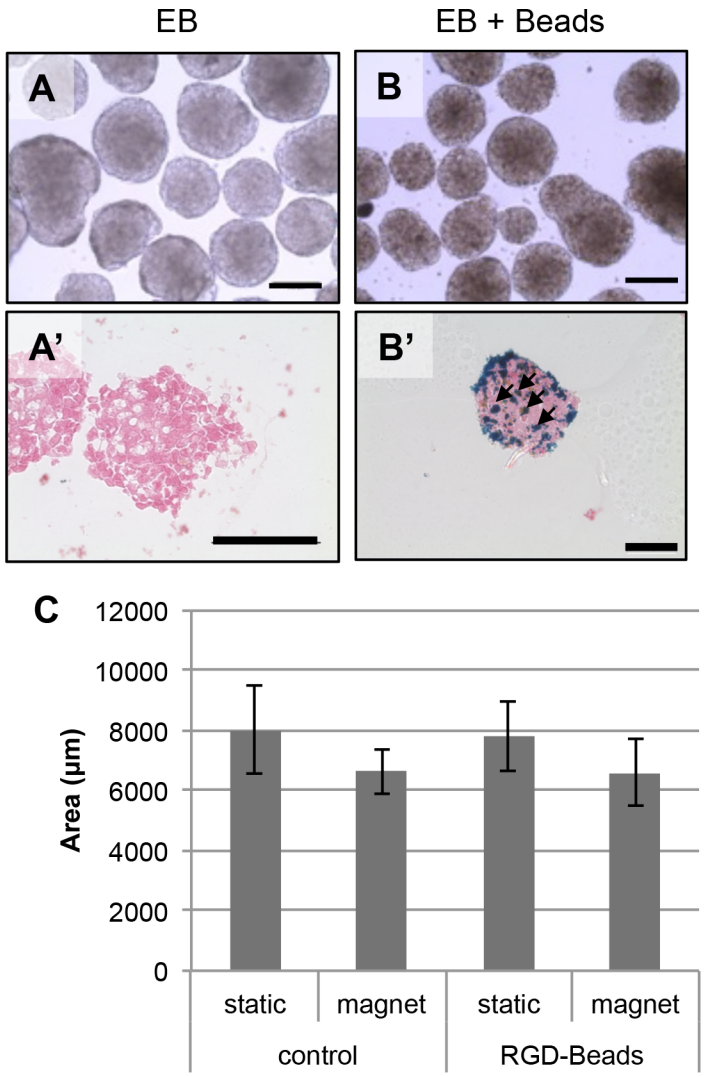

Figure 4.1: Gross morphology of EBs with immobilized beads. Bead incorporation was confirmed by light micrographs (A-B) and Prussian Blue staining (A'-B'). (C) Size comparison of EBs with or without magnetization. Arrows indicate location of beads within EB. Scale: 100 µm.

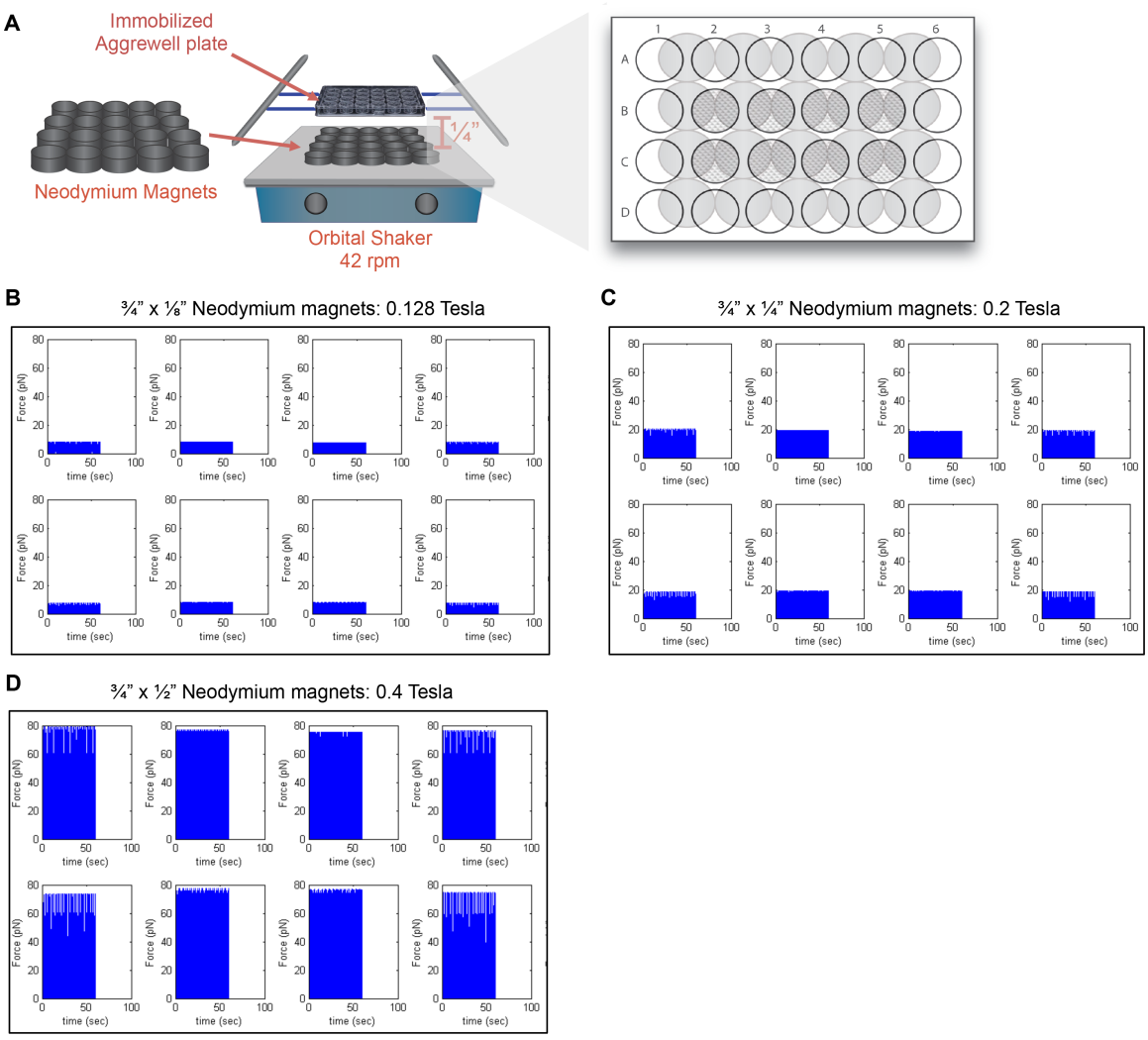

Figure 4.2: Magnetic attraction apparatus setup. (A) An array of N42 permanent neodymium magnets with different thicknesses were arranged on an orbital shaker. The force applied to the cells was modeled using a customized Matlab program over the course of 1 min (42 cycles) at 0.128 Tesla (B), 0.2 Tesla (C), and 0.4 Tesla (D).

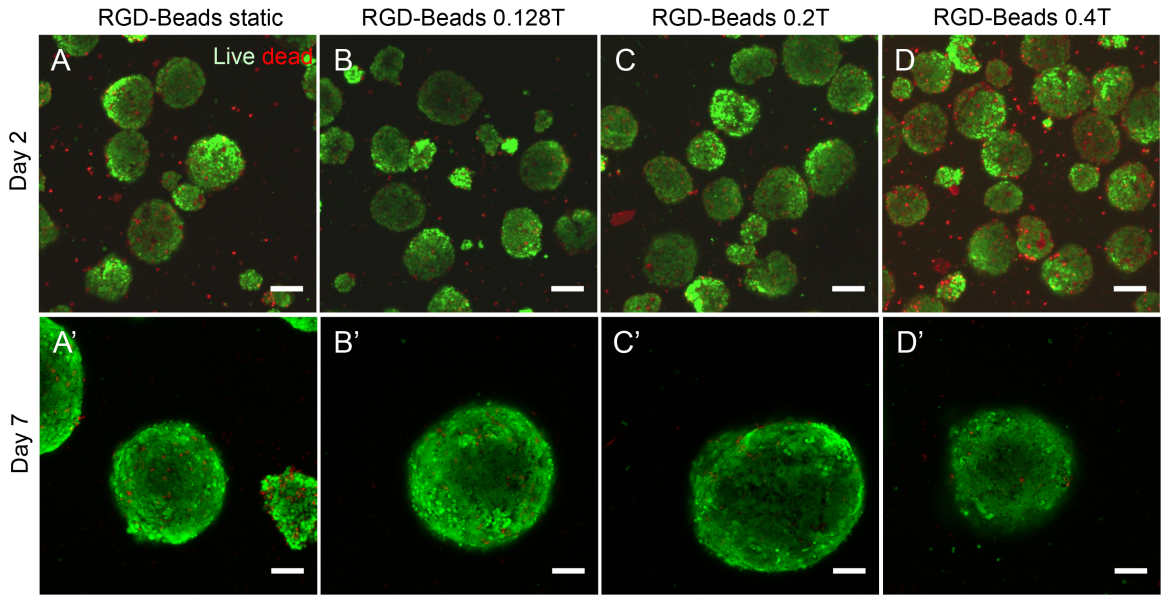

Figure 4.3: Live/dead analysis of EBs containing RGD-Beads following magnetization. Live/dead was analyzed by confocal microscopy 24 hours after magnetic attraction (A-D) or 6 days after magnetic attraction (A'-D'). Scale bar: 100 μm.

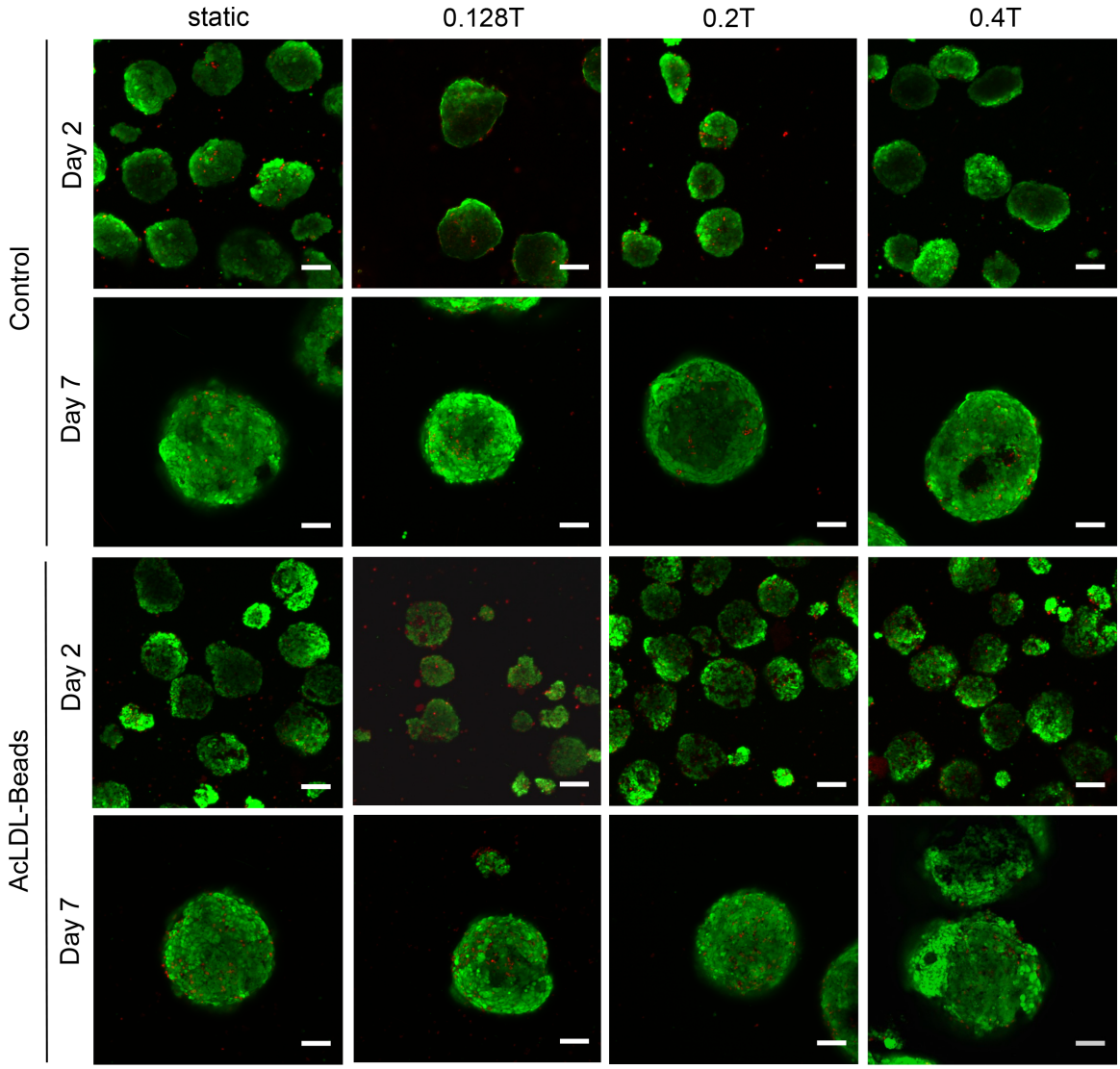

Figure 4.4: Live/dead imaging of EBs with or without AcLDL-Beads. Live cells (green) and dead cells (red) were observed in controls and EBs with AcLDL-beads 24 hours after magnetization and 6 days after magnetization on Day 1. Scale = 100 μm.

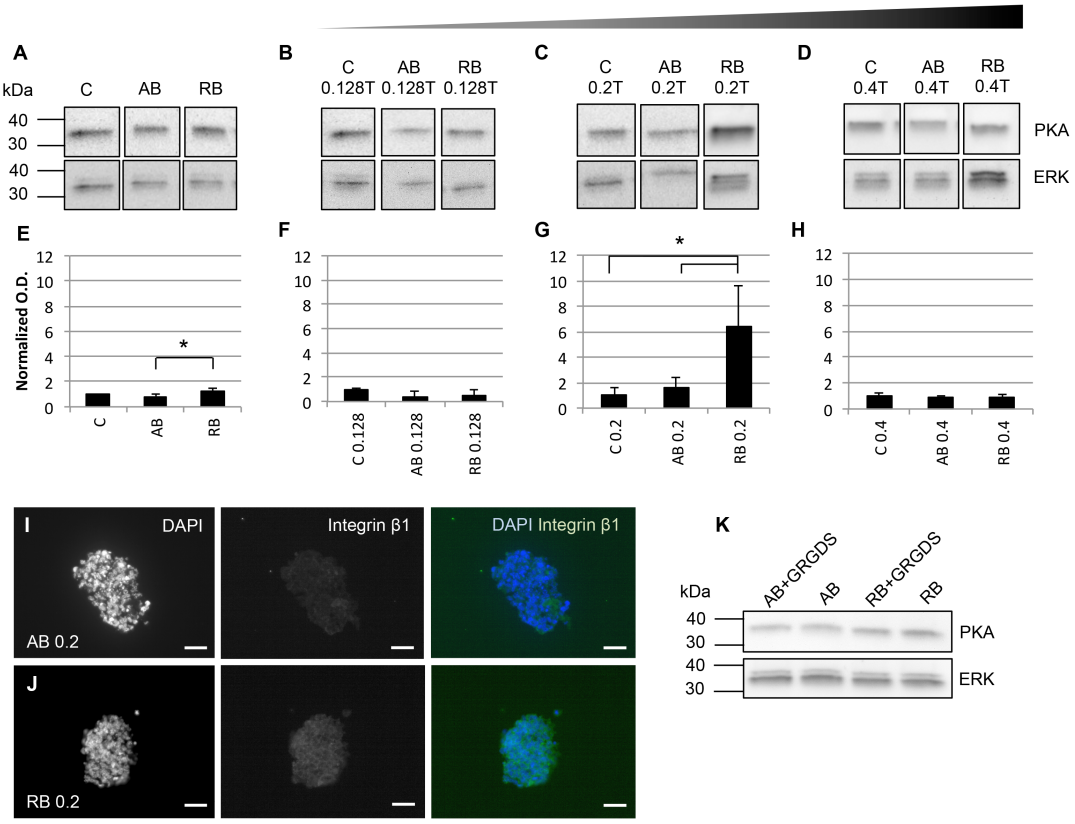

Figure 4.5: Second messenger marker expression in response to magnetic attraction. EBs incubated in static conditions (A,E) were compared to EBs exposed to 0.128 Tesla magnetic fields (B,F), 0.2 Tesla magnetic fields (C,G) and 0.4 Tesla magnetic fields (D,H). (A-D) Representative western blots under each condition. (E-H) Normalized PKA expression relative to ERK. (I) β1 integrin immunostaining in EBs with AcLDL-Beads and (J) RGD-Beads 24 hours following stimulation at 0.2 Tesla. Scale = 20 μm. (K) Effect of β1 integrin inhibition by GRGDS on PKA expression. C: control, AB: AcLDL-Beads, RB: RGD-Beads. *p<0.05

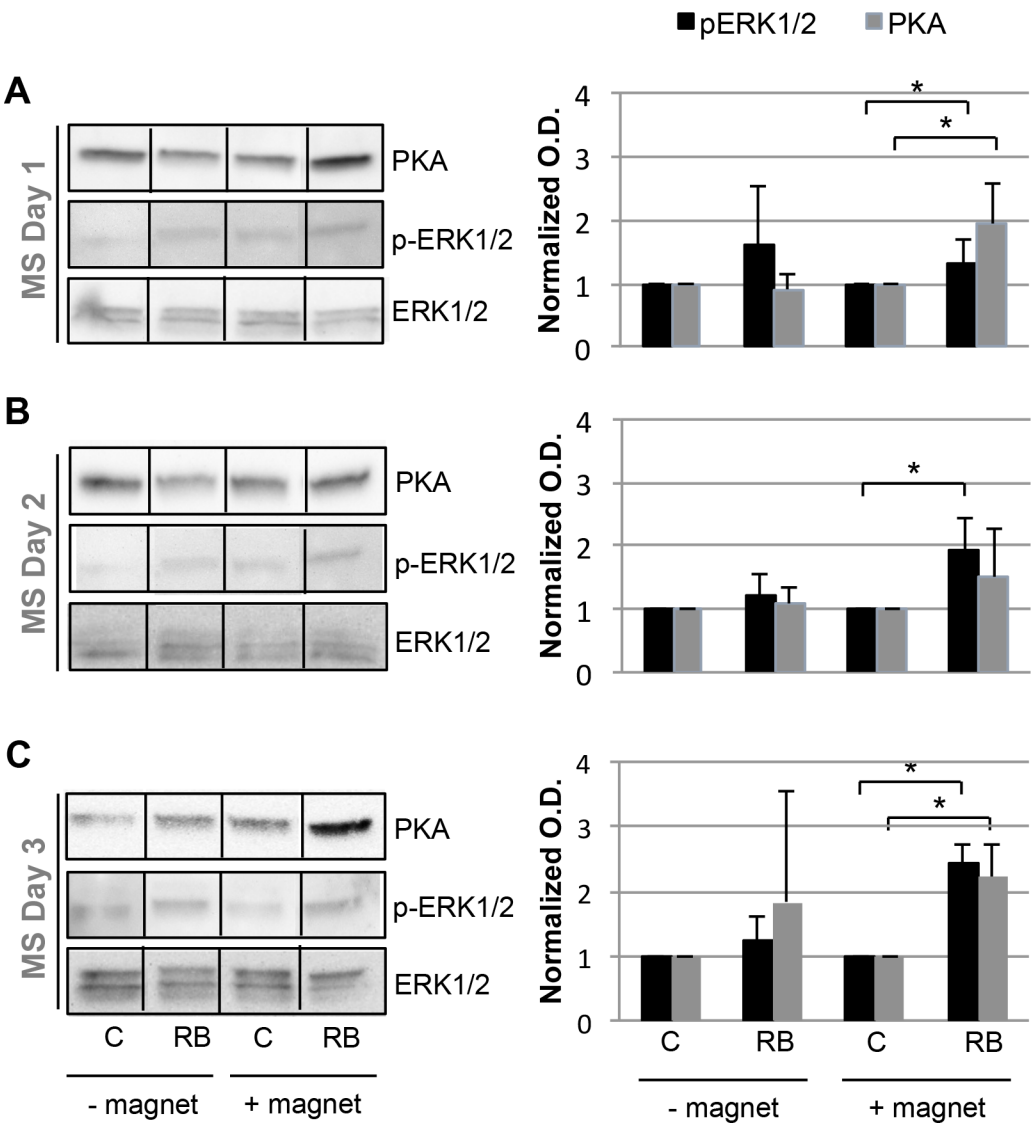

Figure 4.6: Expression of PKA and phosphorylated ERK1/2 in response to magnetic attraction at different stages of EB development. Western blot analysis of EBs stimulated on Day 1 (A), Day 2 (B) or Day 3 (C). Protein expression was normalized to ERK. MS: mechanical stimulation, C: control, RB: RGD-Beads. * $p<0.05$.

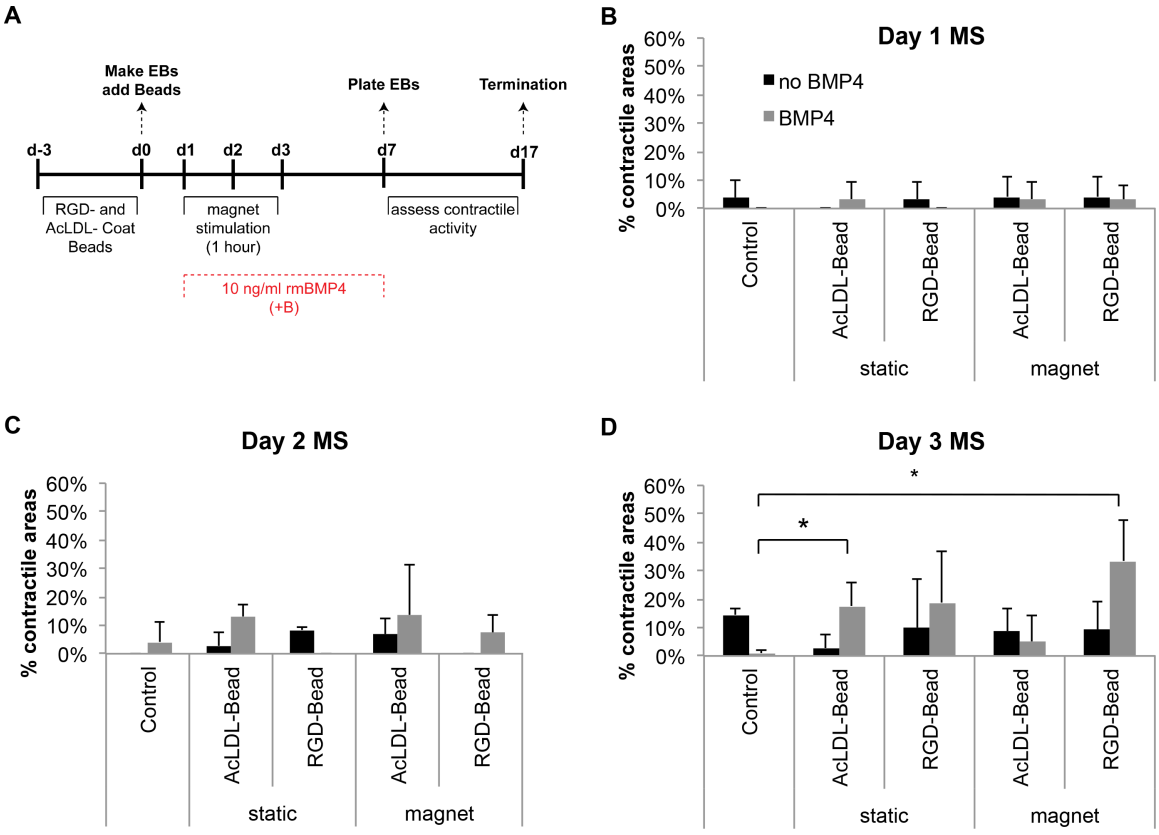

Figure 4.7: Percentage of EBs with contractile areas on Day 17. (A) Timeline of EB mechanical stimulation and culture. BMP4 (10 ng/ml) was added between Days 1-7. EBs were stimulated on Day 1 (B), Day 2 (C), or Day 3 (D) in the presence or absence of BMP4. MS: mechanical stimulation. * $p<0.05$.

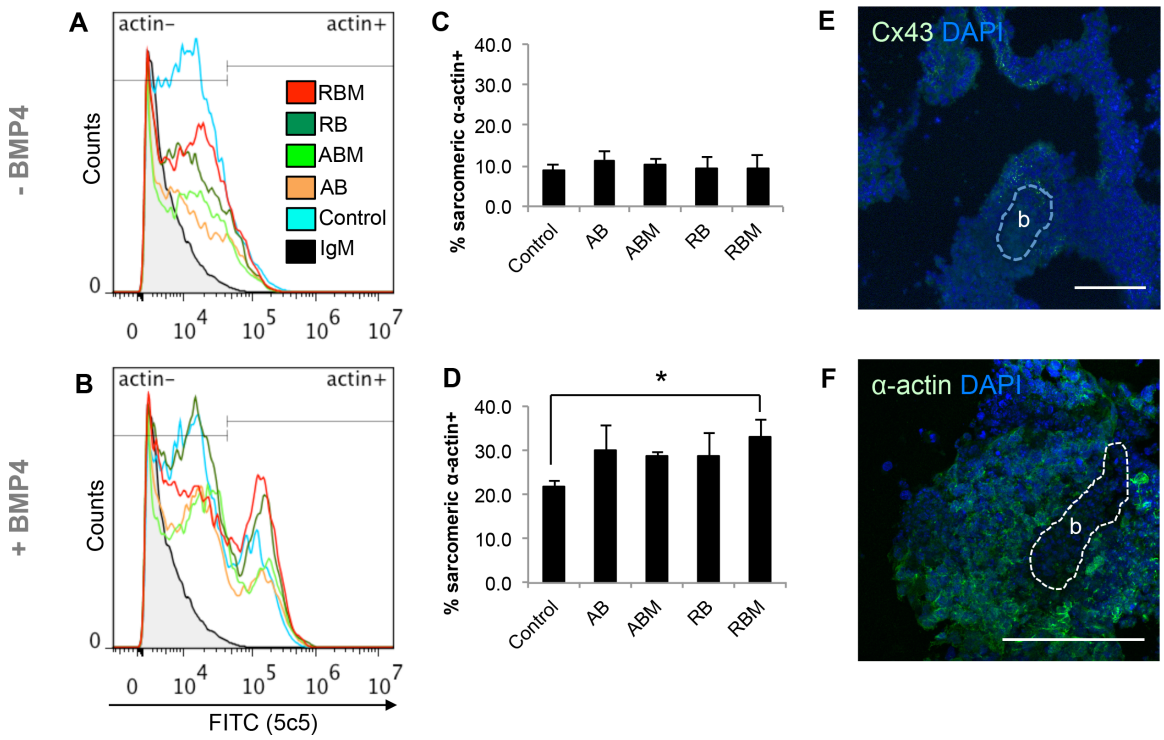

Figure 4.8: Sarcomeric α-actin expression in Day 3-stimulated EBs. Histogram representation of sarcomeric α-actin+ cells in Day 18 EBs without BMP4 (A) and with BMP4 (B). (C-D) Percent of sarcomeric α-actin cells in EBs without (C) and with (D) BMP4 supplementation. (E) Cx43 and (F) sarcomeric α-actin immunostaining of Day 3-stimulated EBs on Day 18. "b": location of beads within confocal micrograph. AB: AcLDL-Beads, RB: RGD-Beads, M: magnetized. *p<0.05. Scale bar: 20 μm.

4.6. REFERENCES

Alenghat, F. J., Tytell, J. D., Thodeti, C. K., Derrien, A., & Ingber, D. E. (2009). Mechanical control of cAMP signaling through integrins is mediated by the heterotrimeric Galphas protein. *Journal of Cellular Biochemistry*, *106*(4), 529–538. doi:10.1002/jcb.22001

Battista, S., Guarnieri, D., Borselli, C., Zeppetelli, S., Borzacchiello, A., Mayol, L., et al. (2005). The effect of matrix composition of 3D constructs on embryonic stem cell differentiation. *Biomaterials*, *26*(31), 6194–6207. doi:10.1016/j.biomaterials.2005.04.003

Boheler, K. R., Czyz, J., Tweedie, D., Yang, H.-T., Anisimov, S. V., & Wobus, A. M. (2002). Differentiation of pluripotent embryonic stem cells into cardiomyocytes. *Circulation Research*, *91*(3), 189–201.

Brafman, D. A., Phung, C., Kumar, N., & Willert, K. (2013). Regulation of endodermal differentiation of human embryonic stem cells through integrin-ECM interactions. *Cell Death and Differentiation*, *20*(3), 369–381. doi:10.1038/cdd.2012.138

Bratt-Leal, A. M., Nguyen, A. H., Hammersmith, K. A., Singh, A., & Mcdevitt, T. C. (2013). A microparticle approach to morphogen delivery within pluripotent stem cell aggregates. *Biomaterials*, *34*(30), 7227–7235. doi:10.1016/j.biomaterials.2013.05.079

Bukoreshtliev, N. V., Haase, K., & Pelling, A. E. (2013). Mechanical cues in cellular signalling and communication. *Cell and Tissue Research*, *352*(1), 77–94. doi:10.1007/s00441-012-1531-4

Chowdhury, F., Na, S., Li, D., Poh, Y.-C., Tanaka, T. S., Wang, F., & Wang, N. (2009). Material properties of the cell dictate stress-induced spreading and differentiation in embryonic stem cells. *Nature Materials*, *9*(1), 82–88. doi:10.1038/nmat2563

Czyz, J., & Wobus, A. (2001). Embryonic stem cell differentiation: the role of extracellular factors. *Differentiation*, *68*(4-5), 167–174.

Dawson, J., Schussler, O., Al-Madhoun, A., Menard, C., Ruel, M., & Skerjanc, I. S. (2011). Collagen scaffolds with or without the addition of RGD peptides support cardiomyogenesis after aggregation of mouse embryonic stem cells. *In Vitro Cellular & Developmental Biology. Animal*, *47*(9), 653–664. doi:10.1007/s11626-011-9453-0

Geuss, L. R., & Suggs, L. J. (2013). Making cardiomyocytes: how mechanical stimulation can influence differentiation of pluripotent stem cells. *Biotechnology*

Progress, *29*(5), 1089–1096. doi:10.1002/btpr.1794

Go, A. S., Mozaffarian, D., Roger, V. L., Benjamin, E. J., Berry, J. D., Borden, W. B., et al. (2013). Heart disease and stroke statistics--2013 update: a report from the American Heart Association. *Circulation*, *127*(1), e6–e245. doi:10.1161/CIR.0b013e31828124ad

Gwak, S.-J., Bhang, S. H., Kim, I.-K., Kim, S.-S., Cho, S.-W., Jeon, O., et al. (2008). The effect of cyclic strain on embryonic stem cell-derived cardiomyocytes. *Biomaterials*, *29*(7), 844–856. doi:10.1016/j.biomaterials.2007.10.050

Heo, J. S., & Lee, J.-C. (2011). β-catenin mediates cyclic strain-stimulated cardiomyogenesis in mouse embryonic stem cells through ROS-dependent and integrin-mediated PI3K/Akt pathways. *Journal of Cellular Biochemistry*, *112*(7), 1880–1889. doi:10.1002/jcb.23108

Hwang, Y.-S., Chung, B. G., Ortmann, D., Hattori, N., Moeller, H.-C., & Khademhosseini, A. (2009). Microwell-mediated control of embryoid body size regulates embryonic stem cell fate via differential expression of WNT5a and WNT11. *Pnas*, *106*(40), 16978–16983. doi:10.1073/pnas.0905550106

Kattman, S. J., Huber, T. L., & Keller, G. M. (2006). Multipotent flk-1+ cardiovascular progenitor cells give rise to the cardiomyocyte, endothelial, and vascular smooth muscle lineages. *Developmental Cell*, *11*(5), 723–732. doi:10.1016/j.devcel.2006.10.002

Laboureau, J., Dubertret, L., Lebreton-De Coster, C., & Coulomb, B. (2004). ERK activation by mechanical strain is regulated by the small G proteins rac-1 and rhoA. *Experimental Dermatology*, *13*(2), 70–77. doi:10.1111/j.0906-6705.2004.00117.x

Lee, M. Y., Bozkulak, E. C., Schliffke, S., Amos, P. J., Ren, Y., Ge, X., et al. (2011). High density cultures of embryoid bodies enhanced cardiac differentiation of murine embryonic stem cells. *Biochemical and Biophysical Research Communications*, *416*(1-2), 51–57. doi:10.1016/j.bbrc.2011.10.140

Lian, X., Zhang, J., Azarin, S. M., Zhu, K., Hazeltine, L. B., Bao, X., et al. (2013). Directed cardiomyocyte differentiation from human pluripotent stem cells by modulating Wnt/β-catenin signaling under fully defined conditions. *Nature Protocols*, *8*(1), 162–175. doi:10.1038/nprot.2012.150

Maniotis, A. J., Chen, C. S., & Ingber, D. E. (1997). Demonstration of mechanical connections between integrins cytoskeletal filaments, and nucleoplasm that stabilize nuclear structure. *Proceedings of the National Academy of Sciences of the United*

States of America, *94*(3), 849–854.

Matthews, B. D., Overby, D. R., Mannix, R., & Ingber, D. E. (2006). Cellular adaptation to mechanical stress: role of integrins, Rho, cytoskeletal tension and mechanosensitive ion channels. *Journal of Cell Science*, *119*(Pt 3), 508–518. doi:10.1242/jcs.02760

Meyer, C. J., Alenghat, F. J., Rim, P., Fong, J. H., Fabry, B., & Ingber, D. E. (2000). Mechanical control of cyclic AMP signalling and gene transcription through integrins. *Nature Cell Biology*, *2*(9), 666–668. doi:10.1038/35023621

Offenberg Sweeney, von, N., Cummins, P. M., Birney, Y. A., Cullen, J. P., Redmond, E. M., & Cahill, P. A. (2004). Cyclic strain-mediated regulation of endothelial matrix metalloproteinase-2 expression and activity. *Cardiovascular Research*, *63*(4), 625–634. doi:10.1016/j.cardiores.2004.05.008

Pimton, P., Sarkar, S., Sheth, N., Perets, A., Marcinkiewicz, C., Lazarovici, P., & Lelkes, P. I. (2011). Fibronectin-mediated upregulation of alpha 5 beta 1 integrin and cell adhesion during differentiation of mouse embryonic stem cells. *Cell Adhesion & Migration*, *5*(1), 73–82. doi:10.4161/cam.5.1.13704

Plopper, G., & Ingber, D. E. (1993). Rapid induction and isolation of focal adhesion complexes. *Biochemical and Biophysical Research Communications*, *193*(2), 571–578. doi:10.1006/bbrc.1993.1662

Saha, S., Ji, L., de Pablo, J. J., & Palecek, S. P. (2006). Inhibition of human embryonic stem cell differentiation by mechanical strain. *Journal of Cellular Physiology*, *206*(1), 126–137. doi:10.1002/jcp.20441

Saha, S., Ji, L., de Pablo, J. J., & Palecek, S. P. (2008). TGFbeta/Activin/Nodal pathway in inhibition of human embryonic stem cell differentiation by mechanical strain. *Biophysical Journal*, *94*(10), 4123–4133. doi:10.1529/biophysj.107.119891

Salameh, A., Wustmann, A., Karl, S., Blanke, K., Apel, D., Rojas-Gomez, D., et al. (2010). Cyclic mechanical stretch induces cardiomyocyte orientation and polarization of the gap junction protein connexin43. *Circulation Research*, *106*(10), 1592–1602. doi:10.1161/CIRCRESAHA.109.214429

Sargent, C. Y., Berguig, G. Y., & Mcdevitt, T. C. (2009). Cardiomyogenic differentiation of embryoid bodies is promoted by rotary orbital suspension culture. *Tissue Engineering Part A*, *15*(2), 331–342. doi:10.1089/ten.tea.2008.0145

Schmelter, M., Ateghang, B., Helmig, S., Wartenberg, M., & Sauer, H. (2006).

Embryonic stem cells utilize reactive oxygen species as transducers of mechanical strain-induced cardiovascular differentiation. *Faseb Journal*, *20*(8), 1182–. doi:10.1096/fj.05-4723fje

Shimizu, N., Yamamoto, K., Obi, S., Kumagaya, S., Masumura, T., Shimano, Y., et al. (2008). Cyclic strain induces mouse embryonic stem cell differentiation into vascular smooth muscle cells by activating PDGF receptor beta. *Journal of Applied Physiology (Bethesda, Md. : 1985)*, *104*(3), 766–772. doi:10.1152/japplphysiol.00870.2007

Taha, M. F., & Valojerdi, M. R. (2008). Effect of bone morphogenetic protein-4 on cardiac differentiation from mouse embryonic stem cells in serum-free and low-serum media. *International Journal of Cardiology*, *127*(1), 78–87. doi:10.1016/j.ijcard.2007.04.173

Toh, Y.-C., & Voldman, J. (2011). Fluid shear stress primes mouse embryonic stem cells for differentiation in a self-renewing environment via heparan sulfate proteoglycans transduction. *The FASEB Journal*, *25*(4), 1208–1217. doi:10.1096/fj.10-168971

Tulloch, N. L., Muskheli, V., Razumova, M. V., Korte, F. S., Regnier, M., Hauch, K. D., et al. (2011). Growth of engineered human myocardium with mechanical loading and vascular coculture. *Circulation Research*, *109*(1), 47–59. doi:10.1161/CIRCRESAHA.110.237206

Uda, Y., Poh, Y.-C., Chowdhury, F., Wu, D. C., Tanaka, T. S., Sato, M., & Wang, N. (2011). Force via integrins but not E-cadherin decreases Oct3/4 expression in embryonic stem cells. *Biochemical and Biophysical Research Communications*, *415*(2), 396–400. doi:10.1016/j.bbrc.2011.10.080

Wan, C.-R., Chung, S., & Kamm, R. D. (2011). Differentiation of embryonic stem cells into cardiomyocytes in a compliant microfluidic system. *Annals of Biomedical Engineering*, *39*(6), 1840–1847. doi:10.1007/s10439-011-0275-8

Wang, N., Butler, J. P., & Ingber, D. E. (1993). Mechanotransduction across the cell surface and through the cytoskeleton. *Science (New York, N.Y.)*, *260*(5111), 1124–1127.

Wang, X., & Ha, T. (2013). Defining Single Molecular Forces Required to Activate Integrin and Notch Signaling. *Science (New York, N.Y.)*, *340*(6135), 991–994. doi:10.1126/science.1231041

Wolfe, R. P., Leleux, J., Nerem, R. M., & Ahsan, T. (2012). Effects of shear stress on germ lineage specification of embryonic stem cells. *Integrative Biology :*

Quantitative Biosciences From Nano to Macro, *4*(10), 1263–1273. doi:10.1039/c2ib20040f

Yamashita, J., Itoh, H., Hirashima, M., Ogawa, M., Nishikawa, S., Yurugi, T., et al. (2000). Flk1-positive cells derived from embryonic stem cells serve as vascular progenitors. *Nature*, *408*(6808), 92–96. doi:10.1038/35040568

Yanada, S., Ochi, M., Adachi, N., Nobuto, H., Agung, M., & Kawamata, S. (2006). Effects of CD44 antibody-- or RGDS peptide--immobilized magnetic beads on cell proliferation and chondrogenesis of mesenchymal stem cells. *Journal of Biomedical Materials Research Part A*, *77*(4), 773–784. doi:10.1002/jbm.a.30635

Zborowski, M., Sun, L., Moore, L. R., Stephen Williams, P., & Chalmers, J. J. (1999). Continuous cell separation using novel magnetic quadrupole flow sorter. *Journal of Magnetism and Magnetic Materials*, *194*(1), 224–230.

CHAPTER FIVE

Effect of PEGylated fibrin gel stiffness on HL-1 and mouse ESC-derived cardiomyocyte maintenance and maturity

Cell transplantation into the damaged myocardium, or cellular cardiomyoplasty, has the potential to promote myocardium regeneration after Myocardial Infarction (MI); however, this strategy is limited due to cell loss shortly after injection. To address this limitation, cells can be incorporated into a compliant matrix, which can physically encapsulate the cells into the host tissue. Encapsulating the cells inside a matrix provides time for cells to remodel their environment by depositing extracellular matrix and electrically coupling with the host tissue. PEGylated fibrin gels are biocompatible, with controllable degradation rates, and have been shown to promote neovascularization and mesenchymal stem cell (MSC) retention in the myocardium. We investigated if PEGylated fibrin gels can promote HL-1 cardiomyocyte functionality and mouse embryonic stem cell-derived cardiomyocyte (mESC-CM) maturation. PEGylated fibrin gels were prepared at concentrations ranging from 10 mg/ml to 25 mg/ml, and cardiomyocytes were either incorporated within the interior of the hydrogel (3D) or cultured on the surface of the gels (2D). We observed that regardless of the seeding density, HL-1 cardiomyocytes are unable to remodel the 10 mg/ml PEGylated fibrin gels, and consequently form non-contractile aggregates. When HL-1 are cultured on the surface of hydrogels, contractile activity is increased on more compliant gels compared to stiffer, more concentrated gels. A 3D-like construct could be fabricated by layering HL-1 in between 10 mg/ml fibrin gels: in this situation, the addition of PEGylated fibrin gel

layers to the cells did not inhibit contractile activity or viability. To examine the potential fibrin gels on mESC-CM maturity, EBs were stimulated using magnetically mediated strain as described in Chapter 4. EBs with contractile areas were dissociated, yielding a 50% sarcomeric a-actin positive population, and seeded onto 2D PEGylated fibrin gels. The mESC-CM and non-cardiomyocytes proliferated to confluency on all of the gels, regardless of the stiffness; however, contractile activity was lost due to the high concentration of non-cardiomyocytes in the cell suspension. This study demonstrates that PEGylated fibrin gels can be used as MI patches; however, both the initial cell population and method of cell seeding must be optimized to promote contractile function.

5.1. INTRODUCTION

Myocardial Infarction (MI), which is one of the most prevalent diseases in the United States, results in scar tissue formation and thinning of the myocardial wall (Christman et al., 2004). Since cardiomyocytes are inherently unable to regenerate and repopulate the infarcted area, MI can result in permanent tissue damage and is lethal if left untreated. Heart transplants are currently the only option for permanent tissue repair; however, there are significant risks associated with this procedure, including tissue rejection.

Cellular cardiomyoplasty, in which viable cells are injected into the injured tissue, is being explored as an alternative and less invasive procedure to repair the myocardium. This was first observed by Soonpaa *et al* in 1994, who demonstrated that fetal cardiomyocytes could form stable intracardiac grafts when implanted into the

myocardium (Soonpa, Koh, Klug, & Field, 1994). Since then, many other groups have investigated the potential of a range of cell types for cellular cardiomyoplasty, including fetal cardiomyocytes (Soonpa et al., 1994), skeletal muscle cells (Laflamme, Zbinden, Epstein, & Murry, 2007), and stem cells such as mesenchymal stem cells (MSC) (ORLIC et al., 2006; J. S. Wang et al., 2000) and pluripotent stem cells (PSC) (Min et al., 2002). A drawback to this approach is cell retention in the infarcted area: In a study with radioactively labeled endothelial progenitor cells, less than 5% of injected cells remained in the myocardium after 96 hours (Aicher et al., 2003).

Tissue engineering, in which cells are combined with biocompatible materials, is an alternative to the direct cell injection method. The addition of the biomaterial can both improve cell viability and increase retention and engraftment at the site of injury (Rask et al., 2010). A variety of methods to incorporate the material into the myocardium have been investigated, including patches (Hidalgo-Bastida et al., 2007; Y.-C. Huang, Khait, & Birla, 2007; Marsano et al., 2010; Robinson et al., 2005; Smith et al., 2012), cell sheets (C.-C. Huang et al., 2010; Matsuura et al., 2011; Sawa & Miyagawa, 2013; Shimizu, Sekine, Yamato, & Okano, 2009), and injectable biomaterials (Christman et al., 2004; Gerard, Forest, Beauregard, Skuk, & Tremblay, 2012; Johnson & Christman, 2012; Shapira-Schweitzer, Habib, Gepstein, & Seliktar, 2009; G. Zhang, Wang, Wang, Zhang, & Suggs, 2006). The combination of cells and the materials significantly decreases infarct size, promotes cell viability and ECM deposition. Cell sheets can be stacked, forming a scaffold-free patch that can be implanted onto the myocardial infarct (Shimizu et al., 2009).

Fibrin-based gels have many advantages for myocardial tissue engineering, including biocompatibility and stable degradation *in vitro* and *in vivo* (Mosesson, 2005). Each Aα chain on fibrinogen molecules have two Arginine-Glycine-Aspartic Acid (RGD) sequences, which promotes cell attachment and proliferation (Yang, Wu, Asakura, Kohno, & Matsuda, 2004). While fibrin hydrogels resorb within 7 days *in vitro* (LIU, Collins, & Suggs, 2006), they can be stabilized by conjugating amine-reactive polyethylene glycol (PEG) prior to the addition of thrombin producing a PEGylated fibrin hydrogel. We have previously demonstrated that PEGylated fibrin gels incorporated with MSCs significantly increases left ventricle ejection fraction function following MI by increasing cell retention and reducing scar formation (G. Zhang et al., 2006). In this study, we examined the potential of using this PEGylated fibrin gel system to maintain cardiomyocytes. Since scaffold stiffness has been observed to play a critical role in cardiomyocyte maturation (Engler et al., 2008; Zoldan et al., 2011), we compared HL-1 and mESC-CM proliferation, viability, contractile activity, and cardiomyocyte-marker expression on PEGylated fibrin gels with different concentrations of fibrinogen. We have observed that fibrinogen concentration does affect cardiomyocyte activity and functionality, and function is also dependent on the method of cardiomyocyte incorporation into the matrix.

5.2. MATERIALS AND METHODS

5.2.1. Embryonic Stem Cell Culture

R1 mouse ESCs (A. Nagy, Toronto, Canada) were expanded feeder-free on 0.1% gelatin-coated cell culture flasks (Stem Cell Technologies, Vancouver, Canada) in Growth Medium containing Knockout Dulbecco's Modified Eagle's Medium (Invitrogen, Grand Island, NY) supplemented with 15% ES-Cult Fetal Bovine Serum (Stem Cell Technologies), 1% Glutamax (Invitrogen), 1% Non-Essential Amino Acids (Invitrogen), 1% Nucleosides (Millipore, Billerica, MA), 1% Penicillin/Streptomycin (Invitrogen), 0.1mM β-Mercaptoethanol (Invitrogen) and 10^3 U/ml Leukemia Inhibitory Factor (LIF; Millipore). Medium was changed in full each day, and cells were passaged every 2 days before reaching approximately 70% confluence.

5.2.2. RGD-Bead preparation

RGD-Beads were prepared as previously described, with a few modifications (Ingber, 2006; Laboureau, Dubertret, Lebreton-De Coster, & Coulomb, 2004). Briefly, 50 μg Peptite 2000 (Advanced Biomatrix, San Diego, CA) was bound to 1 mg of 1μm BcMag™ tosyl-activated paramagnetic beads (Bioclone, San Diego, CA) for 72 hours at 4ºC in 0.1M Carbonate Buffer, pH 9 as suggested by the manufacturer. The RGD-bound beads (RGD-Beads) were rinsed three times in PBS containing calcium and magnesium with a Dynal magnet (Invitrogen) and blocked for 1 hour in PBS containing 5% Bovine Serum Albumin (Sigma-Aldrich, St. Louis, MO). Following an additional three rinses in

PBS, the beads were resuspended in medium and added to the Aggrewell plates at 1 mg beads per well, yielding a final concentration of approximately 500 beads/EB.

5.2.3. Differentiation and isolation of mouse embryonic stem cell derived–cardiomyocytes

ESCs were enzymatically released from the gelatin-coated plates with trypsin/EDTA (ATCC, Manassas, VA) and resuspended in Differentiation Medium (Growth Medium without LIF). Approximately 1.2 million cells were added to each well of a 24-well Aggrewell 400^{TM} plate (Stem Cell Technologies) as directed by the manufacturer. The final EB sizes were approximately 1,000 cells/EB. Once the EBs were allowed to settle for 30 minutes at 37ºC/5%CO_2, the beads were distributed to the appropriate wells. The EBs were kept in the Aggrewell 400^{TM} plates for 3 days, and medium was partially changed daily. On Day 3, the EBs were exposed to magnetic attraction for 1 hour as described in Chapter 4. After stimulation, the EBs were transferred to suspension culture in ultra-low attachment plates and medium was changed in full every 2 days. BMP4 (10 ng/ml) was added to the culture medium from Days 1 through 7. On Day 7, the EBs were allowed to attach to gelatin-coated plates and maintained for up to 18 days at 37ºC/5%CO_2. Approximately 2-3 EBs were plated per well of a 24 well plate.

After 18 days, contractile EBs were incubated in 0.2% collagenase type I (Invitrogen) in DMEM/20% FBS for 1 hour at 37ºC/5%CO_2. The collagenase solution was then removed and the EBs were incubated for 5-7 minutes in 0.25% trypsin/EDTA

(Invitrogen). The EBs were triturated with a 1000 µl pipet and the single cell suspension was neutralized with DMEM/20% FBS and collected by centrifugation for 5 min at 270xg.

5.2.4. HL-1 cardiomyocyte culture

HL-1 cardiomyocytes, a gift from Dr. William Claycomb, are a cardiac muscle cell line from the AT-1 mouse atrial cardiomyocyte tumor lineage (Claycomb et al., 1998). These cells are phenotypically and genotypically similar to mature cardiomyocytes, in that they maintain contractility and express cardiomyocyte-specific genes including α-myosin heavy chain, sarcomeric α-actin and connexin 43. HL-1 from passages 50-60 were maintained in Claycomb medium (Sigma) supplemented with 10% Fetal Bovine Serum (Sigma lot# 12J001), 1% Penicillin/Streptomycin (Invitrogen), 1% Glutamax (Invitrogen), and 0.1mM Norepinephrine. The cells were seeded into flasks at 100,000 cells/cm^2, and were split 1:3 every 4 days.

5.2.5. PEGylated fibrin gel fabrication

PEGylated fibrin hydrogels were prepared as previously described, with a few modifications (G. Zhang, Drinnan, Geuss, & Suggs, 2010). Human fibrinogen (Sigma) was solubilized in PBS (pH 7.8, without calcium and magnesium) at 40 mg/ml, 60 mg/ml, 80 mg/ml and 100 mg/ml. To increase gel stability, homo-bifunctional Succinimidyl Glutarate-Polyethylene Glycol (SG-PEG-SG) was similarly solubilized in PBS at 4 mg/ml, 6 mg/ml, 8 mg/ml and 10 mg/ml. These concentrations correspond to a

10:1 molar ratio of fibrinogen to PEG for final concentrations of 10 mg/ml fibrinogen + 1 mg/ml PEG, 15 mg/ml fibrinogen + 1.5 mg/ml PEG, 20 mg/ml fibrinogen + 2 mg/ml PEG and 25 mg/ml fibrinogen + 2.5 mg/ml PEG, respectively. Human thrombin (Sigma) was diluted to 100 U/ml in nanopure water and further resuspended in 40 mM calcium chloride buffer for a final concentration of 25 U/ml. All solutions were sterile-filtered through a 0.22 μm filter prior to incubation with cells. The volumes of each of the components used are listed in Table 5.1.

For long-term 3D studies, 500 μl gels were prepared in CellCrownTM 12-well plate inserts (Sigma). HL-1 cardiomyocytes were suspended within the gel at final concentrations of 1 Million/ml, 2.5 Million/ml or 5 Million/ml. After 24 hours, the gels were transferred to ultralow attachment 6-well plates containing 5 ml medium. Medium was changed in full every 2 days.

For 2D experiments, 750 μl gels were formed without cells in 35mm glass-bottom petri dishes. After a 2-hour incubation in medium, cardiomyocytes were added to the surface of each hydrogel at 10^5 cells/cm^2. For 2D layer (2DL) gels, an additional 500 μl 10 mg/ml gel was prepared on top of the confluent cardiomyocyte monolayer after 4 days in culture. For 2DL experiments, only 10 mg/ml fibrinogen + 1 mg/ml PEG hydrogels were tested. Medium was changed daily over the course of 7 days.

5.2.6. Rheology

PEGylated fibrin gels were prepared as described in section 5.2.5. A 2-ml layer of 10 mg/ml fibrinogen, 15 mg/ml fibrinogen, 20 mg/ml fibrinogen and 25 mg/ml

fibrinogen was prepared in 6-well plates with 500 µl fibrinogen, 500 µl PEG and 1 ml thrombin. The gels were incubated at 37ºC/5%CO_2 for 2 hours, and samples were collected from the layers using a 40mm diameter punch. The frequency sweep was measured at 1% from 20 to 0.5 rad/sec. All samples were measured at room temperature.

5.2.7. Cell viability

HL-1 and ESC-CM viability were assessed using Calcein-AM (Life Technologies) and Alamar Blue (Life Technologies). For Alamar Blue, cells were incubated in a 1:10 dilution of Alamar Blue reagent in cell culture medium for 1.5 hours at 37ºC/5%CO_2 and fluorescence was read at 560ex/590em. For Calcein-AM imaging, the cells were rinsed 3 times for 5 minutes with PBS containing calcium and magnesium. Calcein-AM (4 µM in PBS containing calcium and magnesium) was added to the cells and incubated for one hour at 37ºC/5% CO_2 in the dark. After three rinses in PBS, the cells were fixed in 4% paraformaldehyde for 15 minutes, rinsed again, and imaged using a Zeiss scanning confocal microscope.

5.2.8. Detection of contractile activity in HL-1

HL-1 Contractile activity was observed 3 days after seeding on hydrogels. Calcium sensitive Fluo-4 AM (10 mM in dimethyl sulfoxide, excitation/emission 494/516nm, Life Technologies) was diluted to 10 µM in HL-1 medium. After 3 rinses in PBS, the gels were incubated in diluted Fluo-4 for 30 minutes at room temperature in the dark. To allow for de-esterification of Fluo-4, the gels were rinsed three times in

Tyrode's solution (1.33 mM $CaCl_2$, 1 mM $MgCl_2$, 5.4 mM KCl, 135 mM NaCl, and 0.33 mM $Na_2H_2PO_4$) containing 5 mM glucose, 5 mM HEPES and 10 mM norepinephrine. The gels were incubated in Tyrode's solution for another 20 minutes at room temperature, and imaged by confocal microscopy within 2 hours as described previously with a few modifications (Mihic et al., 2014; Smith et al., 2012). Briefly, time-lapse images were taken at 195 msec intervals for 100 cycles at 128x128 pixels. A Z-plot profile was developed for three separate regions of interest (ROI) using Fiji image analysis software, and the fluorescence intensity over time (F_0) was normalized to the lowest intensity values (F_{min}) and plotted as F_0/F_{min}.

5.2.9. Immunostaining

To visualize sarcomeric α-actin staining and connexin 43 (cx43) staining patterns, HL-1 cardiomyocytes or mESC-CM were rinsed with PBS and fixed for 15 minutes with 4% paraformaldehyde. For intracellular staining, the cells were permeabilized with 0.25% Triton-X/PBS for 30 minutes at room temperature. Following three rinses in PBS, the samples were blocked in 10% normal goat serum for 1 hour, and incubated overnight in anti-mouse sarcomeric α-actin (5c5, 1:500 in 1% normal goat serum, Sigma Aldrich) or anti-rabbit connexin 43 (1:100 in 1% normal goat serum, Cell Signaling Technologies) at 4°C. The cells were rinsed again three times in TBST (Tris Buffered Saline + 1% Tween-20) and incubated in goat anti-mouse FITC IgM (1:200 in 1% normal goat serum, Santa Cruz Biotechnology) or goat anti-rabbit Alexa Fluor 488 IgG (1:500 in 1% normal goat serum, Abcam) for one hour at room temperature in the dark. The cells were

counterstained with 5 μg/ml 4',6-diamidino-2-phenylindole (DAPI, Life Technologies), rinsed and imaged using a Zeiss scanning confocal microscope.

5.3. RESULTS

5.3.1. Rheology

The viscoelastic properties of PEGylated fibrin gels with fibrinogen concentrations ranging from 10 to 25 mg/ml were assessed by rheology (Figure 5.1A). Increases in storage modulus were observed as the concentration of fibrinogen and PEG increased (Figure 5.1B). The storage moduli of the 10 mg/ml, 15 mg/ml, 20 mg/ml and 25 mg/ml PEGylated fibrin gels were 123.5 ± 29.6, 464.7 ± 77.3, 904.7 ± 71.3 and 966.8 ± 85.5 Pa respectively. No significant differences between the loss moduli were observed.

5.3.2. Effect of PEGylated fibrin matrix on 3D HL-1 cardiomyocyte culture

PEGylated fibrin hydrogels have been shown to effectively promote differentiation of both embryonic stem cells (LIU et al., 2006; Shapira-Schweitzer et al., 2009) and mesenchymal stem cells (G. Zhang et al., 2010) into cardiomyocytes and endothelial cells, respectively. In this study, we investigated the long-term effect of homo-bifunctional PEGylated fibrin hydrogels on HL-1 cardiomyocytes as a potential MI injectable patch. The HL-1 were maintained at three different seeding densities in 10 mg/ml PEGylated fibrin gels: 1 Million/ml, 2.5 Million/ml and 5 Million/ml. At all three concentrations, after 10 days in culture, the HL-1 cardiomyocytes formed cardiosphere-

like aggregates (Figure 5.2A). By day 35, these aggregates increased in size such that they could be observed by eye (Figure 5.2B). Alamar Blue (Figure 5.2C) and PCNA staining (Figure 5.2D) confirmed that the HL-1 cells within these aggregates were proliferative, and maintained the expression of connexin 43 and sarcomeric α-actin (Figure 5.2F)

While the HL-1 did appear to be metabolically active over the course of the culture period (Figure 5.2C,D), contractile behavior was not maintained within the hydrogels. To further examine the effect of 3D HL-1 culture on cell functional behavior, the cells were incubated with Fluo-4 to track changes in calcium concentrations within the aggregates. Calcium transients were observed through the aggregate (Figure 5.2E), indicating that the cells were forming gap-junctions; however, calcium cycles were long in duration and highly variable.

5.3.3. Effect of fibrinogen concentration on HL-1 viability in 2D culture

Since 3D culture of HL-1 appeared to impair functional activity, we examined the effect of (1) culturing the HL-1 on top of PEGylated fibrin gels and (2) the concentration of fibrinogen on HL-1 activity. PEGylated fibrin gels were prepared with final fibrinogen concentrations of 10 mg/ml, 15 mg/ml, 20 mg/ml and 25 mg/ml. The fibrinogen:PEG ratio was kept constant at 10:1 for each concentration (Figure 5.3A). Cell viability was monitored over 14 days by Alamar Blue. Regardless of the fibrinogen concentration, there was no difference in cell number between groups over the culture period (Figure 5.3B).

5.3.4. Effect of PEGylated fibrin concentration on HL-1 viability and morphology

Considering that scaffold stiffness has been well demonstrated to impact cardiomyocyte functional activity *in vitro* (Engler et al., 2008; Shapira-Schweitzer & Seliktar, 2007; Young & Engler, 2011), we examined the effects of 2D PEGylated fibrin gels on the maintenance of cardiomyocyte-specific marker expression. The HL-1 were seeded on top of PEGylated fibrin gels prepared at each fibrinogen concentration (Figure 5.4A,E,I,M). As the concentration of fibrinogen increased, HL-1 cardiomyocytes spread less over the surface of the gel (Figure 5.4A, M); however, there were no evident differences in viability (Figure 5.4B,F,J,N). CX 43 (Figure 5.4C,G,K,O) and sarcomeric α-actin (Figure 5.4D,H,L,P) staining was observed in all samples .

5.3.5. Effect of fibrinogen concentration on HL-1 contractile activity

While we previously observed that incorporation of HL-1 into the interior of PEGylated fibrin gels impairs contractile activity, we next examined the effect of seeding the cells directly on top of the gels in a 2D culture system. Contractile activity was observed in HL-1 by Day 3, and the cells continued to contract through Day 7. During cell contractions, the Fluo-4 GFP intensity increased as calcium was passed through the cells. Over three separate ROI, the HL-1 with the most consistent contractile activity were those seeded on the 10 mg/ml PEGylated fibrin gels, with cell contractions, or calcium peaks, occurring every 0.975 seconds (Figure 5.5A). These contractions were significantly more frequent compared to other PEGylated fibrin gels (Figure 5.5E). As the concentration of fibrinogen increased to 15 mg/ml, the contractions were less

consistent and also less frequent: cells contacted every 1.170±0.195 seconds (Figure 5.5B). At the highest fibrinogen formulations, 20 mg/ml (Figure 5.5C) and 25 mg/ml (Figure 5.5D), the Fluo-4 intensity duration was lowest, at 1.14±0.113 and 1.300±0.113 seconds, respectively.

5.3.6. Effect of PEGylated fibrin gel layers on HL-1 activity

Considering cardiomyocyte activity is enhanced when seeded on 2D PEGylated fibrin surfaces, we investigated how activity is affected when HL-1 are cultured within gel layers (2DL). For these experiments, HL-1 were seeded onto 10 mg/ml 2DL and maintained for 4 days *in vitro*. On Day 4, an additional gel layer was added on top of the cells. After 24 hours, contractile activity and cardiomyocyte-specific marker expression was assessed. Following addition of the gel layer, the cells appeared completely confluent (Figure 5.6A), remained viable (Figure 5.6B) and maintained expression of sarcomeric α-actin (Figure 5.6C) and connexin 43 (Figure 5.6D). Calcium cycle duration was decreased in comparison to 2D gels: HL-1 contracted approximately every 1.17 seconds, which was comparable to that observed on 2D 15 mg/ml gels (Figure 5.6E,F, Figure 5.5B), but significantly higher than on 2D 10 mg/ml gels (Figure 5.6F). In comparison, calcium cycle duration was significantly higher in 3D gels, occurring approximately every 4.8 seconds (Figure 5.6F).

5.3.7. Effect of fibrinogen concentration on mESC-CM maintenance

Since PEGylated fibrin gels appeared sufficient to maintain cardiomyocyte functionality, we next asked whether these fibrin gels could also be used to maintain ESC-CM. To isolate ESC-CM, EBs with contracting areas were isolated from gelatin-coated well plates and the sarcomeric α-actin population was analyzed. From EBs with contracting areas, approximately 48% of the cell population were sarcomeric α-actin positive (ESC-CM) (Figure 5.7).

Recent work has demonstrated that embryonic cardiomyocytes are best maintained on matrices with stiffness that mimic the heart, between approximately 1-11 kPa, as opposed to softer substrates (Engler et al., 2008). Considering our findings that matrix stiffness is proportional to fibrinogen concentrations in PEGylated hydrogels, we examined the effect of fibrinogen concentration on the maintenance of mESC-CM. Cell morphology and viability were compared for both cell types 6 days after seeding onto gel layers ranging from 10 mg/ml to 25 mg/ml (Figure 5.8). Regardless of the gel formulation, the differentiated cells from contractile EBs became fully confluent (Figure 5.8A,D,G,J) and remained viable (Figure 5.8B,E,H,K) regardless of the gel formulation. On 20 mg/ml and 25 mg/ml fibrin gels, sarcomeric α-actin appeared aligned and elongated in mESC-CM (Figure 5.8I,L). Positive staining and some alignment was also observed on 10 mg/ml and 15 mg/ml gels (Figure 5.8C,F); however, the majority of the 10mg/ml fibrin gel had degraded by day 6, and cells began to migrate to the tissue culture plastic (Figure 5.8C).

5.4. DISCUSSION

In this study, we examined the potential of PEGylated fibrin gels as a matrix for the retention of cardiomyocytes. Previously, we reported that PEGylated fibrin gels promote revascularization and decrease fibrosis following myocardial infarction when seeded with mesenchymal stem cells (G. Zhang, Hu, Braunlin, Suggs, & Zhang, 2008). We observed that three-dimensional culture of HL-1 cardiomyocytes promotes the formation of cardiosphere-like aggregates, which while continuing to express cardiac-specific markers and viability, appear to inhibit the functional, contractile phenotype. Alternatively, we found that contractility could be maintained when cells were cultured on layers of PEGylated fibrin, and that the rate of cardiomyocyte contraction was increased on more compliant gels. In addition, contractile activity is maintained when cells are cultured in 2DL, suggesting that a layered PEGylated fibrin gel construct could potentially be used as an MI patch.

Fibrin gels are commonly used in tissue engineering because of its biocompatibility and non-toxic byproducts during degradation (Breen, O'Brien, & Pandit, 2009). These gels can also be used as either an implanted patch or an injectable solution (Christman et al., 2004; Gerard et al., 2012; Johnson & Christman, 2012). In general, the rate at which materials resorb in vivo depends partly on the ability of cells to remodel their environment and deposit ECM. We observed that while HL-1 cardiomyocytes maintain sarcomeric α-actin and connexin 43 expression, they form cardiosphere-like aggregates within the scaffold regardless of the initial seeding density. Recent studies have demonstrated that contractile activity of cardiomyocytes, specifically ESC-CM, is

best maintained in combination with cardiac fibroblasts, which can deposit ECM (Matsuura et al., 2011; Matsuura, Masuda, & Shimizu, 2014). The importance of this co-culture was suggested by our ESC-CM results, as the combination of cell types after EB dissociation and seeding onto gel layers resulted in nearly complete degradation of more compliant PEGylated fibrin gels by Day 5 (Figure 5.8C). Our three-dimensional culture system may have the same requirement, and therefore future studies should examine the potential of cardiac fibroblast and cardiomyocyte co-cultures on 3D PEGylated fibrin remodeling in vitro and in vivo.

As an alternative to true 3D culture, we examined the possibility of creating patch using layers of gels and cells for a sheet-like construct. This cell sheet-like technology offers an alternative to traditional tissue engineered applications by providing a high-cell density construct that can be used as a cardiac patch. These sheets have been produced using both temperature sensitive materials, in which confluent cell layers are detached from temperature-responsive polymer (poly(N-isopropylacrylamide)) coated dishes by changing incubation temperatures from 37ºC to under 32ºC (Bel et al., 2010; Sawa & Miyagawa, 2013; Shimizu et al., 2009). Neonatal cardiomyocyte-sheets have also been fabricated on layers of fibrin gel, which can be easily detached from plates for myocardial patches (Itabashi et al., 2005; Patel & Zhang, 2013). In this study, we examined the possibility of culturing HL-1 between layers of PEGylated fibrin gel, and observed that contractile activity and viability was maintained 24 hours after addition of a second gel layer. While functional properties appear to be unaffected initially by 2DL

culture, future studies should examine long-term effects on proliferation and cardiomyocyte functionality.

Material stiffness also plays an important role in maintaining the expression of cardiomyocyte functional markers. To adjust gel stiffness we increased the initial concentration of fibrinogen in the PEGylated fibrin gels, and in doing so were able to generate materials with storage moduli ranging from 100 Pa to 1 kPa (Figure 5.1B). Initially, we hypothesized that contractile activity in both HL-1 and ESC-CM would be enhanced on stiffer gels, since hydrogels with elastic moduli of 9-14 kPa are optimal for ESC-CM maturity (Engler et al., 2008). In this study, HL-1 seeded on stiffer gels appeared to spread less compared to more compliant gels (Figure 5.4M,P). HL-1 cardiomyocytes are dependent on cell-cell contacts to propagate calcium signals and promote contractility (Claycomb et al., 1998). The inability of HL-1 to become fully confluent on the 25 mg/ml gels may have been the reason for why the contractile frequency is reduced compared to 10 mg/ml gels, and not necessarily because of the elastic modulus. Alternatively, in a report by Shapira-Schweitzer *et al*, ESC-CM expression of cardiomyocyte-specific markers, as well as increases in the number of contractile regions, were observed in PEGylated fibrin gels with elastic moduli of 23 ± 13 Pa (Shapira-Schweitzer et al., 2009; Shapira-Schweitzer & Seliktar, 2007). Therefore, our findings may be attributed to the nature of PEGylated fibrin gels and the ability of HL-1 to proliferate and spread on surfaces with more concentrated fibrinogen networks.

Spontaneous contractile activity is a hallmark of ESC-CM and mature cardiomyocyte functionality (P.-Y. Wang, Yu, Lin, & Tsai, 2011; Xu, Police, Rao, &

Carpenter, 2002). As ESC-CM mature, sarcomeres become more aligned, and beating frequency increases (Robertson, Tran, & George, 2013). The rate largely depends on the study and how the cardiomyocytes are manipulated, such as by electrical or physical stimulation. In this study, we observed HL-1 contractile rates ranging from approximately 0.9 seconds to 1.3 seconds depending on the fibrinogen concentration (Figure 5.5). Interestingly, the contraction rate of HL-1 on 10 mg/ml gels was comparable to that observed on mechanically stimulated scaffolds (Mihic et al., 2014). While HL-1 contracted at a slower rate on other gel formulations, and in 2DL, the rate is still comparable to that observed on PEG-microsphere based scaffolds (Smith et al., 2012) and gelatin sponges (Mihic et al., 2014). Thus, while culturing HL-1 in 2DL may decrease contractile activity, the rate is still within the published range for the cells.

Promoting ESC-CM maturity is an important precursor to their use in vivo for MI treatment. As mentioned previously, contractile activity can be enhanced by co-culture when a percentage of cells are fibroblasts (van Spreeuwel et al., 2014; P.-Y. Wang et al., 2011). We generated ESC-CM from EBs using magnetically mediated strain, and following digestion obtained a cell population that was composed of approximately 50% cardiomyocytes. When these cells were seeded on the PEGylated fibrin gels, the morphology was markedly different compared to HL-1 (Figure 5.8). The cells became completely confluent on all of the gels, and the heterogeneity of this population resulted in partial digestion of the 10 mg/ml gel by Day 6 (Figure 5.8C). Since contractile activity did not persist over the duration of the culture, the concentration of fibroblasts and other ECM-modifying cell types was likely too high to allow for ESC-CM maturation. In the

future, the population of cells within the EB will need to be better assessed to control the ratio of ESC-CM and fibroblastic cell types. By doing so, we can better understand the potential of PEGylated fibrin gels as patches, and confirm findings that compliant gels promote cardiomyocyte functionality.

5.5. CONCLUSIONS

In this study, we observed that while 3D culture of a pure cardiomyocyte population in PEGylated fibrin gels inhibits functionality; however, this can be overcome with a layering approach. HL-1 cultured within layers of hydrogel maintains sarcomeric α-actin alignment, regardless of the concentration of fibrinogen, and promotes contractile activity. While ESC-CM appear to proliferate on the hydrogels, the concentration of non-cardiomyocytes in the EB inhibit cardiomyocyte maturation. Consequently, while PEGylated fibrin gels have potential to be used as patches for MI repair, the phenotype of the starting cell population must be better controlled to optimize hydrogel formulation.

Table 5.1. Volume of components used to fabricate PEGylated fibrin hydrogels for 2D, 2DL, and 3D experiments.

Gel Volume (µl)	Fibrinogen volume (µl)	SG-PEG-SG volume (µl)	Medium/Cell volume (µl)	Thrombin volume (µl)
2D: 750	187.5	187.5	0	375
2DL: 750	93.75	93.75	187.5	375
3D: 500	62.5	62.5	125	250

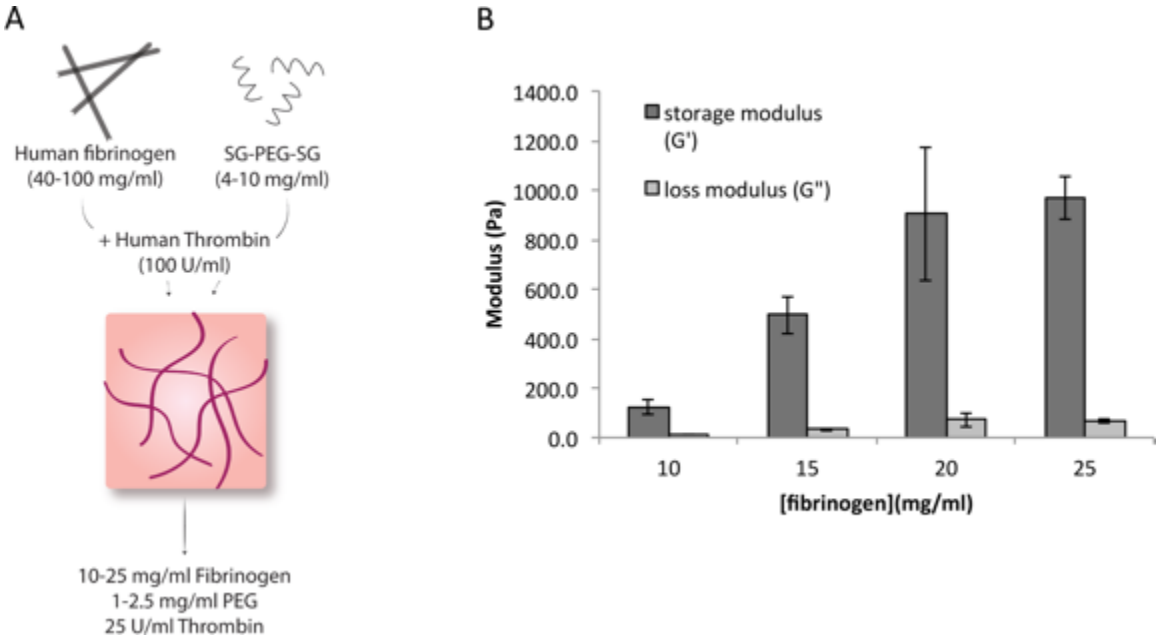

Figure 5.1: (A) Preparation of PEGylated fibrin gels. (B) Effect of fibrinogen concentration on PEGylated fibrin gel stiffness.

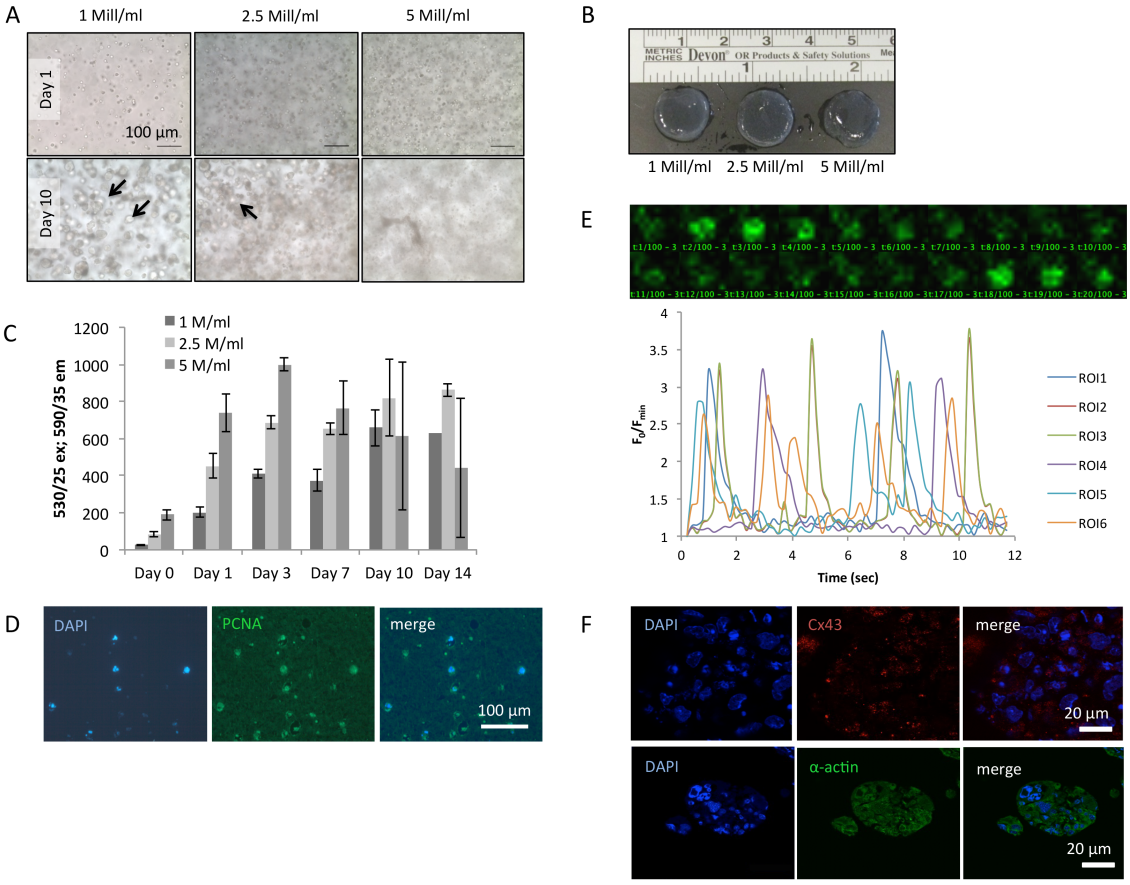

Figure 5.2: HL-1 maintenance in 3D PEGylated fibrin gel matrices. (A) Formation of cardiosphere-like aggregates in matrices (arrows). (B) Gross morphology of 3D PEGylated fibrin gels by day 30. (C) Viability of HL-1 over 14 days in culture. (D) PCNA staining of Day 14 aggregates (1 M/ml). (E) Fluo4 cycling in aggregates over time. (F) Expression of cardiomyocyte-specific markers at Day 15.

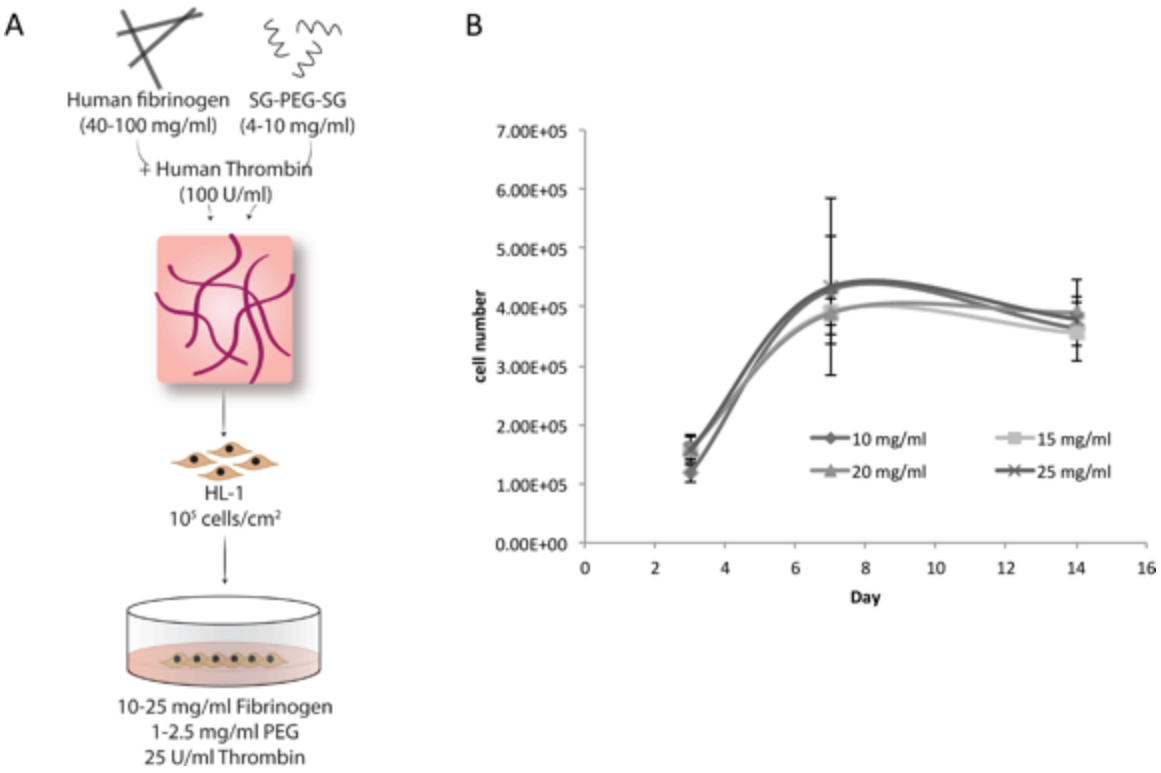

Figure 5.3. Metabolic activity of HL-1 on 2D PEGylated fibrin gels. (A) Formulation of HL-1 seeded hydrogels. (B) Effect of fibrinogen concentration on HL-1 metabolic activity over 14 days.

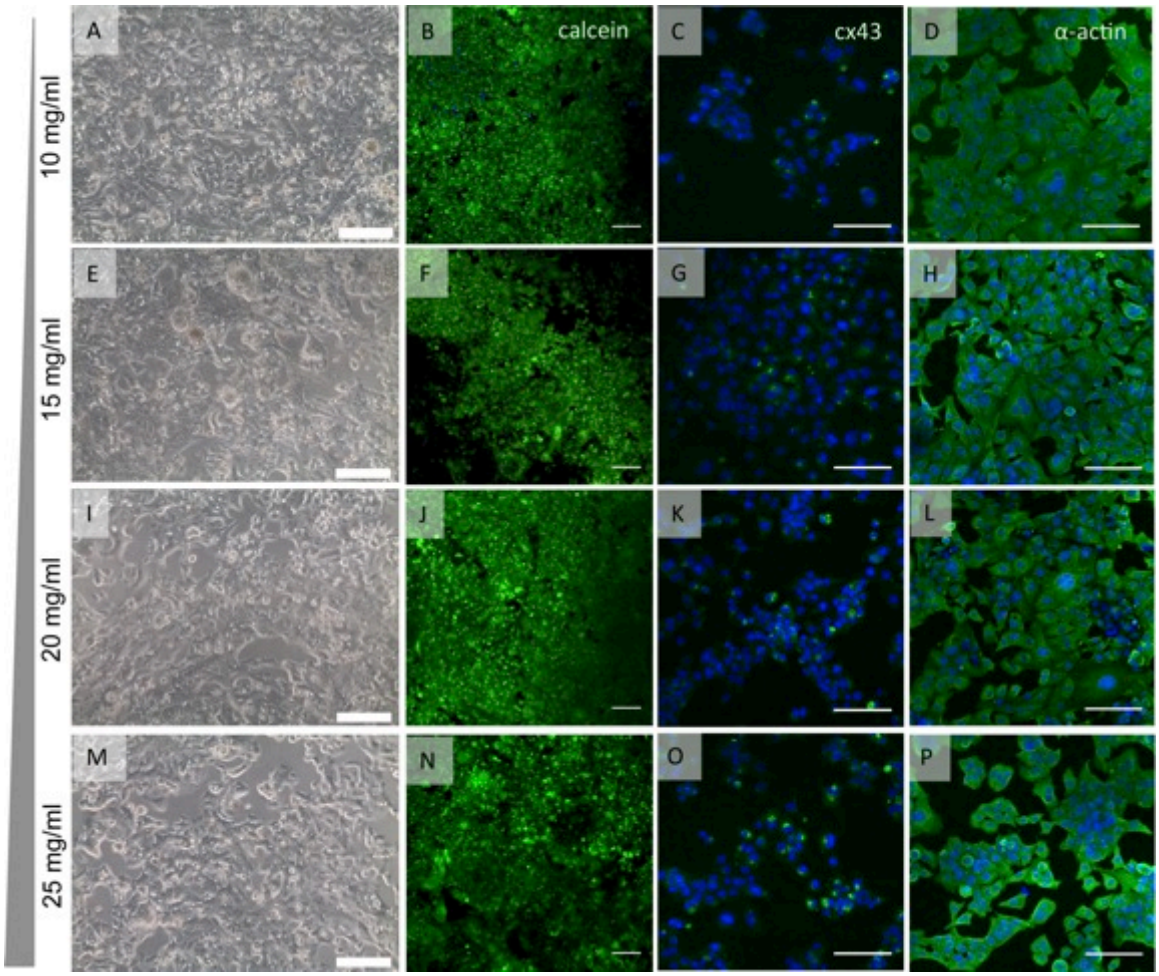

Figure 5.4. Effect of fibrinogen concentration on HL-1 viability and cardiomyocyte-specific marker expression. (A,E,I,M) Phase contrast. (B,F,J,N) Calcein-AM staining. Green = live cells. (C,G,K,O): Connexin 43 (Cx43) immunostaining. (D,H,L,P) Sarcomeric α-actin immunostaining. Scale = 100 μm.

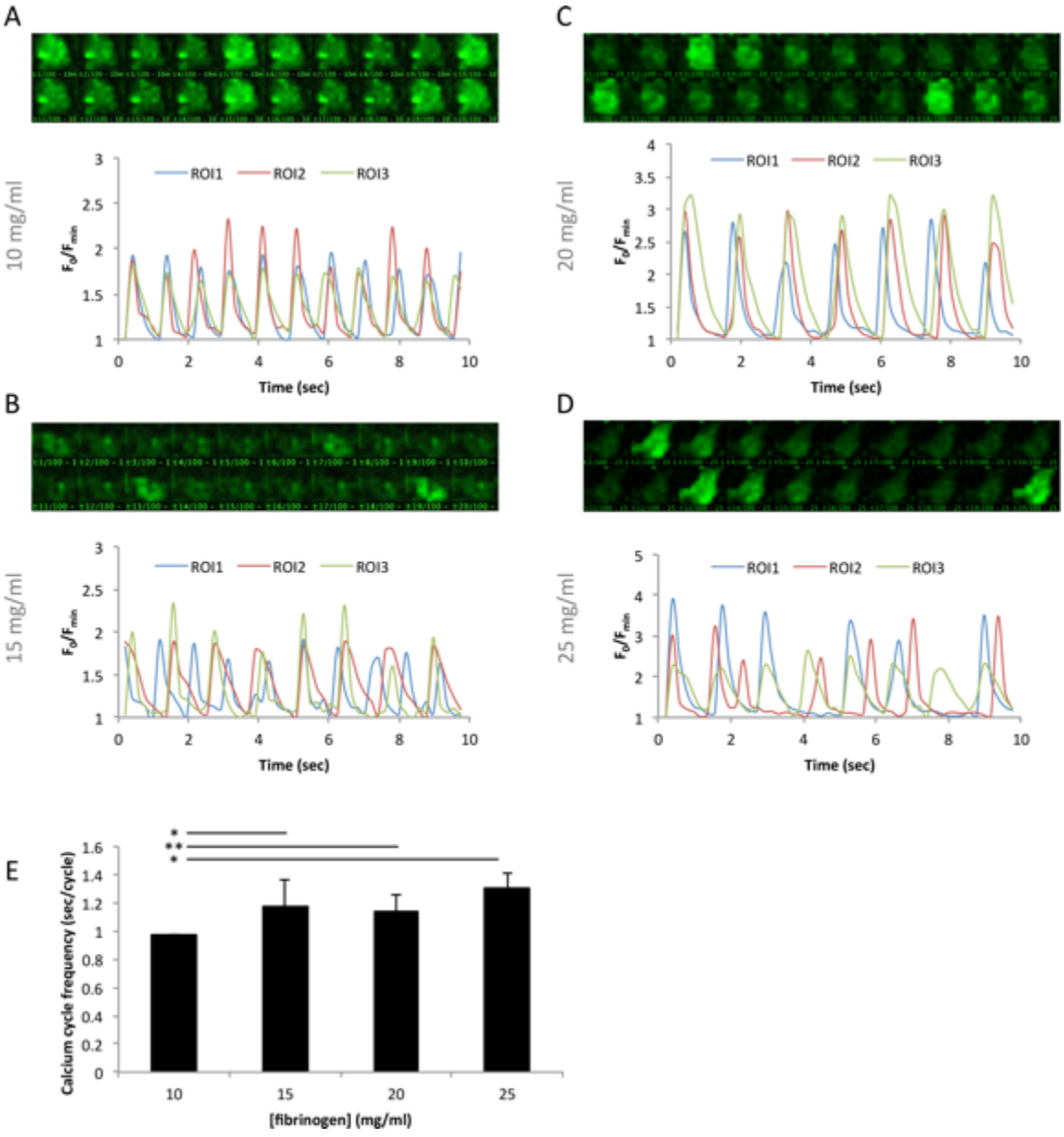

Figure 5.5: Fluo-4 calcium tracking of HL-1 on (A) 10 mg/ml PEGylated fibrin gels, (B) 15 mg/ml PEGylated fibrin gels, (C) 20 mg/ml PEGylated fibrin gels and (D) 25 mg/ml PEGylated fibrin gels. (E) Rate of HL-1 contractile activity on PEGylated fibrin gels. *p<0.05, **p<0.001

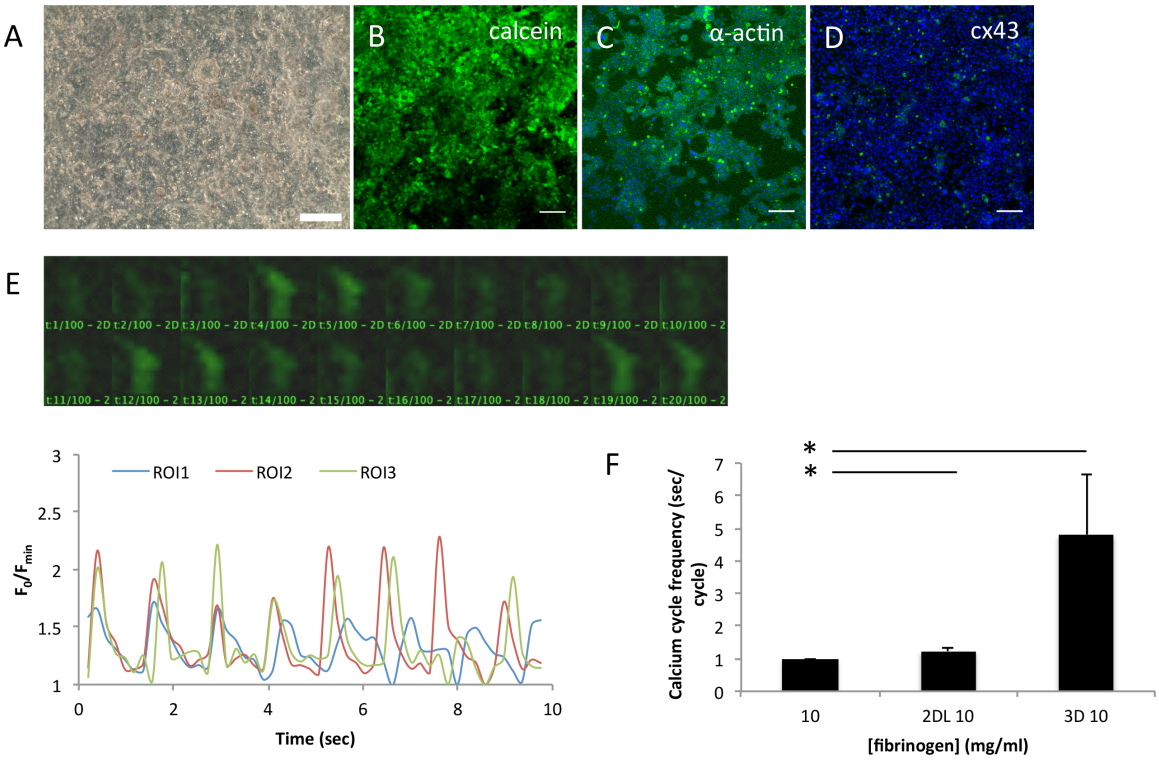

Figure 5.6. Effect of 2DL culture on HL-1 contractile activity and viability. (A) Cells remain completely confluent following addition of a second gel layer. (B) Cell viability after 24 hours. (C) Sarcomeric α-actin and (D) Connexin 43 expression 24 hours after gel layer addition. (E) Fluo-4 tracking of three ROIs after 24 hours. (E) Fluo-4 intensity in HL-1 on 10 mg/ml 2DL gels. (F) Comparison of calcium cycling duration in 10 mg/ml 2D gels, 2DL gels and 3D gels. *p<0.05. Scale = 100 μm.

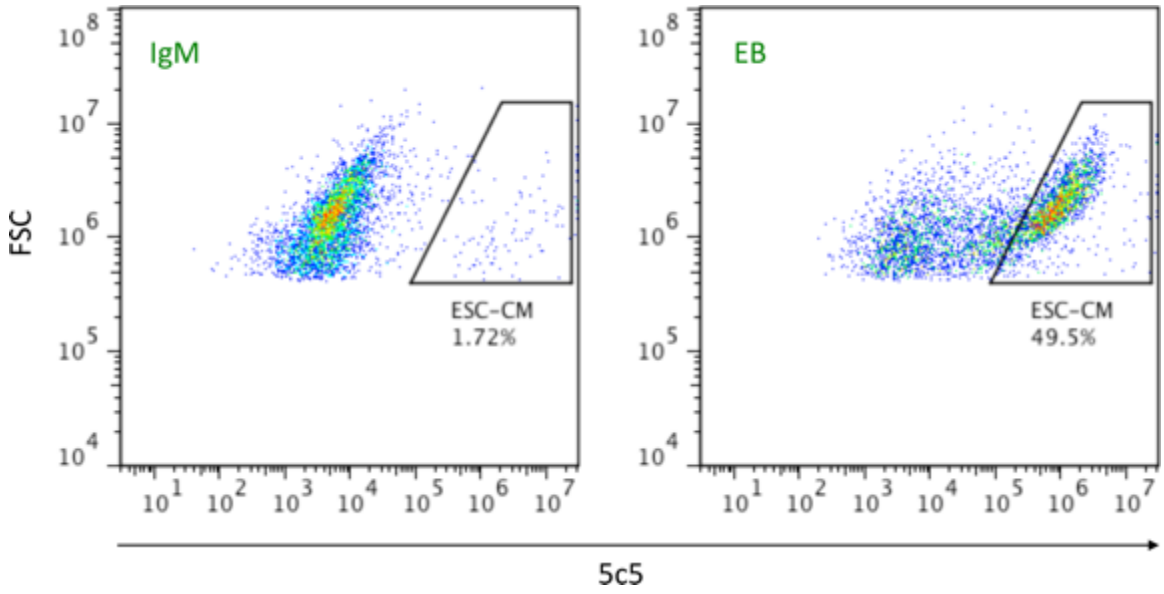

Figure 5.7. Percentage of sarcomeric α-actin expressing cells from EBs with contracting areas.

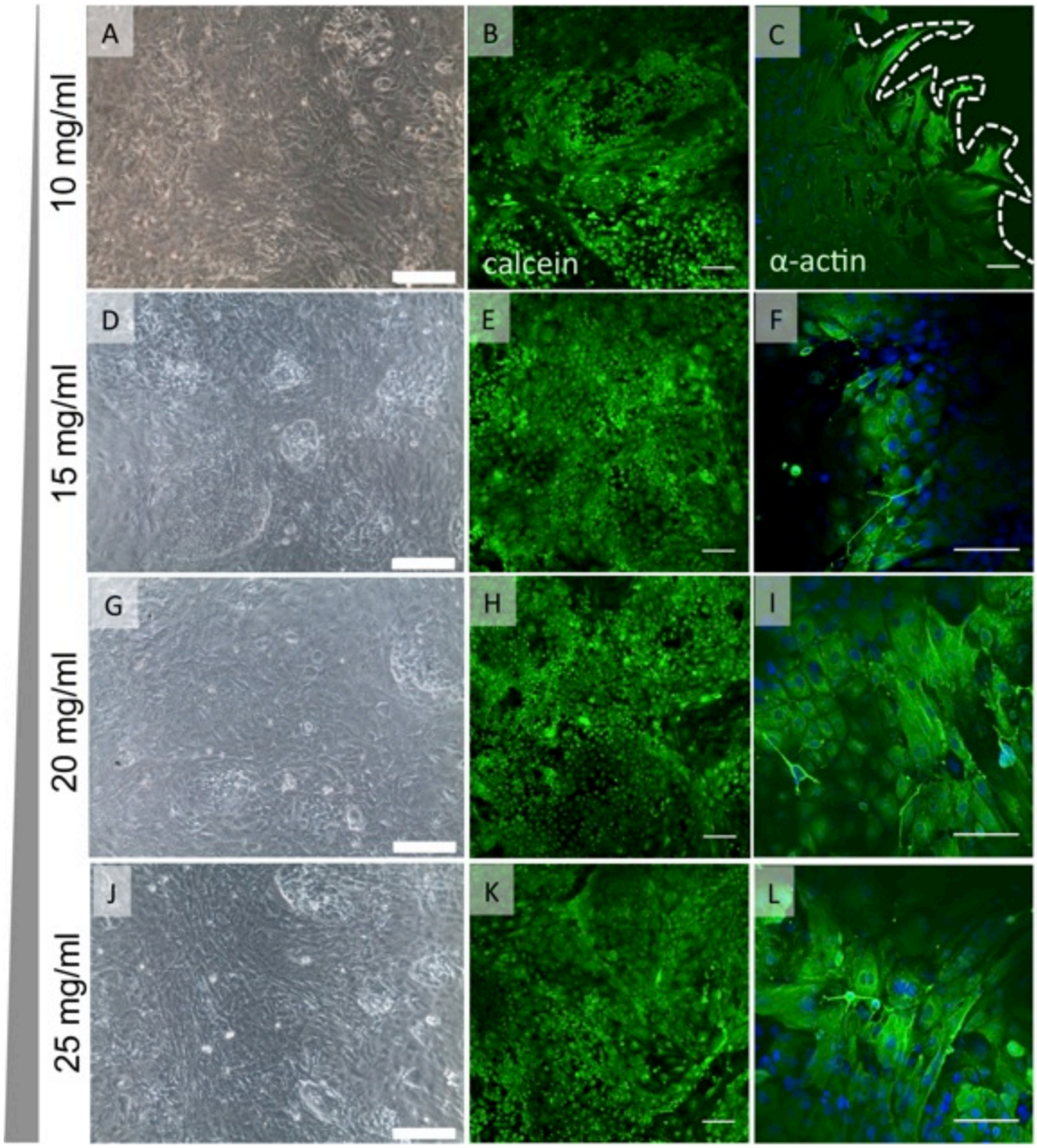

Figure 5.8. Effect of fibrinogen concentration on ESC-CM viability and sarcomeric α-actin expression. (A-C) 10mg/ml PEGylated fibrin gels. Dotted line demarcates interface between cells and degraded hydrogel. (D-F) 15 mg/ml PEGylated fibrin gels, (G-H) 20 mg/ml PEGylated fibrin gels and (J-L) 25 mg/ml PEGylated fibrin gels. Scale = 100 μm.

5.6. REFERENCES

Aicher, A., Brenner, W., Zuhayra, M., Badorff, C., Massoudi, S., Assmus, B., et al. (2003). Assessment of the tissue distribution of transplanted human endothelial progenitor cells by radioactive labeling. *Circulation*, *107*(16), 2134–2139. doi:10.1161/01.CIR.0000062649.63838.C9

Bel, A., Planat-Bernard, V., Saito, A., Bonnevie, L., Bellamy, V., Sabbah, L., et al. (2010). Composite cell sheets: a further step toward safe and effective myocardial regeneration by cardiac progenitors derived from embryonic stem cells. *Circulation*, *122*(11 Suppl), S118–23. doi:10.1161/CIRCULATIONAHA.109.927293

Breen, A., O'Brien, T., & Pandit, A. (2009). Fibrin as a delivery system for therapeutic drugs and biomolecules. *Tissue Engineering Part B, Reviews*, *15*(2), 201–214. doi:10.1089/ten.TEB.2008.0527

Christman, K. L., Vardanian, A. J., Fang, Q., Sievers, R. E., Fok, H. H., & Lee, R. J. (2004). Injectable fibrin scaffold improves cell transplant survival, reduces infarct expansion, and induces neovasculature formation in ischemic myocardium. *Journal of the American College of Cardiology*, *44*(3), 654–660. doi:10.1016/j.jacc.2004.04.040

Claycomb, W., Lanson, N., Stallworth, B., Egeland, D., Delcarpio, J., Bahinski, A., & Izzo, N. (1998). HL-1 cells: A cardiac muscle cell line that contracts and retains phenotypic characteristics of the adult cardiomyocyte. *Proceedings of the National Academy of Sciences of the United States of America*, *95*(6), 2979–2984.

Engler, A. J., Carag-Krieger, C., Johnson, C. P., Raab, M., Tang, H.-Y., Speicher, D. W., et al. (2008). Embryonic cardiomyocytes beat best on a matrix with heart-like elasticity: scar-like rigidity inhibits beating. *Journal of Cell Science*, *121*(Pt 22), 3794–3802. doi:10.1242/jcs.029678

Gerard, C., Forest, M. A., Beauregard, G., Skuk, D., & Tremblay, J. P. (2012). Fibrin gel improves the survival of transplanted myoblasts. *Cell Transplantation*, *21*(1), 127–137. doi:10.3727/096368911X576018

Hidalgo-Bastida, L. A., Barry, J. J. A., Everitt, N. M., Rose, F. R. A. J., Buttery, L. D., Hall, I. P., et al. (2007). Cell adhesion and mechanical properties of a flexible scaffold for cardiac tissue engineering. *Acta Biomaterialia*, *3*(4), 457–462. doi:10.1016/j.actbio.2006.12.006

Huang, C.-C., Liao, C.-K., Yang, M.-J., Chen, C.-H., Hwang, S.-M., Hung, Y.-W., et al.

(2010). A strategy for fabrication of a three-dimensional tissue construct containing uniformly distributed embryoid body-derived cells as a cardiac patch. *Biomaterials*, *31*(24), 6218–6227. doi:10.1016/j.biomaterials.2010.04.067

Huang, Y.-C., Khait, L., & Birla, R. K. (2007). Contractile three-dimensional bioengineered heart muscle for myocardial regeneration. *Journal of Biomedical Materials Research Part A*, *80A*(3), 719–731. doi:10.1002/jbm.a.31090

Ingber, D. E. (2006). Mechanical control of tissue morphogenesis during embryological development. *The International Journal of Developmental Biology*, *50*(2-3), 255–266. doi:10.1387/ijdb.052044di

Itabashi, Y., Miyoshi, S., Kawaguchi, H., Yuasa, S., Tanimoto, K., Furuta, A., et al. (2005). A new method for manufacturing cardiac cell sheets using fibrin-coated dishes and its electrophysiological studies by optical mapping. *Artificial Organs*, *29*(2), 95–103. doi:10.1111/j.1525-1594.2005.29020.x

Johnson, T. D., & Christman, K. L. (2012). Injectable hydrogel therapies and their delivery strategies for treating myocardial infarction. *Expert Opinion on Drug Delivery*. doi:10.1517/17425247.2013.739156

Laboureau, J., Dubertret, L., Lebreton-De Coster, C., & Coulomb, B. (2004). ERK activation by mechanical strain is regulated by the small G proteins rac-1 and rhoA. *Experimental Dermatology*, *13*(2), 70–77. doi:10.1111/j.0906-6705.2004.00117.x

Laflamme, M. A., Zbinden, S., Epstein, S. E., & Murry, C. E. (2007). Cell-based therapy for myocardial ischemia and infarction: pathophysiological mechanisms. *Annual Review of Pathology*, *2*, 307–339. doi:10.1146/annurev.pathol.2.010506.092038

LIU, H., Collins, S. F., & Suggs, L. J. (2006). Three-dimensional culture for expansion and differentiation of mouse embryonic stem cells. *Biomaterials*, *27*(36), 6004–6014. doi:10.1016/j.biomaterials.2006.06.016

Marsano, A., Maidhof, R., Wan, L. Q., Wang, Y., Gao, J., Tandon, N., & Vunjak-Novakovic, G. (2010). Scaffold stiffness affects the contractile function of three-dimensional engineered cardiac constructs. *Biotechnology Progress*, *26*(5), 1382–1390. doi:10.1002/btpr.435

Matsuura, K., Masuda, S., & Shimizu, T. (2014). Cell Sheet-Based Cardiac Tissue Engineering. *Anatomical Record-Advances in Integrative Anatomy and Evolutionary Biology*, *297*(1), 65–72. doi:10.1002/ar.22834

Matsuura, K., Masuda, S., Haraguchi, Y., Yasuda, N., Shimizu, T., Hagiwara, N., et al.

(2011). Creation of mouse embryonic stem cell-derived cardiac cell sheets. *Biomaterials*, *32*(30), 7355–7362. doi:10.1016/j.biomaterials.2011.05.042

Mihic, A., Li, J., Miyagi, Y., Gagliardi, M., Li, S.-H., Zu, J., et al. (2014). The effect of cyclic stretch on maturation and 3D tissue formation of human embryonic stem cell-derived cardiomyocytes. *Biomaterials*. doi:10.1016/j.biomaterials.2013.12.052

Min, J. Y., Yang, Y. K., Converso, K. L., Liu, L. X., Huang, Q., Morgan, J. P., & Xiao, Y. F. (2002). Transplantation of embryonic stem cells improves cardiac function in postinfarcted rats. *Journal of Applied Physiology (Bethesda, Md. : 1985)*, *92*(1), 288–296.

Mosesson, M. W. (2005). Fibrinogen and fibrin structure and functions. *Journal of Thrombosis and Haemostasis : JTH*, *3*(8), 1894–1904. doi:10.1111/j.1538-7836.2005.01365.x

ORLIC, D., KAJSTURA, J., Chimenti, S., BODINE, D. M., LERI, A., & ANVERSA, P. (2006). Transplanted Adult Bone Marrow Cells Repair Myocardial Infarcts in Mice. *Annals of the New York Academy of Sciences*, *938*(1), 221–230. doi:10.1111/j.1749-6632.2001.tb03592.x

Patel, N. G., & Zhang, G. (2013). Responsive systems for cell sheet detachment. *Organogenesis*, *9*(2), 93–100. doi:10.4161/org.25149

Rask, F., Mihic, A., Reis, L., Dallabrida, S. M., Ismail, N. S., Sider, K., et al. (2010). Hydrogels modified with QHREDGS peptide support cardiomyocyte survival in vitro and after sub-cutaneous implantation. *Soft Matter*, *6*(20), 5089–5099. doi:10.1039/c0sm00362j

Robertson, C., Tran, D. D., & George, S. C. (2013). Concise review: maturation phases of human pluripotent stem cell-derived cardiomyocytes. *Stem Cells*, *31*(5), 829–837. doi:10.1002/stem.1331

Robinson, K. A., Li, J., Mathison, M., Redkar, A., Cui, J., Chronos, N. A. F., et al. (2005). Extracellular matrix scaffold for cardiac repair. *Circulation*, *112*(9 Suppl), I135–43. doi:10.1161/CIRCULATIONAHA.104.525436

Sawa, Y., & Miyagawa, S. (2013). Cell sheet technology for heart failure. *Current Pharmaceutical Biotechnology*, *14*(1), 61–66.

Shapira-Schweitzer, K., & Seliktar, D. (2007). Matrix stiffness affects spontaneous contraction of cardiomyocytes cultured within a PEGylated fibrinogen biomaterial. *Acta Biomaterialia*, *3*(1), 33–41. doi:10.1016/j.actbio.2006.09.003

Shapira-Schweitzer, K., Habib, M., Gepstein, L., & Seliktar, D. (2009). A photopolymerizable hydrogel for 3-D culture of human embryonic stem cell-derived cardiomyocytes and rat neonatal cardiac cells. *Journal of Molecular and Cellular Cardiology*, *46*(2), 213–224. doi:10.1016/j.yjmcc.2008.10.018

Shimizu, T., Sekine, H., Yamato, M., & Okano, T. (2009). Cell Sheet-Based Myocardial Tissue Engineering: New Hope for Damaged Heart Rescue. *Current Pharmaceutical Design*, *15*(24), 2807–2814.

Smith, A. W., Segar, C. E., Nguyen, P. K., MacEwan, M. R., Efimov, I. R., & Elbert, D. L. (2012). Long-term culture of HL-1 cardiomyocytes in modular poly(ethylene glycol) microsphere-based scaffolds crosslinked in the phase-separated state. *Acta Biomaterialia*, *8*(1), 31–40. doi:10.1016/j.actbio.2011.08.021

SOONPAA, M. H., KOH, G. Y., KLUG, M. G., & Field, L. J. (1994). Formation of Nascent Intercalated Disks Between Grafted Fetal Cardiomyocytes and Host Myocardium. *Science (New York, N.Y.)*, *264*(5155), 98–101.

van Spreeuwel, A. C. C., Bax, N. A. M., Bastiaens, A. J., Foolen, J., Loerakker, S., Borochin, M., et al. (2014). The influence of matrix (an)isotropy on cardiomyocyte contraction in engineered cardiac microtissues. *Integrative Biology : Quantitative Biosciences From Nano to Macro*, *6*(4), 422–429. doi:10.1039/c3ib40219c

Wang, J. S., Shum-Tim, D., Galipeau, J., Chedrawy, E., Eliopoulos, N., & Chiu, R. (2000). Marrow stromal cells for cellular cardiomyoplasty: Feasibility and potential clinical advantages. *Journal of Thoracic and Cardiovascular Surgery*, *120*(5), 999–1006. doi:10.1067/mtc.2000.110250

Wang, P.-Y., Yu, J., Lin, J.-H., & Tsai, W.-B. (2011). Modulation of alignment, elongation and contraction of cardiomyocytes through a combination of nanotopography and rigidity of substrates. *Acta Biomaterialia*, *7*(9), 3285–3293. doi:10.1016/j.actbio.2011.05.021

Xu, C., Police, S., Rao, N., & Carpenter, M. K. (2002). Characterization and enrichment of cardiomyocytes derived from human embryonic stem cells. *Circulation Research*, *91*(6), 501–508.

Yang, W., Wu, B., Asakura, S., Kohno, I., & Matsuda, M. (2004). Soluble fibrin augments spreading of fibroblasts by providing RGD sequences of fibrinogen in soluble fibrin. *Thrombosis Research*, *114*(4), 293–300. doi:10.1016/j.thromres.2004.06.022

Young, J. L., & Engler, A. J. (2011). Hydrogels with time-dependent material properties enhance cardiomyocyte differentiation in vitro. *Biomaterials*, *32*(4), 1002–1009. doi:10.1016/j.biomaterials.2010.10.020

Zhang, G., Drinnan, C. T., Geuss, L. R., & Suggs, L. J. (2010). Vascular differentiation of bone marrow stem cells is directed by a tunable three-dimensional matrix. *Acta Biomaterialia*, *6*(9), 3395–3403. doi:10.1016/j.actbio.2010.03.019

Zhang, G., Hu, Q., Braunlin, E. A., Suggs, L. J., & Zhang, J. (2008). Enhancing efficacy of stem cell transplantation to the heart with a PEGylated fibrin biomatrix. *Tissue Engineering Part A*, *14*(6), 1025–1036. doi:10.1089/ten.tea.2007.0289

Zhang, G., Wang, X., Wang, Z., Zhang, J., & Suggs, L. (2006). A PEGylated fibrin patch for mesenchymal stem cell delivery. *Tissue Engineering*, *12*(1), 9–19. doi:10.1089/ten.2006.12.9

Zoldan, J., Karagiannis, E. D., Lee, C. Y., Anderson, D. G., Langer, R., & Levenberg, S. (2011). The influence of scaffold elasticity on germ layer specification of human embryonic stem cells. *Biomaterials*, *32*(36), 9612–9621. doi:10.1016/j.biomaterials.2011.09.012

CHAPTER SIX

Conclusion and future directions

6.1. SUMMARY

Cell therapy has promise to be the gold standard for Myocardial Infarction (MI) treatment (Min et al., 2002). Pluripotent stem cells (PSCs) are ideal candidates for this procedure due to their potential to differentiate into many different cell types. To this end, there are specific scientific challenges that must be overcome to make their use in the clinic a reality: (1) determine more effective methods to direct differentiation into cardiomyocytes (Xu, Yi, & Chien, 2011), (2) improve upon current culture conditions to both maintain and promote maturation of stem cell derived cardiomyocytes (Nunes et al., 2013; Robinson et al., 2005), and (3) improve upon current delivery methods to retain cardiomyocytes in the myocardium to enhance integration with the host tissue (Ye, Zhou, Cai, & Tan, 2011).

In this study, we investigated alternative methods to preferentially guide ESC differentiation towards cardiomyocytes using the EB model. Since there are diffusional limitations associated with EB culture, we hypothesized that delivery of pro-cardiomyogenic proteins into the EB interior would increase exposure of ESCs within the EB to these proteins. While these proteins could be immobilized to paramagnetic beads and incorporated within the EB, the beads alone appeared to play a significant role in increasing cardiomyogenesis. By coupling Arginine-Glycine-Aspartic acid (RGD)

sequences to the beads, we can further guide differentiation by manipulating integrins using permanent magnets. We observed that by combining this stimulation regimen with current biochemical stimulation protocols, we could enhance cardiomyogenesis in mouse EBs.

Finally, we also investigated the potential of PEGylated fibrin gels to maintain and/or promote cardiomyocyte maturation. As a model, we used HL-1 cardiomyocytes, which are derived from a mouse atrial tumor lineage. HL-1 cardiomyocytes were cultured within and on top of fibrin hydrogels crosslinked with homobifunctional succinimidylglutarate polyethylene glycol (SG-PEG-SG). Functional characteristics of cardiomyocytes, such as contractile activity and expression of cardiac-specific markers sarcomeric α-actin and connexin 43, were examined during the culture process. As a comparison, ESC-CM derived from EBs were seeded on PEGylated fibrin gels with different fibrinogen concentrations and stiffness. We observed that PEGylated fibrin gels do have the potential to be used as MI patches; however, the starting cell population is critical to maintain cardiomyocyte functionality.

6.2. CONCLUSION ON SHH AND BMP4 DELIVERY STUDIES

Supplementation of Bone Morphogenetic Protein 4 (BMP4) to culture medium is currently the most effective protocol for deriving cardiomyocytes from mouse ESCs (Jamali, Karamboulas, Rogerson, & Skerjanc, 2001; Taha & Valojerdi, 2008). Recent reports suggest that Sonic Hedgehog (SHH) can also induce cardiovascular fates from embryonic stem cells (Gianakopoulos & Skerjanc, 2009; Kusano et al., 2005). In

Chapter 3, we attempted to overcome diffusional limitations of EB culture by immobilizing both BMP4 and SHH to paramagnetic beads and incorporating them into the EB during aggregation. While there were early increases in most mesodermal markers, gene expression data indicated that differentiation was not directed towards any specific phenotype. This is due possibly to decreased potency of tagged proteins compared to those without His- or MBP-tags. Interestingly, cardiomyocyte differentiation was affected by the presence of beads that were not immobilized with proteins: the only condition that significantly increased contractile activity were the EBs with beads alone. Using a focal adhesion protein array, integrin $\alpha 1$ was most changed in response to bead presence, suggesting an integrin-mediated interaction, which is ultimately increasing cardiomyogenesis.

6.3. CONCLUSION ON MAGNETIC ATTRACTION STUDIES

The results from Chapter 3 suggested that mechanical interactions with paramagnetic beads could increase cardiomyogenesis by mechanotransduction. In Chapter 4, we adapted the magnetic twisting cytometry (MTC) technique, which immobilizes RGD-sequences to paramagnetic beads and magnetizes the cells, to induce a stress on ESCs within the EBs. We hypothesized that MTC, which was previously demonstrated to decrease pluripotency in mESCs (Min et al., 2002; Uda et al., 2011), could also guide differentiation. We observed that magnetization could be used to apply stress to EBs at field strengths around 0.2 Tesla. This stress activates integrin-mediated signaling pathways via protein kinase A (PKA) and ERK1/2. In addition, this method

could be used to study the effects of mechanical stress on early EB time points: combining BMP4 with magnetically mediated strain increases cardiomyocyte differentiation over control groups when applied on Day 3. This is evident by the significant increase in contractile areas and percentage of sarcomeric α-actin positive cells by Day 18.

6.4. CONCLUSION ON PEGYLATED FIBRIN GEL STUDIES FOR MAINTENANCE OF MATURE AND IMMATURE CARDIOMYOCYTES

In Chapter 5, we investigated a tissue engineering approach to MI patch fabrication, in which PEGylated fibrin gels are seeded with cardiomyocytes. HL-1 cardiomyocytes are an ideal model because they are genotypically and phenotypically similar to mature cardiomyocytes (Claycomb et al., 1998; Xu et al., 2011). Regardless of the initial seeding density, HL-1 cardiomyocytes seeded within 10 mg/ml PEGylated fibrin gels proliferate into cardiosphere-like aggregates. These aggregates are viable, are proliferative and express both connexin 43 and sarcomeric α-actin; however, contractile activity is inhibited. Cells seeded on top of PEGylated fibrin gels proliferate and maintain sarcomeric α-actin expression, although cells spread differently on the gels depending on the concentration. Cardiomyocytes cultured on less concentrated and more compliant gels spread more, and as a result the rate of contractile activity is increased. In contrast, cells that are cultured on more concentrated gels contract at a significantly lower rate.

Since contractile activity on 2D gels was maintained within the published range for HL-1, we attempted to create a 3D-like patch by layering cells in between PEGylated fibrin gels. Similar approaches have been used with cell sheets to generate 3D constructs *ex vivo* (Leung & Sefton, 2010; Matsuura, Masuda, & Shimizu, 2014; Nunes et al., 2013; Robinson et al., 2005; Sakaguchi et al., 2013). To assess this possibility with our hydrogel technology, an additional gel layer was added to the top of confluent, contractile HL-1 cardiomyocytes. After 24 hours, contractile activity and viability was maintained, albeit at a slightly decreased rate.

In addition, we performed preliminary studies examining the behavior of ESC-CM on the hydrogels. ESC-CM were derived from EBs using the mechanical stimulation regimen described in Chapter 4. After seeding onto gels, contractile activity was lost; however, only approximately 48% of the population was comprised of cardiomyocytes.

6.5. FUTURE DIRECTIONS

The results described in this thesis demonstrate the potential of mechanical stimulation on directed differentiation of mESCs into cardiomyocytes. A potential drawback to the work presented here is that experiments were performed in mouse pluripotent cells. While this can serve as a model, to better elucidate their clinical use, understanding how these stimulation regimens direct differentiation of human ESCs and iPSCs will be important.

In our protein delivery studies, we were unable to detect statistical differences in cell phenotype over the course of EB culture. Possible reasons for this include (1) timing

of protein delivery and (2) the amount of immobilized protein delivered into the EB interior. For the former, SHH exposure at early timepoints may not be adequate to direct differentiation into cardiomyocytes. Pre-differentiation into mesendoderm may be necessary in order to guide cells towards cardiovascular fates. In addition, the high variability made analysis of the SHH potential to guide differentiation difficult. There is a possibility that Shh can direct differentiation; however, the potency of tagged-SHH is not sufficient for biological stimulation. To verify that the lack of response is due to His-tagged SHH potency alone, purmorphamine can be supplemented to the culture medium during ESC differentiation. In addition, co-delivery of beads with different proteins may further enhance cardiomyogenesis in EBs.

In Chapter 4, we observed that the magnetic field strength had a significant role in integrin-mediated signaling following the delivery of RGD-immobilized beads. Intermediate field strengths of approximately 0.2 T are sufficient to activate the MAPK/ERK signaling cascades. While 0.128 T was not sufficient to activate mechanotransduction and 0.4 T increased cell death, a better understanding of the range of field strengths may be helpful to optimize the mechanical stimulation regimen.

Another outstanding question from this study is exactly what the forces exerted on the cells within the EB are in response to magnetically mediated strain. The most relevant model we found was that developed by Zborowski *et al* (1999), which approximates the force experienced by a cell in a quadripole field while bound to a magnetic particle (Ye et al., 2011; Zborowski, Sun, Moore, Stephen Williams, & Chalmers, 1999). The EB microenvironment is more complex than this model can

account for, and consequently a more quantitative understanding of these forces would be beneficial.

In addition, in Chapter 4 we focused on a narrow window of EB development: the effect of magnetically mediated strain was only examined between Days 1 and 3. While we were primarily interested in the effects of stress at early timepoints, since this data is lacking from current stimulation protocols, examining the effects of magnetically mediated strain on later stages of EB development would also be interesting. Specifically, cardiomyogenesis may be even further stimulated when stress is applied on Day 4 or later. A better understanding of the effects of magnetically mediated strain on lineage commitment will improve the potential of this method.

Finally in Chapter 5, we examined the phenotypic and functional effects of PEGylated fibrin gels on cardiomyocyte maintenance and maturity. The lack of contractile activity when HL-1 were cultured in 3D may be due to the inability of cardiomyocytes to modify their environment. Cardiomyocytes account for only 20% of the entire cell population in the myocardium (Bergmann et al., 2009; Jamali et al., 2001; Taha & Valojerdi, 2008), and the addition of fibroblasts was observed to be critical to maintain contractile activity in cell sheets (Gianakopoulos & Skerjanc, 2005; Kusano et al., 2005; Matsuura et al., 2012). Three-dimensional culture of cardiomyocytes in PEGylated fibrin gels may be improved by fine-tuning the proportion of cardiomyocytes and non-cardiomyocytes. While a 50:50 ratio is too high (Figure 5.8), a lower percentage of cardiac fibroblasts may be sufficient for ECM remodeling and stimulation of contractile activity.

In this chapter, we also investigated the possibility of culturing cardiomyocytes in gel layers as an alternative to true 3D culture. This strategy combines sheets of cells and materials, which the cells will eventually remodel. When the cardiomyocytes started displaying contractile activity (Day 4), an additional gel layer was added to the cells, and contractile activity and viability was maintained after 24 hours. To further validate this method, the effects on long-term viability will also need to be assessed. Since matrix remodeling is an important part of developing the 3D cardiac patch, optimization of the material properties and cell population may also be necessary. For the former, producing nanostructured fibrinogen materials, such as by electrospinning (Frisman, Seliktar, & Bianco-Peled, 2011; H. Hosseinkhani, Hosseinkhani, Hattori, Matsuoka, & Kawaguchi, 2010; Massumi et al., 2011), can minimize material thickness while providing the surface topography that is ideal for cardiomyocytes. In addition, matrix remodeling can also be improved by altering the concentration of cardiomyocytes and non-cardiomyocytes.

6.6. REFERENCES

Bergmann, O., Bhardwaj, R. D., Bernard, S., Zdunek, S., Barnabe-Heider, F., Walsh, S., et al. (2009). Evidence for Cardiomyocyte Renewal in Humans. *Science (New York, N.Y.)*, *324*(5923), 98–102. doi:10.1126/science.1164680

Claycomb, W., Lanson, N., Stallworth, B., Egeland, D., Delcarpio, J., Bahinski, A., & Izzo, N. (1998). HL-1 cells: A cardiac muscle cell line that contracts and retains phenotypic characteristics of the adult cardiomyocyte. *Proceedings of the National Academy of Sciences of the United States of America*, *95*(6), 2979–2984.

Frisman, I., Seliktar, D., & Bianco-Peled, H. (2011). Nanostructuring PEG-fibrinogen hydrogels to control cellular morphogenesis. *Biomaterials*, *32*(31), 7839–7846. doi:10.1016/j.biomaterials.2011.06.078

Gianakopoulos, P. J., & Skerjanc, I. S. (2005). Hedgehog signaling induces cardiomyogenesis in P19 cells. *The Journal of Biological Chemistry*, *280*(22), 21022–21028. doi:10.1074/jbc.M502977200

Gianakopoulos, P. J., & Skerjanc, I. S. (2009). Cross talk between hedgehog and bone morphogenetic proteins occurs during cardiomyogenesis in P19 cells. *In Vitro Cellular & Developmental Biology. Animal*, *45*(9), 566–572. doi:10.1007/s11626-009-9228-z

Hosseinkhani, H., Hosseinkhani, M., Hattori, S., Matsuoka, R., & Kawaguchi, N. (2010). Micro and nano-scale in vitro 3D culture system for cardiac stem cells. *Journal of Biomedical Materials Research Part A*, *94*(1), 1–8. doi:10.1002/jbm.a.32676

Jamali, M., Karamboulas, C., Rogerson, P. J., & Skerjanc, I. S. (2001). BMP signaling regulates Nkx2-5 activity during cardiomyogenesis. *FEBS Letters*, *509*(1), 126–130.

Kusano, K. F., Pola, R., Murayama, T., Curry, C., Kawamoto, A., Iwakura, A., et al. (2005). Sonic hedgehog myocardial gene therapy: tissue repair through transient reconstitution of embryonic signaling. *Nature Medicine*, *11*(11), 1197–1204. doi:10.1038/nm1313

Leung, B. M., & Sefton, M. V. (2010). A modular approach to cardiac tissue engineering. *Tissue Engineering Part A*, *16*(10), 3207–3218. doi:10.1089/ten.TEA.2009.0746

Massumi, M., Abasi, M., Babaloo, H., Terraf, P., Safi, M., Saeed, M., et al. (2011). The Effect of Topography on Differentiation Fates of Matrigel-Coated Mouse Embryonic Stem (mES) Cells Cultured on PLGA Nanofibrous Scaffolds. *Tissue Engineering Part A*. doi:10.1089/ten.TEA.2011.0368

Matsuura, K., Masuda, S., & Shimizu, T. (2014). Cell Sheet-Based Cardiac Tissue Engineering. *Anatomical Record-Advances in Integrative Anatomy and Evolutionary Biology*, *297*(1), 65–72. doi:10.1002/ar.22834

Matsuura, K., Wada, M., Konishi, K., Sato, M., Iwamoto, U., Sato, Y., et al. (2012). Fabrication of mouse embryonic stem cell-derived layered cardiac cell sheets using a bioreactor culture system. *Plos One*, *7*(12), e52176–e52176. doi:10.1371/journal.pone.0052176

Min, J. Y., Yang, Y. K., Converso, K. L., Liu, L. X., Huang, Q., Morgan, J. P., & Xiao, Y. F. (2002). Transplantation of embryonic stem cells improves cardiac function in postinfarcted rats. *Journal of Applied Physiology (Bethesda, Md. : 1985)*, *92*(1), 288–296.

Nunes, S. S., Miklas, J. W., Liu, J., Aschar-Sobbi, R., Xiao, Y., Zhang, B., et al. (2013). Biowire: a platform for maturation of human pluripotent stem cell-derived cardiomyocytes. *Nature Methods*. doi:10.1038/nmeth.2524

Robinson, K. A., Li, J., Mathison, M., Redkar, A., Cui, J., Chronos, N. A. F., et al. (2005). Extracellular matrix scaffold for cardiac repair. *Circulation*, *112*(9 Suppl), I135–43. doi:10.1161/CIRCULATIONAHA.104.525436

Sakaguchi, K., Shimizu, T., Horaguchi, S., Sekine, H., Yamato, M., Umezu, M., & Okano, T. (2013). In Vitro Engineering of Vascularized Tissue Surrogates. *Scientific Reports*, *3*. doi:10.1038/srep01316

Taha, M. F., & Valojerdi, M. R. (2008). Effect of bone morphogenetic protein-4 on cardiac differentiation from mouse embryonic stem cells in serum-free and low-serum media. *International Journal of Cardiology*, *127*(1), 78–87. doi:10.1016/j.ijcard.2007.04.173

Uda, Y., Poh, Y.-C., Chowdhury, F., Wu, D. C., Tanaka, T. S., Sato, M., & Wang, N. (2011). Force via integrins but not E-cadherin decreases Oct3/4 expression in embryonic stem cells. *Biochemical and Biophysical Research Communications*, *415*(2), 396–400. doi:10.1016/j.bbrc.2011.10.080

Xu, H., Yi, B. A., & Chien, K. R. (2011). Shortcuts to making cardiomyocytes. *Nature Cell Biology*, *13*(3), 191–193. doi:10.1038/ncb0311-191

Ye, Z., Zhou, Y., Cai, H., & Tan, W. (2011). Myocardial regeneration: Roles of stem cells and hydrogels. *Advanced Drug Delivery Reviews*, *63*(8), 688–697. doi:10.1016/j.addr.2011.02.007

Zborowski, M., Sun, L., Moore, L. R., Stephen Williams, P., & Chalmers, J. J. (1999). Continuous cell separation using novel magnetic quadrupole flow sorter. *Journal of Magnetism and Magnetic Materials*, *194*(1), 224–230.

BIBLIOGRAPHY

Adamo, L., & García-Cardeña, G. (2011). Directed stem cell differentiation by fluid mechanical forces. *Antioxidants & Redox Signaling*, *15*(5), 1463–1473. doi:10.1089/ars.2011.3907

Ahmed, R. P. H., Haider, K. H., Shujia, J., Afzal, M. R., & Ashraf, M. (2010). Sonic Hedgehog gene delivery to the rodent heart promotes angiogenesis via iNOS/netrin-1/PKC pathway. *Plos One*, *5*(1), e8576. doi:10.1371/journal.pone.0008576

Ahsan, T., & Nerem, R. M. (2010). Fluid shear stress promotes an endothelial-like phenotype during the early differentiation of embryonic stem cells. *Tissue Engineering Part A*, *16*(11), 3547–3553. doi:10.1089/ten.TEA.2010.0014

Aicher, A., Brenner, W., Zuhayra, M., Badorff, C., Massoudi, S., Assmus, B., et al. (2003). Assessment of the tissue distribution of transplanted human endothelial progenitor cells by radioactive labeling. *Circulation*, *107*(16), 2134–2139. doi:10.1161/01.CIR.0000062649.63838.C9

Aikawa, R., Nagai, T., Kudoh, S., Zou, Y., Tanaka, M., Tamura, M., et al. (2002). Integrins play a critical role in mechanical stress-induced p38 MAPK activation. *Hypertension*, *39*(2), 233–238.

Alenghat, F. J., Tytell, J. D., Thodeti, C. K., Derrien, A., & Ingber, D. E. (2009). Mechanical control of cAMP signaling through integrins is mediated by the heterotrimeric Galphas protein. *Journal of Cellular Biochemistry*, *106*(4), 529–538. doi:10.1002/jcb.22001

Alexander, J. M., & Bruneau, B. G. (2010). Lessons for cardiac regeneration and repair through development. *Trends in Molecular Medicine*, *16*(9), 426–434. doi:10.1016/j.molmed.2010.06.003

Anderson, G. J., & Darshan, D. (2008). Small-molecule dissection of BMP signaling. *Nature Chemical Biology*, *4*(1), 15–16. doi:10.1038/nchembio0108-15

Astorga, J., & Carlsson, P. (2007). Hedgehog induction of murine vasculogenesis is mediated by Foxf1 and Bmp4. *Development*, *134*(20), 3753–3761. doi:10.1242/dev.004432

Bai, H., Gao, Y., Arzigian, M., Wojchowski, D. M., Wu, W.-S., & Wang, Z. Z. (2010). BMP4 regulates vascular progenitor development in human embryonic stem cells through a Smad-dependent pathway. *Journal of Cellular Biochemistry*, *109*(2), 363–

374. doi:10.1002/jcb.22410

Bartsch, C., Bekhite, M. M., Wolheim, A., Richter, M., Ruhe, C., Wissuwa, B., et al. (2011). NADPH oxidase and eNOS control cardiomyogenesis in mouse embryonic stem cells on ascorbic acid treatment. *Free Radical Biology & Medicine*, *51*(2), 432–443. doi:10.1016/j.freeradbiomed.2011.04.029

Battista, S., Guarnieri, D., Borselli, C., Zeppetelli, S., Borzacchiello, A., Mayol, L., et al. (2005). The effect of matrix composition of 3D constructs on embryonic stem cell differentiation. *Biomaterials*, *26*(31), 6194–6207. doi:10.1016/j.biomaterials.2005.04.003

Bel, A., Planat-Bernard, V., Saito, A., Bonnevie, L., Bellamy, V., Sabbah, L., et al. (2010). Composite cell sheets: a further step toward safe and effective myocardial regeneration by cardiac progenitors derived from embryonic stem cells. *Circulation*, *122*(11 Suppl), S118–23. doi:10.1161/CIRCULATIONAHA.109.927293

Berge, ten, D., Koole, W., Fuerer, C., Fish, M., Eroglu, E., & Nusse, R. (2008). Wnt signaling mediates self-organization and axis formation in embryoid bodies. *Cell Stem Cell*, *3*(5), 508–518. doi:10.1016/j.stem.2008.09.013

Bergmann, O., Bhardwaj, R. D., Bernard, S., Zdunek, S., Barnabe-Heider, F., Walsh, S., et al. (2009). Evidence for Cardiomyocyte Renewal in Humans. *Science (New York, N.Y.)*, *324*(5923), 98–102. doi:10.1126/science.1164680

Berry, M. F., Engler, A. J., Woo, Y. J., Pirolli, T. J., Bish, L. T., Jayasankar, V., et al. (2006). Mesenchymal stem cell injection after myocardial infarction improves myocardial compliance. *American Journal of Physiology Heart and Circulatory Physiology*, *290*(6), H2196–203. doi:10.1152/ajpheart.01017.2005

Bijlsma, M. F., & Spek, C. A. (2010). The Hedgehog morphogen in myocardial ischemia-reperfusion injury. *Experimental Biology and Medicine (Maywood, N.J.)*, *235*(4), 447–454. doi:10.1258/ebm.2009.009303

Bistola, V., Nikolopoulou, M., Derventzi, A., Kataki, A., Sfyras, N., Nikou, N., et al. (2008). Long-term primary cultures of human adult atrial cardiac myocytes: Cell viability, structural properties and BNP secretion in vitro. *International Journal of Cardiology*, *131*(1), 113–122. doi:10.1016/j.ijcard.2007.10.058

Black, L. D., Meyers, J. D., Weinbaum, J. S., Shvelidze, Y. A., & Tranquillo, R. T. (2009). Cell-induced alignment augments twitch force in fibrin gel-based engineered myocardium via gap junction modification. *Tissue Engineering Part A*, *15*(10), 3099–3108. doi:10.1089/ten.TEA.2008.0502

Blan, N. R., & Birla, R. K. (2008). Design and fabrication of heart muscle using scaffold-based tissue engineering. *Journal of Biomedical Materials Research Part A*, *86A*(1), 195–208. doi:10.1002/jbm.a.31642

Boheler, K. R., Czyz, J., Tweedie, D., Yang, H.-T., Anisimov, S. V., & Wobus, A. M. (2002). Differentiation of pluripotent embryonic stem cells into cardiomyocytes. *Circulation Research*, *91*(3), 189–201.

Brafman, D. A., Phung, C., Kumar, N., & Willert, K. (2013). Regulation of endodermal differentiation of human embryonic stem cells through integrin-ECM interactions. *Cell Death and Differentiation*, *20*(3), 369–381. doi:10.1038/cdd.2012.138

Bratt-Leal, A. M., Carpenedo, R. L., & Mcdevitt, T. C. (2009). Engineering the embryoid body microenvironment to direct embryonic stem cell differentiation. *Biotechnology Progress*, *25*(1), 43–51. doi:10.1002/btpr.139

Bratt-Leal, A. M., Carpenedo, R. L., Ungrin, M. D., Zandstra, P. W., & Mcdevitt, T. C. (2011). Incorporation of biomaterials in multicellular aggregates modulates pluripotent stem cell differentiation. *Biomaterials*, *32*(1), 48–56. doi:10.1016/j.biomaterials.2010.08.113

Bratt-Leal, A. M., Nguyen, A. H., Hammersmith, K. A., Singh, A., & Mcdevitt, T. C. (2013). A microparticle approach to morphogen delivery within pluripotent stem cell aggregates. *Biomaterials*, *34*(30), 7227–7235. doi:10.1016/j.biomaterials.2013.05.079

Breen, A., O'Brien, T., & Pandit, A. (2009). Fibrin as a delivery system for therapeutic drugs and biomolecules. *Tissue Engineering Part B, Reviews*, *15*(2), 201–214. doi:10.1089/ten.TEB.2008.0527

Brewer, A. C., & Shah, A. M. (2009). Redox signalling and miRNA function in cardiomyocytes. *Journal of Molecular and Cellular Cardiology*, *47*(1), 2–4. doi:10.1016/j.yjmcc.2009.02.024

Buggisch, M., Ateghang, B., Ruhe, C., Strobel, C., Lange, S., Wartenberg, M., & Sauer, H. (2007). Stimulation of ES-cell-derived cardiomyogenesis and neonatal cardiac cell proliferation by reactive oxygen species and NADPH oxidase. *Journal of Cell Science*, *120*(Pt 5), 885–894. doi:10.1242/jcs.03386

Bukoreshtliev, N. V., Haase, K., & Pelling, A. E. (2013). Mechanical cues in cellular signalling and communication. *Cell and Tissue Research*, *352*(1), 77–94. doi:10.1007/s00441-012-1531-4

Burdon, T., Smith, A., & Savatier, P. (2002). Signalling, cell cycle and pluripotency in embryonic stem cells. *Trends in Cell Biology*, *12*(9), 432–438.

Byrd, N., Becker, S., Maye, P., Narasimhaiah, R., St-Jacques, B., Zhang, X., et al. (2002). Hedgehog is required for murine yolk sac angiogenesis. *Development*, *129*(2), 361–372.

Cai, J., Chen, J., Liu, Y., Miura, T., Luo, Y., Loring, J. F., et al. (2006). Assessing self-renewal and differentiation in human embryonic stem cell lines. *Stem Cells*, *24*(3), 516–530. doi:10.1634/stemcells.2005-0143

Carpenedo, R. L., Bratt-Leal, A. M., Marklein, R. A., Seaman, S. A., Bowen, N. J., Mcdonald, J. F., & Mcdevitt, T. C. (2009). Homogeneous and organized differentiation within embryoid bodies induced by microsphere-mediated delivery of small molecules. *Biomaterials*, *30*(13), 2507–2515. doi:10.1016/j.biomaterials.2009.01.007

Chen, J., Fabry, B., Schiffrin, E. L., & Wang, N. (2001). Twisting integrin receptors increases endothelin-1 gene expression in endothelial cells. *American Journal of Physiology-Cell Physiology*, *280*(6), C1475–84.

Chen, M., Lin, Y.-Q., Xie, S.-L., Wu, H.-F., & Wang, J.-F. (2011). Enrichment of cardiac differentiation of mouse embryonic stem cells by optimizing the hanging drop method. *Biotechnology Letters*, *33*(4), 853–858. doi:10.1007/s10529-010-0494-3

Chowdhury, F., Na, S., Li, D., Poh, Y.-C., Tanaka, T. S., Wang, F., & Wang, N. (2009). Material properties of the cell dictate stress-induced spreading and differentiation in embryonic stem cells. *Nature Materials*, *9*(1), 82–88. doi:10.1038/nmat2563

Christman, K. L., Vardanian, A. J., Fang, Q., Sievers, R. E., Fok, H. H., & Lee, R. J. (2004). Injectable fibrin scaffold improves cell transplant survival, reduces infarct expansion, and induces neovasculature formation in ischemic myocardium. *Journal of the American College of Cardiology*, *44*(3), 654–660. doi:10.1016/j.jacc.2004.04.040

Claycomb, W., Lanson, N., Stallworth, B., Egeland, D., Delcarpio, J., Bahinski, A., & Izzo, N. (1998). HL-1 cells: A cardiac muscle cell line that contracts and retains phenotypic characteristics of the adult cardiomyocyte. *Proceedings of the National Academy of Sciences of the United States of America*, *95*(6), 2979–2984.

Clement, C. A., Kristensen, S. G., Møllgård, K., Pazour, G. J., Yoder, B. K., Larsen, L. A., & Christensen, S. T. (2009). The primary cilium coordinates early cardiogenesis

and hedgehog signaling in cardiomyocyte differentiation. *Journal of Cell Science*, *122*(17), 3070–3082. doi:10.1242/jcs.049676

Czyz, J., & Wobus, A. (2001). Embryonic stem cell differentiation: the role of extracellular factors. *Differentiation*, *68*(4-5), 167–174.

Dar, A., Shachar, M., Leor, J., & Cohen, S. (2002). Cardiac tissue engineering - Optimization of cardiac cell seeding and distribution in 3D porous alginate scaffolds. *Biotechnology and Bioengineering*, *80*(3), 305–312. doi:10.1002/bit.10372

Davies, P. F., Remuzzi, A., Gordon, E. J., Dewey, C. F., & Gimbrone, M. A. (1986). Turbulent fluid shear stress induces vascular endothelial cell turnover in vitro. *Proceedings of the National Academy of Sciences of the United States of America*, *83*(7), 2114–2117.

Dawson, J., Schussler, O., Al-Madhoun, A., Menard, C., Ruel, M., & Skerjanc, I. S. (2011). Collagen scaffolds with or without the addition of RGD peptides support cardiomyogenesis after aggregation of mouse embryonic stem cells. *In Vitro Cellular & Developmental Biology. Animal*, *47*(9), 653–664. doi:10.1007/s11626-011-9453-0

Dias, J. V., Benslimane-Ahmim, Z., Egot, M., Lokajczyk, A., Grelac, F., Galy-Fauroux, I., et al. (2012). A motif within the N-terminal domain of TSP-1 specifically promotes the proangiogenic activity of endothelial colony-forming cells. *Biochemical Pharmacology*, *84*(8), 1014–1023. doi:10.1016/j.bcp.2012.07.006

Drinnan, C. T., Zhang, G., Alexander, M. A., Pulido, A. S., & Suggs, L. J. (2010). Multimodal release of transforming growth factor-β1 and the BB isoform of platelet derived growth factor from PEGylated fibrin gels. *Journal of Controlled Release : Official Journal of the Controlled Release Society*, *147*(2), 180–186. doi:10.1016/j.jconrel.2010.03.026

Duranteau, J. (1998). Intracellular Signaling by Reactive Oxygen Species during Hypoxia in Cardiomyocytes. *Journal of Biological Chemistry*, *273*(19), 11619–11624. doi:10.1074/jbc.273.19.11619

Engler, A. J., Carag-Krieger, C., Johnson, C. P., Raab, M., Tang, H.-Y., Speicher, D. W., et al. (2008). Embryonic cardiomyocytes beat best on a matrix with heart-like elasticity: scar-like rigidity inhibits beating. *Journal of Cell Science*, *121*(Pt 22), 3794–3802. doi:10.1242/jcs.029678

Engler, A. J., Sen, S., Sweeney, H. L., & Discher, D. E. (2006). Matrix elasticity directs stem cell lineage specification. *Cell*, *126*(4), 677–689. doi:10.1016/j.cell.2006.06.044

Evans, T. (2008). Embryonic Stem Cells as a Model for Cardiac Development and Disease. *Drug Discovery Today Disease Models*, *5*(3), 147–155. doi:10.1016/j.ddmod.2009.03.004

Frank-Kamenetsky, M., Zhang, X. M., Bottega, S., Guicherit, O., Wichterle, H., Dudek, H., et al. (2002). Small-molecule modulators of Hedgehog signaling: identification and characterization of Smoothened agonists and antagonists. *Journal of Biology*, *1*(2), 10.

Frisman, I., Seliktar, D., & Bianco-Peled, H. (2011). Nanostructuring PEG-fibrinogen hydrogels to control cellular morphogenesis. *Biomaterials*, *32*(31), 7839–7846. doi:10.1016/j.biomaterials.2011.06.078

Gasimli, L., Linhardt, R. J., & Dordick, J. S. (2012). Proteoglycans in stem cells. *Biotechnology and Applied Biochemistry*, *59*(2), 65–76. doi:10.1002/bab.1002

Gerard, C., Forest, M. A., Beauregard, G., Skuk, D., & Tremblay, J. P. (2012). Fibrin gel improves the survival of transplanted myoblasts. *Cell Transplantation*, *21*(1), 127–137. doi:10.3727/096368911X576018

Geuss, L. R., & Suggs, L. J. (2013). Making cardiomyocytes: how mechanical stimulation can influence differentiation of pluripotent stem cells. *Biotechnology Progress*, *29*(5), 1089–1096. doi:10.1002/btpr.1794

Gianakopoulos, P. J., & Skerjanc, I. S. (2005). Hedgehog signaling induces cardiomyogenesis in P19 cells. *The Journal of Biological Chemistry*, *280*(22), 21022–21028. doi:10.1074/jbc.M502977200

Gianakopoulos, P. J., & Skerjanc, I. S. (2009). Cross talk between hedgehog and bone morphogenetic proteins occurs during cardiomyogenesis in P19 cells. *In Vitro Cellular & Developmental Biology. Animal*, *45*(9), 566–572. doi:10.1007/s11626-009-9228-z

Ginis, I., Luo, Y., Miura, T., Thies, S., Brandenberger, R., Gerecht-Nir, S., et al. (2004). Differences between human and mouse embryonic stem cells. *Developmental Biology*, *269*(2), 360–380. doi:10.1016/j.ydbio.2003.12.034

Go, A. S., Mozaffarian, D., Roger, V. L., Benjamin, E. J., Berry, J. D., Borden, W. B., et al. (2013). Heart disease and stroke statistics--2013 update: a report from the American Heart Association. *Circulation*, *127*(1), e6–e245. doi:10.1161/CIR.0b013e31828124ad

Gonnerman, E. A., Kelkhoff, D. O., McGregor, L. M., & Harley, B. A. C. (2012). The

promotion of HL-1 cardiomyocyte beating using anisotropic collagen-GAG scaffolds. *Biomaterials*, *33*(34), 8812–8821. doi:10.1016/j.biomaterials.2012.08.051

Gwak, S.-J., Bhang, S. H., Kim, I.-K., Kim, S.-S., Cho, S.-W., Jeon, O., et al. (2008). The effect of cyclic strain on embryonic stem cell-derived cardiomyocytes. *Biomaterials*, *29*(7), 844–856. doi:10.1016/j.biomaterials.2007.10.050

Harvey, R. P. (2002). Patterning the vertebrate heart. *Nature Reviews Genetics*, *3*(7), 544–556. doi:10.1038/nrg843

Hayashi, Y., Furue, M. K., Okamoto, T., Ohnuma, K., Myoishi, Y., Fukuhara, Y., et al. (2007). Integrins regulate mouse embryonic stem cell self-renewal. *Stem Cells*, *25*(12), 3005–3015. doi:10.1634/stemcells.2007-0103

Heo, J. S., & Lee, J.-C. (2011). β-catenin mediates cyclic strain-stimulated cardiomyogenesis in mouse embryonic stem cells through ROS-dependent and integrin-mediated PI3K/Akt pathways. *Journal of Cellular Biochemistry*, *112*(7), 1880–1889. doi:10.1002/jcb.23108

Hidalgo-Bastida, L. A., Barry, J. J. A., Everitt, N. M., Rose, F. R. A. J., Buttery, L. D., Hall, I. P., et al. (2007). Cell adhesion and mechanical properties of a flexible scaffold for cardiac tissue engineering. *Acta Biomaterialia*, *3*(4), 457–462. doi:10.1016/j.actbio.2006.12.006

Holtzinger, A., Rosenfeld, G. E., & Evans, T. (2010). Gata4 directs development of cardiac-inducing endoderm from ES cells. *Developmental Biology*, *337*(1), 63–73. doi:10.1016/j.ydbio.2009.10.003

Horiuchi, R., Akimoto, T., Hong, Z., & Ushida, T. (2012). Cyclic mechanical strain maintains Nanog expression through PI3K/Akt signaling in mouse embryonic stem cells. *Experimental Cell Research*. doi:10.1016/j.yexcr.2012.05.021

Hosseinkhani, H., Hosseinkhani, M., Hattori, S., Matsuoka, R., & Kawaguchi, N. (2010). Micro and nano-scale in vitro 3D culture system for cardiac stem cells. *Journal of Biomedical Materials Research Part A*, *94*(1), 1–8. doi:10.1002/jbm.a.32676

Hove, J. R., Köster, R. W., Forouhar, A. S., Acevedo-Bolton, G., Fraser, S. E., & Gharib, M. (2003). Intracardiac fluid forces are an essential epigenetic factor for embryonic cardiogenesis. *Nature*, *421*(6919), 172–177. doi:10.1038/nature01282

Huang, C.-C., Liao, C.-K., Yang, M.-J., Chen, C.-H., Hwang, S.-M., Hung, Y.-W., et al. (2010). A strategy for fabrication of a three-dimensional tissue construct containing uniformly distributed embryoid body-derived cells as a cardiac patch. *Biomaterials*,

31(24), 6218–6227. doi:10.1016/j.biomaterials.2010.04.067

Huang, Y.-C., Khait, L., & Birla, R. K. (2007). Contractile three-dimensional bioengineered heart muscle for myocardial regeneration. *Journal of Biomedical Materials Research Part A*, *80A*(3), 719–731. doi:10.1002/jbm.a.31090

Hwang, Y.-S., Chung, B. G., Ortmann, D., Hattori, N., Moeller, H.-C., & Khademhosseini, A. (2009). Microwell-mediated control of embryoid body size regulates embryonic stem cell fate via differential expression of WNT5a and WNT11. *Pnas*, *106*(40), 16978–16983. doi:10.1073/pnas.0905550106

Illi, B., Scopece, A., Nanni, S., Farsetti, A., Morgante, L., Biglioli, P., et al. (2005). Epigenetic histone modification and cardiovascular lineage programming in mouse embryonic stem cells exposed to laminar shear stress. *Circulation Research*, *96*(5), 501–508. doi:10.1161/01.RES.0000159181.06379.63

Ingber, D. E. (2006). Mechanical control of tissue morphogenesis during embryological development. *The International Journal of Developmental Biology*, *50*(2-3), 255–266. doi:10.1387/ijdb.052044di

Ingham, P. W., & McMahon, A. P. (2001). Hedgehog signaling in animal development: paradigms and principles. *Genes & Development*, *15*(23), 3059–3087. doi:10.1101/gad.938601

Itabashi, Y., Miyoshi, S., Kawaguchi, H., Yuasa, S., Tanimoto, K., Furuta, A., et al. (2005). A new method for manufacturing cardiac cell sheets using fibrin-coated dishes and its electrophysiological studies by optical mapping. *Artificial Organs*, *29*(2), 95–103. doi:10.1111/j.1525-1594.2005.29020.x

Jamali, M., Karamboulas, C., Rogerson, P. J., & Skerjanc, I. S. (2001). BMP signaling regulates Nkx2-5 activity during cardiomyogenesis. *FEBS Letters*, *509*(1), 126–130.

Johnson, T. D., & Christman, K. L. (2012). Injectable hydrogel therapies and their delivery strategies for treating myocardial infarction. *Expert Opinion on Drug Delivery*. doi:10.1517/17425247.2013.739156

Kalaskar, D. M., Downes, J. E., Murray, P., Edgar, D. H., & Williams, R. L. (2013). Characterization of the interface between adsorbed fibronectin and human embryonic stem cells. *Journal of the Royal Society, Interface / the Royal Society*, *10*(83), 20130139. doi:10.1098/rsif.2013.0139

Kattman, S. J., Huber, T. L., & Keller, G. M. (2006). Multipotent flk-1+ cardiovascular progenitor cells give rise to the cardiomyocyte, endothelial, and vascular smooth

muscle lineages. *Developmental Cell*, *11*(5), 723–732. doi:10.1016/j.devcel.2006.10.002

Keung, A. J., Healy, K. E., Kumar, S., & Schaffer, D. V. (2009). Biophysics and dynamics of natural and engineered stem cell microenvironments. *Wiley Interdisciplinary Reviews. Systems Biology and Medicine*, *2*(1), 49–64. doi:10.1002/wsbm.46

Khan, S. A., Nelson, M. S., Pan, C., Gaffney, P. M., & Gupta, P. (2008). Endogenous heparan sulfate and heparin modulate bone morphogenetic protein-4 signaling and activity. *American Journal of Physiology-Cell Physiology*, *294*(6), C1387–97. doi:10.1152/ajpcell.00346.2007

Kolossov, E., Bostani, T., Roell, W., Breitbach, M., Pillekamp, F., Nygren, J. M., et al. (2006). Engraftment of engineered ES cell-derived cardiomyocytes but not BM cells restores contractile function to the infarcted myocardium. *The Journal of Experimental Medicine*, *203*(10), 2315–2327. doi:10.1084/jem.20061469

Kumar, D., Kamp, T. J., & LeWinter, M. M. (2005). Embryonic stem cells: differentiation into cardiomyocytes and potential for heart repair and regeneration. *Coronary Artery Disease*, *16*(2), 111–116.

Kusano, K. F., Pola, R., Murayama, T., Curry, C., Kawamoto, A., Iwakura, A., et al. (2005). Sonic hedgehog myocardial gene therapy: tissue repair through transient reconstitution of embryonic signaling. *Nature Medicine*, *11*(11), 1197–1204. doi:10.1038/nm1313

Labouesse, M. (2011). *Forces and Tension in Development*. Academic Press. doi:10.1016/B978-0-12-385065-2.00008-6

Laboureau, J., Dubertret, L., Lebreton-De Coster, C., & Coulomb, B. (2004). ERK activation by mechanical strain is regulated by the small G proteins rac-1 and rhoA. *Experimental Dermatology*, *13*(2), 70–77. doi:10.1111/j.0906-6705.2004.00117.x

Laflamme, M. A., Chen, K. Y., Naumova, A. V., Muskheli, V., Fugate, J. A., Dupras, S. K., et al. (2007a). Cardiomyocytes derived from human embryonic stem cells in pro-survival factors enhance function of infarcted rat hearts. *Nature Biotechnology*, *25*(9), 1015–1024. doi:10.1038/nbt1327

Laflamme, M. A., Zbinden, S., Epstein, S. E., & Murry, C. E. (2007b). Cell-based therapy for myocardial ischemia and infarction: pathophysiological mechanisms. *Annual Review of Pathology*, *2*, 307–339. doi:10.1146/annurev.pathol.2.010506.092038

Lanner, F., & Rossant, J. (2010). The role of FGF/Erk signaling in pluripotent cells. *Development*, *137*(20), 3351–3360. doi:10.1242/dev.050146

Lavine, K. J., Kovacs, A., & Ornitz, D. M. (2008). Hedgehog signaling is critical for maintenance of the adult coronary vasculature in mice. *The Journal of Clinical Investigation*, *118*(7), 2404–2414. doi:10.1172/JCI34561

Lee, M. Y., Bozkulak, E. C., Schliffke, S., Amos, P. J., Ren, Y., Ge, X., et al. (2011a). High density cultures of embryoid bodies enhanced cardiac differentiation of murine embryonic stem cells. *Biochemical and Biophysical Research Communications*, *416*(1-2), 51–57. doi:10.1016/j.bbrc.2011.10.140

Lee, S. H., Lee, Y. J., Park, S. W., Kim, H. S., & Han, H. J. (2011b). Caveolin-1 and integrin β1 regulate embryonic stem cell proliferation via p38 MAPK and FAK in high glucose. *Journal of Cellular Physiology*, *226*(7), 1850–1859. doi:10.1002/jcp.22510

Lee, S. T., Yun, J. I., van der Vlies, A. J., Kontos, S., Jang, M., Gong, S. P., et al. (2012). Long-term maintenance of mouse embryonic stem cell pluripotency by manipulating integrin signaling within 3D scaffolds without active Stat3. *Biomaterials*, *33*(35), 8934–8942. doi:10.1016/j.biomaterials.2012.08.062

Lehoux, S. (2006). Redox signalling in vascular responses to shear and stretch. *Cardiovascular Research*, *71*(2), 269–279. doi:10.1016/j.cardiores.2006.05.008

Leung, B. M., & Sefton, M. V. (2010). A modular approach to cardiac tissue engineering. *Tissue Engineering Part A*, *16*(10), 3207–3218. doi:10.1089/ten.TEA.2009.0746

Li, Y.-S., & Gao, B.-R. (2007). Transplantation of neonatal cardiomyocytes plus fibrin sealant restores myocardial function in a rat model of myocardial infarction. *Chinese Medical Journal*, *120*(22), 2022–2027.

Lian, X., Zhang, J., Azarin, S. M., Zhu, K., Hazeltine, L. B., Bao, X., et al. (2013). Directed cardiomyocyte differentiation from human pluripotent stem cells by modulating Wnt/β-catenin signaling under fully defined conditions. *Nature Protocols*, *8*(1), 162–175. doi:10.1038/nprot.2012.150

LIU, H., Collins, S. F., & Suggs, L. J. (2006). Three-dimensional culture for expansion and differentiation of mouse embryonic stem cells. *Biomaterials*, *27*(36), 6004–6014. doi:10.1016/j.biomaterials.2006.06.016

Louis, H., Kakou, A., Regnault, V., Labat, C., Bressenot, A., Gao-Li, J., et al. (2007).

Role of alpha(1)beta(1)-integrin in arterial stiffness and angiotensin-induced arterial wall hypertrophy in mice. *American Journal of Physiology Heart and Circulatory Physiology*, *293*(4), H2597–H2604. doi:10.1152/ajpheart.00299.2007

Lucitti, J. L., Jones, E. A. V., Huang, C., Chen, J., Fraser, S. E., & Dickinson, M. E. (2007). Vascular remodeling of the mouse yolk sac requires hemodynamic force. *Development*, *134*(18), 3317–3326. doi:10.1242/dev.02883

Luong, E., & Gerecht, S. (2008). Stem Cells and Scaffolds for Vascularizing Engineered Tissue Constructs. *Advances in Biochemical Engineering/Biotechnology*, *114*, 129–172. doi:10.1007/10_2008_8

Lyngbaek, S., Schneider, M., Hansen, J. L., & Sheikh, S. P. (2007). Cardiac regeneration by resident stem and progenitor cells in the adult heart. *Basic Research in Cardiology*, *102*(2), 101–114. doi:10.1007/s00395-007-0638-3

Makino, S., Fukuda, K., Miyoshi, S., Konishi, F., Kodama, H., Pan, J., et al. (1999). Cardiomyocytes can be generated from marrow stromal cells in vitro. *The Journal of Clinical Investigation*, *103*(5), 697–705. doi:10.1172/JCI5298

Mammoto, A., Mammoto, T., & Ingber, D. E. (2012). Mechanosensitive mechanisms in transcriptional regulation. *Journal of Cell Science*, *125*(Pt 13), 3061–3073. doi:10.1242/jcs.093005

Mammoto, T., & Ingber, D. E. (2010). Mechanical control of tissue and organ development. *Development*, *137*(9), 1407–1420. doi:10.1242/dev.024166

Maniotis, A. J., Chen, C. S., & Ingber, D. E. (1997). Demonstration of mechanical connections between integrins cytoskeletal filaments, and nucleoplasm that stabilize nuclear structure. *Proceedings of the National Academy of Sciences of the United States of America*, *94*(3), 849–854.

Marsano, A., Maidhof, R., Wan, L. Q., Wang, Y., Gao, J., Tandon, N., & Vunjak-Novakovic, G. (2010). Scaffold stiffness affects the contractile function of three-dimensional engineered cardiac constructs. *Biotechnology Progress*, *26*(5), 1382–1390. doi:10.1002/btpr.435

Martin, G. R. (1981). Isolation of a pluripotent cell line from early mouse embryos cultured in medium conditioned by teratocarcinoma stem cells. *Proceedings of the National Academy of Sciences of the United States of America*, *78*(12), 7634–7638.

Massumi, M., Abasi, M., Babaloo, H., Terraf, P., Safi, M., Saeed, M., et al. (2011). The Effect of Topography on Differentiation Fates of Matrigel-Coated Mouse Embryonic

Stem (mES) Cells Cultured on PLGA Nanofibrous Scaffolds. *Tissue Engineering Part A*. doi:10.1089/ten.TEA.2011.0368

Masumura, T., Yamamoto, K., Shimizu, N., Obi, S., & Ando, J. (2009). Shear stress increases expression of the arterial endothelial marker ephrinB2 in murine ES cells via the VEGF-Notch signaling pathways. *Arteriosclerosis, Thrombosis, and Vascular Biology*, *29*(12), 2125–2131. doi:10.1161/ATVBAHA.109.193185

Matsuura, K., Masuda, S., & Shimizu, T. (2014). Cell Sheet-Based Cardiac Tissue Engineering. *Anatomical Record-Advances in Integrative Anatomy and Evolutionary Biology*, *297*(1), 65–72. doi:10.1002/ar.22834

Matsuura, K., Masuda, S., Haraguchi, Y., Yasuda, N., Shimizu, T., Hagiwara, N., et al. (2011). Creation of mouse embryonic stem cell-derived cardiac cell sheets. *Biomaterials*, *32*(30), 7355–7362. doi:10.1016/j.biomaterials.2011.05.042

Matsuura, K., Wada, M., Konishi, K., Sato, M., Iwamoto, U., Sato, Y., et al. (2012). Fabrication of mouse embryonic stem cell-derived layered cardiac cell sheets using a bioreactor culture system. *Plos One*, *7*(12), e52176–e52176. doi:10.1371/journal.pone.0052176

Matthews, B. D., Overby, D. R., Mannix, R., & Ingber, D. E. (2006). Cellular adaptation to mechanical stress: role of integrins, Rho, cytoskeletal tension and mechanosensitive ion channels. *Journal of Cell Science*, *119*(Pt 3), 508–518. doi:10.1242/jcs.02760

Metallo, C. M., Vodyanik, M. A., de Pablo, J. J., Slukvin, I. I., & Palecek, S. P. (2008). The response of human embryonic stem cell-derived endothelial cells to shear stress. *Biotechnology and Bioengineering*, *100*(4), 830–837. doi:10.1002/bit.21809

Meyer, C. J., Alenghat, F. J., Rim, P., Fong, J. H., Fabry, B., & Ingber, D. E. (2000). Mechanical control of cyclic AMP signalling and gene transcription through integrins. *Nature Cell Biology*, *2*(9), 666–668. doi:10.1038/35023621

Mihic, A., Li, J., Miyagi, Y., Gagliardi, M., Li, S.-H., Zu, J., et al. (2014). The effect of cyclic stretch on maturation and 3D tissue formation of human embryonic stem cell-derived cardiomyocytes. *Biomaterials*. doi:10.1016/j.biomaterials.2013.12.052

Min, J. Y., Yang, Y. K., Converso, K. L., Liu, L. X., Huang, Q., Morgan, J. P., & Xiao, Y. F. (2002). Transplantation of embryonic stem cells improves cardiac function in postinfarcted rats. *Journal of Applied Physiology (Bethesda, Md. : 1985)*, *92*(1), 288–296.

Mosesson, M. W. (2005). Fibrinogen and fibrin structure and functions. *Journal of Thrombosis and Haemostasis : JTH*, *3*(8), 1894–1904. doi:10.1111/j.1538-7836.2005.01365.x

Murry, C. E., & Keller, G. (2010). Differentiation of Embryonic Stem Cells to Clinically Relevant Populations: Lessons from Embryonic Development
. *Cell*, *132*, 661–680. doi:10.1016/j.cell.2008.02.008

Nakajima, Y., Yamagishi, T., Ando, K., & Nakamura, H. (2002). Significance of bone morphogenetic protein-4 function in the initial myofibrillogenesis of chick cardiogenesis. *Developmental Biology*, *245*(2), 291–303. doi:10.1006/dbio.2002.0637

Neal, R. A., Jean, A., Park, H., Wu, P. B., Hsiao, J., Engelmayr, G. C., et al. (2013). Three-dimensional elastomeric scaffolds designed with cardiac-mimetic structural and mechanical features. *Tissue Engineering Part A*, *19*(5-6), 793–807. doi:10.1089/ten.tea.2012.0330

Nieden, zur, N. I., Cormier, J. T., Rancourt, D. E., & Kallos, M. S. (2007). Embryonic stem cells remain highly pluripotent following long term expansion as aggregates in suspension bioreactors. *Journal of Biotechnology*, *129*(3), 421–432. doi:10.1016/j.jbiotec.2007.01.006

Nikmanesh, M., Shi, Z.-D., & Tarbell, J. M. (2012). Heparan sulfate proteoglycan mediates shear stress-induced endothelial gene expression in mouse embryonic stem cell-derived endothelial cells. *Biotechnology and Bioengineering*, *109*(2), 583–594. doi:10.1002/bit.23302

Nunes, S. S., Miklas, J. W., Liu, J., Aschar-Sobbi, R., Xiao, Y., Zhang, B., et al. (2013). Biowire: a platform for maturation of human pluripotent stem cell-derived cardiomyocytes. *Nature Methods*. doi:10.1038/nmeth.2524

Offenberg Sweeney, von, N., Cummins, P. M., Birney, Y. A., Cullen, J. P., Redmond, E. M., & Cahill, P. A. (2004). Cyclic strain-mediated regulation of endothelial matrix metalloproteinase-2 expression and activity. *Cardiovascular Research*, *63*(4), 625–634. doi:10.1016/j.cardiores.2004.05.008

ORLIC, D., KAJSTURA, J., Chimenti, S., BODINE, D. M., LERI, A., & ANVERSA, P. (2006). Transplanted Adult Bone Marrow Cells Repair Myocardial Infarcts in Mice. *Annals of the New York Academy of Sciences*, *938*(1), 221–230. doi:10.1111/j.1749-6632.2001.tb03592.x

Pandur, P. (2005). What does it take to make a heart? *Biology of the Cell / Under the*

Auspices of the European Cell Biology Organization, *97*(3), 197–210. doi:10.1042/BC20040109

Patel, N. G., & Zhang, G. (2013). Responsive systems for cell sheet detachment. *Organogenesis*, *9*(2), 93–100. doi:10.4161/org.25149

Patwari, P., & Lee, R. T. (2008). Mechanical control of tissue morphogenesis. *Circulation Research*, *103*(3), 234–243. doi:10.1161/CIRCRESAHA.108.175331

Pimton, P., Sarkar, S., Sheth, N., Perets, A., Marcinkiewicz, C., Lazarovici, P., & Lelkes, P. I. (2011). Fibronectin-mediated upregulation of alpha 5 beta 1 integrin and cell adhesion during differentiation of mouse embryonic stem cells. *Cell Adhesion & Migration*, *5*(1), 73–82. doi:10.4161/cam.5.1.13704

Plopper, G., & Ingber, D. E. (1993). Rapid induction and isolation of focal adhesion complexes. *Biochemical and Biophysical Research Communications*, *193*(2), 571–578. doi:10.1006/bbrc.1993.1662

Prowse, A. B. J., Chong, F., Gray, P. P., & Munro, T. P. (2011). Stem cell integrins: implications for ex-vivo culture and cellular therapies. *Stem Cell Research*, *6*(1), 1–12. doi:10.1016/j.scr.2010.09.005

Rask, F., Mihic, A., Reis, L., Dallabrida, S. M., Ismail, N. S., Sider, K., et al. (2010). Hydrogels modified with QHREDGS peptide support cardiomyocyte survival in vitro and after sub-cutaneous implantation. *Soft Matter*, *6*(20), 5089–5099. doi:10.1039/c0sm00362j

Renault, M.-A., Roncalli, J., Tongers, J., Thorne, T., Klyachko, E., Misener, S., et al. (2010). Sonic hedgehog induces angiogenesis via Rho kinase-dependent signaling in endothelial cells. *Journal of Molecular and Cellular Cardiology*, *49*(3), 490–498. doi:10.1016/j.yjmcc.2010.05.003

Riha, G. M., Wang, X., Wang, H., Chai, H., Mu, H., Lin, P. H., et al. (2007). Cyclic strain induces vascular smooth muscle cell differentiation from murine embryonic mesenchymal progenitor cells. *Surgery*, *141*(3), 394–402. doi:10.1016/j.surg.2006.07.043

Roberts, D. J., Johnson, R. L., Burke, A. C., Nelson, C. E., Morgan, B. A., & Tabin, C. (1995). Sonic hedgehog is an endodermal signal inducing Bmp-4 and Hox genes during induction and regionalization of the chick hindgut. *Development*, *121*(10), 3163–3174.

Robertson, C., Tran, D. D., & George, S. C. (2013). Concise review: maturation phases

of human pluripotent stem cell-derived cardiomyocytes. *Stem Cells*, *31*(5), 829–837. doi:10.1002/stem.1331

Robinson, K. A., Li, J., Mathison, M., Redkar, A., Cui, J., Chronos, N. A. F., et al. (2005). Extracellular matrix scaffold for cardiac repair. *Circulation*, *112*(9 Suppl), I135–43. doi:10.1161/CIRCULATIONAHA.104.525436

Roger, V. L., Go, A. S., Lloyd-Jones, D. M., Benjamin, E. J., Berry, J. D., Borden, W. B., et al. (2012). Heart Disease and Stroke Statistics—2012 Update A Report From the American Heart Association. *Circulation*, *125*(1), e2–e220.

Rowland, T. J., Miller, L. M., Blaschke, A. J., Doss, E. L., Bonham, A. J., Hikita, S. T., et al. (2010). Roles of integrins in human induced pluripotent stem cell growth on Matrigel and vitronectin. *Stem Cells and Development*, *19*(8), 1231–1240. doi:10.1089/scd.2009.0328

Sachlos, E., & Auguste, D. T. (2008). Embryoid body morphology influences diffusive transport of inductive biochemicals: A strategy for stem cell differentiation. *Biomaterials*, *29*(34), 4471–4480. doi:10.1016/j.biomaterials.2008.08.012

Saha, S., Ji, L., de Pablo, J. J., & Palecek, S. P. (2006). Inhibition of human embryonic stem cell differentiation by mechanical strain. *Journal of Cellular Physiology*, *206*(1), 126–137. doi:10.1002/jcp.20441

Saha, S., Ji, L., de Pablo, J. J., & Palecek, S. P. (2008). TGFbeta/Activin/Nodal pathway in inhibition of human embryonic stem cell differentiation by mechanical strain. *Biophysical Journal*, *94*(10), 4123–4133. doi:10.1529/biophysj.107.119891

Sakaguchi, K., Shimizu, T., Horaguchi, S., Sekine, H., Yamato, M., Umezu, M., & Okano, T. (2013). In Vitro Engineering of Vascularized Tissue Surrogates. *Scientific Reports*, *3*. doi:10.1038/srep01316

Salameh, A., Wustmann, A., Karl, S., Blanke, K., Apel, D., Rojas-Gomez, D., et al. (2010). Cyclic mechanical stretch induces cardiomyocyte orientation and polarization of the gap junction protein connexin43. *Circulation Research*, *106*(10), 1592–1602. doi:10.1161/CIRCRESAHA.109.214429

Sargent, C. Y., Berguig, G. Y., & Mcdevitt, T. C. (2009). Cardiomyogenic differentiation of embryoid bodies is promoted by rotary orbital suspension culture. *Tissue Engineering Part A*, *15*(2), 331–342. doi:10.1089/ten.tea.2008.0145

Sauer, H., & Wartenberg, M. (2005). Reactive oxygen species as signaling molecules in cardiovascular differentiation of embryonic stem cells and tumor-induced

angiogenesis. *Antioxidants & Redox Signaling*, *7*(11-12), 1423–1434. doi:10.1089/ars.2005.7.1423

Sauer, H., Rahimi, C., Hescheler, J., & Wartenberg, M. (2000). Role of reactive oxygen species and phosphatidylinositol 3-kinase in cardiomyocyte differentiation of embryonic stem cells. *FEBS Letters*, *476*(3), 218–223.

Sawa, Y., & Miyagawa, S. (2013). Cell sheet technology for heart failure. *Current Pharmaceutical Biotechnology*, *14*(1), 61–66.

Schmelter, M., Ateghang, B., Helmig, S., Wartenberg, M., & Sauer, H. (2006). Embryonic stem cells utilize reactive oxygen species as transducers of mechanical strain-induced cardiovascular differentiation. *Faseb Journal*, *20*(8), 1182–. doi:10.1096/fj.05-4723fje

Serena, E., Figallo, E., Tandon, N., Cannizzaro, C., Gerecht, S., Elvassore, N., & Vunjak-Novakovic, G. (2009). Electrical stimulation of human embryonic stem cells: Cardiac differentiation and the generation of reactive oxygen species. *Experimental Cell Research*, *315*(20), 3611–3619. doi:10.1016/j.yexcr.2009.08.015

Shapira-Schweitzer, K., & Seliktar, D. (2007). Matrix stiffness affects spontaneous contraction of cardiomyocytes cultured within a PEGylated fibrinogen biomaterial. *Acta Biomaterialia*, *3*(1), 33–41. doi:10.1016/j.actbio.2006.09.003

Shapira-Schweitzer, K., Habib, M., Gepstein, L., & Seliktar, D. (2009). A photopolymerizable hydrogel for 3-D culture of human embryonic stem cell-derived cardiomyocytes and rat neonatal cardiac cells. *Journal of Molecular and Cellular Cardiology*, *46*(2), 213–224. doi:10.1016/j.yjmcc.2008.10.018

Shimizu, N., Yamamoto, K., Obi, S., Kumagaya, S., Masumura, T., Shimano, Y., et al. (2008). Cyclic strain induces mouse embryonic stem cell differentiation into vascular smooth muscle cells by activating PDGF receptor beta. *Journal of Applied Physiology (Bethesda, Md. : 1985)*, *104*(3), 766–772. doi:10.1152/japplphysiol.00870.2007

Shimizu, T., Sekine, H., Yamato, M., & Okano, T. (2009). Cell Sheet-Based Myocardial Tissue Engineering: New Hope for Damaged Heart Rescue. *Current Pharmaceutical Design*, *15*(24), 2807–2814.

Singh, A., Suri, S., Lee, T., Chilton, J. M., Cooke, M. T., Chen, W., et al. (2013). Adhesion strength-based, label-free isolation of human pluripotent stem cells. *Nature Methods*. doi:10.1038/nmeth.2437

Smith, A. W., Segar, C. E., Nguyen, P. K., MacEwan, M. R., Efimov, I. R., & Elbert, D. L. (2012). Long-term culture of HL-1 cardiomyocytes in modular poly(ethylene glycol) microsphere-based scaffolds crosslinked in the phase-separated state. *Acta Biomaterialia*, *8*(1), 31–40. doi:10.1016/j.actbio.2011.08.021

Son, Y., Cheong, Y.-K., Kim, N.-H., Chung, H.-T., Kang, D. G., & Pae, H.-O. (2011). Mitogen-Activated Protein Kinases and Reactive Oxygen Species: How Can ROS Activate MAPK Pathways? *Journal of Signal Transduction*, *2011*, 792639. doi:10.1155/2011/792639

SOONPAA, M. H., KOH, G. Y., KLUG, M. G., & Field, L. J. (1994). Formation of Nascent Intercalated Disks Between Grafted Fetal Cardiomyocytes and Host Myocardium. *Science (New York, N.Y.)*, *264*(5155), 98–101.

Srichai, M. B., & Zent, R. (2009). Integrin Structure and Function. In R. Zent & A. Pozzi, (pp. 19–41). New York, NY: Springer New York. doi:10.1007/978-1-4419-0814-8_2

Stolberg, S., & McCloskey, K. E. (2009). Can shear stress direct stem cell fate? *Biotechnology Progress*, *25*(1), 10–19. doi:10.1002/btpr.124

Sucov, H. M. (1998). Molecular insights into cardiac development. *Annual Review of Physiology*, *60*, 287–308. doi:10.1146/annurev.physiol.60.1.287

Taha, M. F., & Valojerdi, M. R. (2008). Effect of bone morphogenetic protein-4 on cardiac differentiation from mouse embryonic stem cells in serum-free and low-serum media. *International Journal of Cardiology*, *127*(1), 78–87. doi:10.1016/j.ijcard.2007.04.173

Tan, M. Y., Zhi, W., Wei, R. Q., Huang, Y. C., Zhou, K. P., Tan, B., et al. (2009). Repair of infarcted myocardium using mesenchymal stem cell seeded small intestinal submucosa in rabbits. *Biomaterials*, *30*(19), 3234–3240. doi:10.1016/j.biomaterials.2009.02.013

Tehrani, D. M., & Seto, A. H. (2013). Third universal definition of myocardial infarction: update, caveats, differential diagnoses. *Cleveland Clinic Journal of Medicine*, *80*(12), 777–786. doi:10.3949/ccjm.80a.12158

Teramura, T., Takehara, T., Onodera, Y., Nakagawa, K., Hamanishi, C., & Fukuda, K. (2012). Mechanical stimulation of cyclic tensile strain induces reduction of pluripotent related gene expressions via activation of Rho/ROCK and subsequent decreasing of AKT phosphorylation in human induced pluripotent stem cells. *Biochemical and Biophysical Research Communications*, *417*(2), 836–841. doi:10.1016/j.bbrc.2011.12.052

Thomas, N. A., Koudijs, M., van Eeden, F. J. M., Joyner, A. L., & Yelon, D. (2008). Hedgehog signaling plays a cell-autonomous role in maximizing cardiac developmental potential. *Development*, *135*(22), 3789–3799. doi:10.1242/dev.024083

Thygesen, K., Alpert, J. S., Jaffe, A. S., Simoons, M. L., Chaitman, B. R., White, H. D., et al. (2012). Third universal definition of myocardial infarction. (Vol. 126, pp. 2020–2035). Presented at the Circulation. doi:10.1161/CIR.0b013e31826e1058

Thygesen, K., Alpert, J. S., Jaffe, A. S., Simoons, M. L., Chaitman, B. R., White, H. D., Katus, H. A., et al. (2012b). Third universal definition of myocardial infarction. *Nature Reviews Cardiology*, *9*(11), 620–633. doi:10.1038/nrcardio.2012.122

Tirosh-Finkel, L., Zeisel, A., Brodt-Ivenshitz, M., Shamai, A., Yao, Z., Seger, R., et al. (2010). BMP-mediated inhibition of FGF signaling promotes cardiomyocyte differentiation of anterior heart field progenitors. *Development*, *137*(18), 2989–3000. doi:10.1242/dev.051649

Toh, Y.-C., & Voldman, J. (2011). Fluid shear stress primes mouse embryonic stem cells for differentiation in a self-renewing environment via heparan sulfate proteoglycans transduction. *The FASEB Journal*, *25*(4), 1208–1217. doi:10.1096/fj.10-168971

Tulloch, N. L., Muskheli, V., Razumova, M. V., Korte, F. S., Regnier, M., Hauch, K. D., et al. (2011). Growth of engineered human myocardium with mechanical loading and vascular coculture. *Circulation Research*, *109*(1), 47–59. doi:10.1161/CIRCRESAHA.110.237206

Uda, Y., Poh, Y.-C., Chowdhury, F., Wu, D. C., Tanaka, T. S., Sato, M., & Wang, N. (2011). Force via integrins but not E-cadherin decreases Oct3/4 expression in embryonic stem cells. *Biochemical and Biophysical Research Communications*, *415*(2), 396–400. doi:10.1016/j.bbrc.2011.10.080

van Spreeuwel, A. C. C., Bax, N. A. M., Bastiaens, A. J., Foolen, J., Loerakker, S., Borochin, M., et al. (2014). The influence of matrix (an)isotropy on cardiomyocyte contraction in engineered cardiac microtissues. *Integrative Biology : Quantitative Biosciences From Nano to Macro*, *6*(4), 422–429. doi:10.1039/c3ib40219c

Van Vliet, P., Wu, S. M., Zaffran, S., & Pucéat, M. (2012). Early cardiac development: a view from stem cells to embryos. *Cardiovascular Research*, *96*(3), 352–362. doi:10.1093/cvr/cvs270

Vokes, S. A., Yatskievych, T. A., Heimark, R. L., McMahon, J., McMahon, A. P., Antin,

P. B., & Krieg, P. A. (2004). Hedgehog signaling is essential for endothelial tube formation during vasculogenesis. *Development*, *131*(17), 4371–4380. doi:10.1242/dev.01304

Wan, C.-R., Chung, S., & Kamm, R. D. (2011). Differentiation of embryonic stem cells into cardiomyocytes in a compliant microfluidic system. *Annals of Biomedical Engineering*, *39*(6), 1840–1847. doi:10.1007/s10439-011-0275-8

Wang, B., Wang, G., To, F., Butler, J. R., Claude, A., McLaughlin, R. M., et al. (2013). Myocardial scaffold-based cardiac tissue engineering: application of coordinated mechanical and electrical stimulations. *Langmuir*, *29*(35), 11109–11117. doi:10.1021/la401702w

Wang, J. S., Shum-Tim, D., Galipeau, J., Chedrawy, E., Eliopoulos, N., & Chiu, R. (2000). Marrow stromal cells for cellular cardiomyoplasty: Feasibility and potential clinical advantages. *Journal of Thoracic and Cardiovascular Surgery*, *120*(5), 999–1006. doi:10.1067/mtc.2000.110250

Wang, N., Butler, J. P., & Ingber, D. E. (1993). Mechanotransduction across the cell surface and through the cytoskeleton. *Science (New York, N.Y.)*, *260*(5111), 1124–1127.

Wang, P.-Y., Yu, J., Lin, J.-H., & Tsai, W.-B. (2011). Modulation of alignment, elongation and contraction of cardiomyocytes through a combination of nanotopography and rigidity of substrates. *Acta Biomaterialia*, *7*(9), 3285–3293. doi:10.1016/j.actbio.2011.05.021

Wang, X., & Ha, T. (2013). Defining Single Molecular Forces Required to Activate Integrin and Notch Signaling. *Science (New York, N.Y.)*, *340*(6135), 991–994. doi:10.1126/science.1231041

Watanabe, S., Umehara, H., Murayama, K., Okabe, M., Kimura, T., & Nakano, T. (2006). Activation of Akt signaling is sufficient to maintain pluripotency in mouse and primate embryonic stem cells. *Oncogene*, *25*(19), 2697–2707. doi:10.1038/sj.onc.1209307

Willems, E., Spiering, S., Davidovics, H., Lanier, M., Xia, Z., Dawson, M., et al. (2011). Small-molecule inhibitors of the Wnt pathway potently promote cardiomyocytes from human embryonic stem cell-derived mesoderm. *Circulation Research*, *109*(4), 360–364. doi:10.1161/CIRCRESAHA.111.249540

Williams, C., Johnson, S. L., Robinson, P. S., & Tranquillo, R. T. (2006). Cell sourcing and culture conditions for fibrin-based valve constructs. *Tissue Engineering*, *12*(6),

1489–1502.

Wolfe, R. P., Leleux, J., Nerem, R. M., & Ahsan, T. (2012). Effects of shear stress on germ lineage specification of embryonic stem cells. *Integrative Biology : Quantitative Biosciences From Nano to Macro*, *4*(10), 1263–1273. doi:10.1039/c2ib20040f

Wu, S. M., Choo, A. B. H., Yap, M. G. S., & Chan, K. K.-K. (2010). Role of Sonic hedgehog signaling and the expression of its components in human embryonic stem cells. *Stem Cell Research*, *4*(1), 38–49. doi:10.1016/j.scr.2009.09.002

Xin, M., Olson, E. N., & Bassel-Duby, R. (2013). Mending broken hearts: cardiac development as a basis for adult heart regeneration and repair. *Nature Reviews. Molecular Cell Biology*, *14*(8), 529–541. doi:doi:10.1038/nrm3619

Xu, C., Police, S., Rao, N., & Carpenter, M. K. (2002). Characterization and enrichment of cardiomyocytes derived from human embryonic stem cells. *Circulation Research*, *91*(6), 501–508.

Xu, H., Yi, B. A., & Chien, K. R. (2011). Shortcuts to making cardiomyocytes. *Nature Cell Biology*, *13*(3), 191–193. doi:10.1038/ncb0311-191

Yamashita, J., Itoh, H., Hirashima, M., Ogawa, M., Nishikawa, S., Yurugi, T., et al. (2000). Flk1-positive cells derived from embryonic stem cells serve as vascular progenitors. *Nature*, *408*(6808), 92–96. doi:10.1038/35040568

Yanada, S., Ochi, M., Adachi, N., Nobuto, H., Agung, M., & Kawamata, S. (2006). Effects of CD44 antibody-- or RGDS peptide--immobilized magnetic beads on cell proliferation and chondrogenesis of mesenchymal stem cells. *Journal of Biomedical Materials Research Part A*, *77*(4), 773–784. doi:10.1002/jbm.a.30635

Yang, W., Wu, B., Asakura, S., Kohno, I., & Matsuda, M. (2004). Soluble fibrin augments spreading of fibroblasts by providing RGD sequences of fibrinogen in soluble fibrin. *Thrombosis Research*, *114*(4), 293–300. doi:10.1016/j.thromres.2004.06.022

Ye, Z., Zhou, Y., Cai, H., & Tan, W. (2011). Myocardial regeneration: Roles of stem cells and hydrogels. *Advanced Drug Delivery Reviews*, *63*(8), 688–697. doi:10.1016/j.addr.2011.02.007

Young, J. L., & Engler, A. J. (2011). Hydrogels with time-dependent material properties enhance cardiomyocyte differentiation in vitro. *Biomaterials*, *32*(4), 1002–1009. doi:10.1016/j.biomaterials.2010.10.020

Zborowski, M., Sun, L., Moore, L. R., Stephen Williams, P., & Chalmers, J. J. (1999). Continuous cell separation using novel magnetic quadrupole flow sorter. *Journal of Magnetism and Magnetic Materials*, *194*(1), 224–230.

Zeng, D., Ou, D.-B., Wei, T., Ding, L., Liu, X.-T., Hu, X.-L., et al. (2013). Collagen/β(1) integrin interaction is required for embryoid body formation during cardiogenesis from murine induced pluripotent stem cells. *BMC Cell Biology*, *14*, 5. doi:10.1186/1471-2121-14-5

Zhang, G., Drinnan, C. T., Geuss, L. R., & Suggs, L. J. (2010). Vascular differentiation of bone marrow stem cells is directed by a tunable three-dimensional matrix. *Acta Biomaterialia*, *6*(9), 3395–3403. doi:10.1016/j.actbio.2010.03.019

Zhang, G., Hu, Q., Braunlin, E. A., Suggs, L. J., & Zhang, J. (2008a). Enhancing efficacy of stem cell transplantation to the heart with a PEGylated fibrin biomatrix. *Tissue Engineering Part A*, *14*(6), 1025–1036. doi:10.1089/ten.tea.2007.0289

Zhang, G., Wang, X., Wang, Z., Zhang, J., & Suggs, L. (2006). A PEGylated fibrin patch for mesenchymal stem cell delivery. *Tissue Engineering*, *12*(1), 9–19. doi:10.1089/ten.2006.12.9

Zhang, P., Li, J., Tan, Z., Wang, C., Liu, T., Chen, L., et al. (2008b). Short-term BMP-4 treatment initiates mesoderm induction in human embryonic stem cells. *Blood*, *111*(4), 1933–1941. doi:10.1182/blood-2007-02-074120

Zhao, S., Suciu, A., Ziegler, T., Moore, J. E., Bürki, E., Meister, J. J., & Brunner, H. R. (1995). Synergistic effects of fluid shear stress and cyclic circumferential stretch on vascular endothelial cell morphology and cytoskeleton. *Arteriosclerosis, Thrombosis, and Vascular Biology*, *15*(10), 1781–1786.

Zoldan, J., Karagiannis, E. D., Lee, C. Y., Anderson, D. G., Langer, R., & Levenberg, S. (2011). The influence of scaffold elasticity on germ layer specification of human embryonic stem cells. *Biomaterials*, *32*(36), 9612–9621. doi:10.1016/j.biomaterials.2011.09.012

VITA

Laura Roslye Geuss graduated from the International School of Luxembourg in 2000. In 2004, she graduated from Wellesley College in Wellesley, MA with a Bachelor of the Arts in Neuroscience. After college, she went to Tufts University to pursue a Master of Science degree in Biology/Biotechnology. While pursuing a Masters, she worked as a Junior Research Scientist in Research and Development for Serica, Inc. Following commencement in 2006, she was employed as a Research Associate in the Research and Development group at Histogenics Corp from 2006-2008. In June 2008, she entered the Cell and Molecular Biology graduate program at the University of Texas at Austin.

This manuscript was typed by the author.